ALINE DO AMARAL LEITE

POULTRY-MANURE BIOCHAR AND PHOSPHORUS AVAILABILITY: INFLUENCE OF MAGNESIUM ENRICHMENT AND BACTERIAL SOLUBILIZATION

LAVRAS – MG
2023

ALINE DO AMARAL LEITE

POULTRY-MANURE BIOCHAR AND PHOSPHORUS AVAILABILITY: INFLUENCE OF MAGNESIUM ENRICHMENT AND BACTERIAL SOLUBILIZATION

Thesis presented to the Federal University of Lavras, as part of the requirements of the Graduate Program in Soil Science, concentration area Soil Fertility and Plant Nutrition, to obtain the title of Doctor.

Advisor
Prof. Dr. Leônidas Carrijo Azevedo Melo

Co-advisor
Prof. Dr. Johannes Lehmann

Co-advisor
Prof. Dr. Fatima Maria de Souza Moreira

LAVRAS - MG
2023

Ficha catalográfica elaborada pelo Sistema de Geração de Ficha Catalográfica da Biblioteca Universitária da UFLA, com dados informados pelo(a) próprio(a) autor(a).

Leite, Aline do Amaral.
Poultry-Manure Biochar and Phosphorus Availability : Poultry-Manure Biochar and Phosphorus Availability: Influence of Magnesium Enrichment and Bacterial Solubilization / Aline do Amaral Leite. - 2022.
95 p. : il.

Orientador(a): Leônidas Carijo Azevedo Melo.
Coorientador(a): Fatima Maria de Souza Moreira, Johannes Lehmann.
Tese (doutorado) - Universidade Federal de Lavras, 2022.
Bibliografia.

1. Pyrolysis of poultry manure. 2. Phosphate-solubilizing bacteria. 3. Plant growth. I. Melo, Leônidas Carijo Azevedo. II. Moreira, Fatima Maria de Souza. III. Lehmann, Johannes. IV.

ALINE DO AMARAL LEITE

POULTRY-MANURE BIOCHAR AND PHOSPHORUS AVAILABILITY: INFLUENCE OF MAGNESIUM ENRICHMENT AND BACTERIAL SOLUBILIZATION

BIOCARVÃO DE ESTERCO DE AVES E DISPONIBILIDADE DE FÓSFORO: INFLUÊNCIA DO ENRIQUECIMENTO COM MAGNÉSIO E DA SOLUBILIZAÇÃO BACTERIANA

Thesis presented to the Federal University of Lavras, as part of the requirements of the Postgraduate Program in Soil Science, area of concentration in Soil Fertility and Plant Nutrition, to obtain the title of Doctor.

Approved on December 29, 2022.

Dr. Leônidas Carrijo Azevedo Melo – Federal University of Lavras (UFLA)
Dr. Marco Aurelio Carbone Carneiro – Federal University of Lavras (UFLA)
Dr. Flávio Henrique Silveira Rabelo – Federal University of Lavras (UFLA)
Dr. Marcos Gervasio Pereira – Federal Rural University of Rio de Janeiro (UFRRJ)
Dr. Ederson da Conceição Jesus – Embrapa Agrobiology

gov.br
Documento assinado digitalmente
LEONIDAS CARRIJO AZEVEDO MELO
Data: 19/01/2023 12:02:45-0300
Verifique em https://verificador.iti.br

Advisor
Prof. Dr. Leônidas Carrijo Azevedo Melo

Co-advisor
Prof. Dr. Johannes Lehmann

Co-advisor
Prof. Dr. Fatima Maria de Souza Moreira

LAVRAS - MG
2023

To God,

To my parents, Amélia S. Amaral. and Aurelino A. Leite and my brother João Paulo A. Leite,

To my stepfather Nilson Gonçalves,

To my grandmother, Prezilina Santos.

I DEDICATE.

ACKNOWLEDGMENTS

I acknowledge for all the support during my doctorate:

The Federal University of Lavras, the School of Agricultural Sciences of Lavras and especially to the Department of Soil Science.

The Coordination of Improvement of Higher Education Personnel (CAPES) for the grant of the student scholarship.

The Institutional Internationalization Program (CAPES PrInt) for the grant of the student scholarship.

The National Council of Scientific and Technological Development (CNPq) and the Foundation for Research Support of Minas Gerais (FAPEMIG) for the financial subsidy.

To Cornell University.

My advisor at UFLA, Prof. Dr. Leônidas Carrijo Azevedo Melo, and my co-advisor, Prof. Dr. Fátima Maria de Souza Moreira.

My advisor at Cornell University, Prof. Dr. Johannes Lehmann.

All professors of the Department of Soil Science of Federal University of Lavras.

The Prof. Dr. Carlos Silva.

All laboratory technicians, specially Lívia Botelho, Mariene Duarte, Aline Mesquita, Geila Carvalho, Lidiany Lima, Franciane Campos and Jacqueline Savana.

My research group, colleagues and friends – Arnon Cardoso, Rafael Almeida, Bárbara Nardis, Jefferson Carneiro, Ivan Ribeiro, Bruno Lago, Thiago Pereira, Isabela Durães, Daniela Queiroz, Thiago Viana, Ana Maria Barrera, Evanise Penido, Andrés Montes, Felipe Sarto, Silvia Oliveira-Longatti and Giovanna Fontes.

.

TABLE OF CONTENTS

RESUMO

O biocarvão é um subproduto da pirólise e suas aplicações estão relacionadas principalmente ao condicionamento do solo. Produzir biocarvão a partir de um resíduo orgânico como o esterco de frango é uma alternativa para aumentar o valor fertilizante da biomassa, favorecer a reciclagem e evitar perdas. A baixa disponibilidade de nutrientes em água é importante para aumentar a eficiência do uso do fósforo (P), principalmente em solos tropicais devido à sua alta afinidade com a fração argila (óxidos e hidróxidos de Fe e Al). No entanto, o teor de Ca no esterco de aves é relativamente alto (~10%) e, com a pirólise, a disponibilidade de P diminui. Além disso, é necessário desenvolver métodos para aumentar a disponibilidade de P sem aumentar a solubilidade de P em água. Por exemplo, modificações químicas pela adição de magnésio (Mg) e/ou inoculação com bactérias solubilizadoras de fosfato podem melhorar a capacidade do biocarvão de fornecer P. Assim, os objetivos deste estudo foram: (1) Determinar como a temperatura de pirólise e o aumento da razão Mg/Ca afetam a solubilidade do P; (2) Avaliar como mudanças nas espécies de P e sua cristalinidade afetam a extensão em que as bactérias solubilizadoras de fosfato (BSF) aumentam a solubilização de P; (3) Avaliar como o crescimento de plantas de milho e a absorção de P na parte aérea são afetados com fertilização de P usando biocarvão e biocarvão enriquecido com Mg produzidos em temperaturas de pirólise crescentes e inoculação bacteriana. Para isso, biocarvões modificados com Mg foram produzidos em uma taxa de aquecimento de 10 ºC por min até a temperatura alvo e um período de espera de 30 min. Após a produção, o biocarvão foi completamente caracterizado, e a disponibilidade de P (ácido fórmico e cítrico 2%) e a especiação de P por espectroscopia de XANES foram estudadas. Experimentos *in vitro* e *in vivo* foram realizados, determinando-se a solubilização de P, o crescimento de plantas de milho e a absorção de P. Com a adição de Mg, a disponibilidade de P aumentou até uma temperatura de pirólise de 600 °C em comparação com o biochar puro. A adição de Mg à também impediu ou diminuiu a formação de minerais mais cristalinos, como hidroxiapatita e pirofosfato. Já para a inoculação com BFS, a fonte de P influenciou a produção de ácidos orgânicos específicos, mas não necessariamente com aumento da solubilização de P. A estirpe *Pseudomonas* sp. liberou maiores quantidades de P do biocarvão com Mg a 350 °C (condição *in vitro*). Da mesma forma, o biocarvão enriquecido com Mg (350 °C) e a inoculação de BSF aumentaram a absorção e o acúmulo de P do milho. Assim, a adição de Mg antes da pirólise do esterco de frango é uma alternativa atraente para aumentar seu valor fertilizante para crescimento das plantas. Estudos futuros devem se concentrar em compreender as transformações de P em biocarvão produzido em temperaturas mais altas (>350 °C) e como aumentar o potencial de enriquecimento de Mg e inoculação de PSB na disponibilidade de P.

Palavras-chave: Bactérias solubilizadoras de fosfato. Especiação de P. Crescimento da planta. Plantas de milho.

ABSTRACT

Biochar is a stable and recalcitrant byproduct of pyrolysis, and its applications are related primarily to soil conditioning. Producing biochar from an organic residue such as poultry manure is an alternative to increase the fertilizer value, increase nutrient recycling, and prevent nutrient losses by decreasing nutrient availability in water. A low water availability is important specially to enhance phosphorus (P) use efficiency in soils, especially in tropical soils due to their high affinity to clay mineral fraction (Fe and Al oxides and hydroxides). However, Ca content in poultry manure is relatively high (~10%), and with pyrolysis, P availability decreases due to thermal transformation. Moreover, is it necessary to develop methods to increase P availability from poultry manure biochar without increasing P availability in water. For instance, chemical modifications by introducing additives such as magnesium (Mg) in the feedstock and/or inoculation with phosphate-solubilizing bacteria may improve the biochar's ability to supply P in soil. Thus, the objectives of this study were: (1) To determine how pyrolysis temperature and increasing the ratio of Mg/Ca affects P solubility; (2) To evaluate how changes in P species and their crystallinity affect the extent to which phosphate-solubilizing bacteria (PSB) increase P solubilization; (3) To evaluate how maize plants growth and P uptake in shoots are affected with P fertilization using biochar and Mg-enriched biochar at increasing pyrolysis temperature and bacterial inoculation. For this, Mg modified-biochars were produced in a laboratory-scale pyrolysis system, performed with a heating rate of 10 ºC/min to their target temperature and a holding period of 30 min. After the production, biochar was completely characterized, and P availability (formic and citric acid 2%) and P speciation by using XANES spectroscopy were studied. *In vitro* and *in vivo* experiments were performed, and P solubilization, maize plant growth, and P uptake in plant shoots were determined. With Mg addition, P availability increased up to a pyrolysis temperature of 600 °C compared to the pristine biochar. Adding Mg to poultry manure biomass prevented or decreased the formation of more crystalline minerals, such as hydroxyapatite and pyrophosphate. As for PSB, the P source influenced specific organic acid production, but not necessarily with increased P solubilization. The strain *Pseudomonas* sp. released higher amounts of P from Mg-biochar at 350 °C (*in vitro* condition). Similarly, Mg-enriched biochar (350 °C) and PSB inoculation increased P uptake and accumulation in maize shoot tissues. Thus, adding Mg prior to the pyrolysis of poultry manure is an attractive alternative to increase its fertilizer value for further plant growth. Future studies should focus on comprising the P transformations in biochar produced at higher pyrolysis temperatures (>350 °C) and how to enhance the potential of Mg enrichment and PSB inoculation on P availability in soil.

Keywords: Phosphate-solubilizing bacteria. P speciation. Plant growth. Maize plants.

General introduction

Brazil has a great diversity of soils due to the abundant soil environments and soil formation factors that they are exposed. The Oxisols, Argisols and Neosols together are distributed over approximately 70% of the national territory, and these are highly weathered, possesses an acidic condition and low natural fertility (Santos, 2018). Besides, Natural P scarcity is a major issue in these soils (Du et al., 2020), which have higher P fixing capacity and low efficiency of P fertilization, which is applied primarily in the soluble form (Shen et al., 2011). For crop production in Brazil, P fertilizers are mostly dependent from mining of external sources since the quality of internal P reserves are very low (ANDA, 2017; Pavinato et al., 2020). For agriculture expansion, P management must use alternative strategies rather than P extraction and acquire P from sustainable sources, aiming to reduce P mining and the cost of P fertilization.

Biochar is the solid fraction of the thermal degradation (pyrolysis) of organic feedstocks and can aid plant production. The pyrolysis process occurs at relatively high temperatures (300 – 700 °C), under limited or oxygen-free conditions, reduces volume, and the byproduct resulting has higher nutrient concentration and carbon stability than the unpyrolyzed biomass (Ippolito et al., 2020). When applied to soil, biochar function as a conditioner and improves the chemical, physical and biological properties, providing a better environment for plant growth and microbial biomass activity and development (Kocsis et al., 2022; Oni et al., 2019). However, the feedstock choice creates distinctive chemical composition amidst biochars. For instance, wood-based feedstocks contain more C and low nutrient concentrations, while manure biomasses originate biochar with smaller C content and higher mineral composition, such as P (Freitas et al., 2020; Satoshi Higashikawa et al., 2010). Moreover, biochar produced from nutrient-rich organic residues functions not only as a soil conditioner, but also as a slow-release fertilizer (Hossain et al., 2020). However, the above purposes vary not only according to feedstock selection, but also with its modification and pyrolysis conditions, which greatly influence the final biochar product, properties, and application (Cao and Harris, 2010).

Overall, pyrolysis temperature, the heating rate, and holding time play a significant role in biochar physicochemical and morphological properties. In general, higher pyrolysis temperatures lead to higher biochar-specific surface area, pH and carbon stability and carbon content; however, these vary according to feedstock, as mentioned (Keiluweit et al., 2010; Zhang et al., 2015; Zhao

et al., 2017). Biochar yield also changes with increasing pyrolysis temperatures, and temperatures above 500 °C decrease biochar yield and the ratios of O/C and H/C, indicating higher aromaticity and persistence in the environment (Hassan et al., 2020). For instance, a yield decrease between temperatures of 350 and 500 °C is likely due to the combustion of organic matter (Cao and Harris, 2010). Regarding nutrients availability, in temperatures higher than 500 °C induces the production of less soluble forms of nutrients due to higher crystal propagation, as observed for phosphates (Tomczyk et al., 2020; Xu et al., 2016).

Among plant nutrients in biochar matrix, many studies have reported that biochar efficiently supplies phosphorus (P) for plant growth (Glaser and Lehr, 2019), and among feedstocks poultry manure could be suitable for pyrolysis due to its chemical P composition (~1.6 g kg^{-1}), which concentrates in the biochar (Darby et al., 2016; Tsai and Chang, 2021). Poultry for meat production in Brazil achieved 1.55 billion of birds in 2022 (IBGE, 2022), and poultry manure production is in the order of 1.1 kg per broiler and 9-13 pounds per commercial layer during poultry life cycle (Ritz and Merka, 2013). Furthermore, poultry manure processing is necessary to decrease moisture (~ 60 % *in natura*) and sanitize the material (Rehman et al., 2020). Pyrolysis might be a solution to reduce the polluting potential of poultry manure, and consequently, reduce environmental impacts such as eutrophication of water bodies through the release of N and P (Abassi et al., 2019). However, when pyrolyzed at high temperatures, poultry manure biochar becomes either a slow-release P fertilizer or P storage, which needs to be optimized to be used as P fertilizer in soils (Bruun et al., 2017; Sarvi et al., 2021). However, it has yet to be discovered which conditions could increase P availability in poultry manure biochar. One alternative could be chemical modification through enrichment poultry manure biomass with Mg before pyrolysis and solubilization by phosphate-solubilizing bacteria (PSB).

Some studies have already reported the influence of Mg on phosphate crystallinity after thermal degradation. In synthetic hydroxyapatite production, for example, partially substituting Ca with Mg inhibited crystal growth by inducing structural decomposition with heat treatments (Cao and Harris, 2010; Hilger et al., 2020). Thus, increasing the concentration of a smaller ion (Mg) in poultry manure biomass might similarly cause structural changes during pyrolysis and influence P speciation in favor of higher availability and enhanced proportions of Mg-phosphates. In contrast, inoculating PSB strains could be another alternative to increase P availability from poultry manure biochar and Mg-enriched poultry manure biochar (Sharma et al., 2013). Studies have demonstrated

that PSB inoculation increases plant growth in soil fertilized with insoluble P sources (Marra et al., 2012; Costa et al., 2015), also including biochar (Leite et al., 2020). It is also well-documented that the association of bacteria and biochar could facilitate nutrient cycling (Atkinson et al., 2010; Lavakush et al., 2014; Lehmann et al., 2011). Biochar characteristics, such as pores and surface structure, can beneficiate microbial communities in soil. The surface area likely interferes with microbial attachment, while the porous structure can assist microorganisms, working as a safe habitat (Jaafar et al., 2015, 2014; Lehmann et al., 2011). Therefore, it is necessary to unravel the solubilization mechanisms from selected PSB strains from P-Ca compared to P-Mg minerals and Mg-enriched biochar.

Thesis objectives and research questions

The major purpose of this research was to develop a novel biochar of higher P availability and consequently enhanced potential for P use efficiency in tropical soils. The following questions will be answered posteriorly.

Would Mg-enriched poultry manure biochars, through increasing Mg/Ca ratio in poultry manure, present higher phosphorus availability than pristine biochar? And in which pyrolysis conditions would that be true?

Would Mg-enriched poultry manure biochars affected the extent by which phosphate-solubilizing bacteria (PSB) released P and enhance plant growth and P uptake by maize plants? On which Mg/Ca levels and pyrolysis temperatures would that be possible?

Dissertation outline

The above research questions were addressed and answered in two chapters.

In chapter 1, we discussed P availability of 5 levels of Mg/Ca ration in poultry manure and four pyrolysis temperatures. For that we used chemical extractors and biochar characterization through advanced synchrotron techniques (XANES), X-ray diffraction (XRD), Fourier transform infrared spectroscopy (FTIR), scanning electron microscopy (SEM-EDS) and P-release kinetics in water.

In chapter 2, Magnesium and calcium phosphates were subjected to PSB inoculation and the medium acidification and organic acid production were investigated. We also discussed the

effect of three levels of Mg/Ca ratio under PSB inoculation and the effect as phosphate fertilizer for maize plants growth under tropical soil.

REFERENCES

ABBASI, F., FAKHUR-UN-NISA, T., LIU, J., LUO, X., ABBASI, I.H.R., 2019. Low digestibility of phytate phosphorus, their impacts on the environment, and phytase opportunity in the poultry industry. **Environmental Science and Pollution Research**. https://doi.org/10.1007/s11356-018-4000-0

ANDA - Associação Nacional para Difusão de Adubos, 2017. Indicadores - Fertilizantes entregues ao mercado. https://anda.org.br/index.php?mpg=03.00.00

ATKINSON, C.J., FITZGERALD, J.D., HIPPS, N.A., 2010. Potential mechanisms for achieving agricultural benefits from biochar application to temperate soils: A review. **Plant Soil**. https://doi.org/10.1007/s11104-010-0464-5

BRUUN, S., HARMER, S.L., BEKIARIS, G., CHRISTEL, W., ZUIN, L., HU, Y., JENSEN, L.S., LOMBI, E., 2017. The effect of different pyrolysis temperatures on the speciation and availability in soil of P in biochar produced from the solid fraction of manure. **Chemosphere** 169, 377–386. https://doi.org/10.1016/j.chemosphere.2016.11.058

CAO, X., HARRIS, W., 2010. Properties of dairy-manure-derived biochar pertinent to its potential use in remediation. **Bioresour Technol** 101, 5222–5228. https://doi.org/10.1016/j.biortech.2010.02.052

DARBY, I., XU, C.Y., WALLACE, H.M., JOSEPH, S., PACE, B., BAI, S.H., 2016. Short-term dynamics of carbon and nitrogen using compost, compost-biochar mixture and organo-mineral biochar. **Environmental Science and Pollution Research** 23, 11267–11278. https://doi.org/10.1007/s11356-016-6336-7

DU, E., TERRER, C., PELLEGRINI, A. F. A., AHLSTRÖM, A., VAN LISSA, C. J., ZHAO, X., XIA, N., WU, X., AND JACKSON, R. B., 2020. Global patterns of terrestrial nitrogen and phosphorus limitation. **Nature Geoscience** 13, 221–226. https://doi.org/10.1038/s41561-019-0530-4

LEITE, A., DE SOUZA CARDOSO, A.A., DE ALMEIDA LEITE, R., DE OLIVEIRA-LONGATTI, S.M., FILHO, J.F.L., DE SOUZA MOREIRA, F.M., MELO, L.C.A., 2020. Selected bacterial strains enhance phosphorus availability from biochar-based rock phosphate fertilizer. **Ann Microbiol** 70. https://doi.org/10.1186/s13213-020-01550-3

FREITAS, A.M., NAIR, V.D., HARRIS, W.G., 2020. Biochar as Influenced by Feedstock Variability: Implications and Opportunities for Phosphorus Management. **Front Sustain Food Syst** 4. https://doi.org/10.3389/fsufs.2020.510982

GLASER, B., LEHR, V.I., 2019. Biochar effects on phosphorus availability in agricultural soils: A meta-analysis. **Sci Rep** 9. https://doi.org/10.1038/s41598-019-45693-z

HASSAN, M., LIU, Y., NAIDU, R., PARIKH, S.J., DU, J., QI, F., WILLETT, I.R., 2020. Influences of feedstock sources and pyrolysis temperature on the properties of biochar and functionality as adsorbents: A meta-analysis. **Science of the Total Environment**. https://doi.org/10.1016/j.scitotenv.2020.140714

HILGER, D.M., HAMILTON, J.G., PEAK, D., 2020. The influences of magnesium upon calcium phosphate mineral formation and structure as monitored by x-ray and vibrational spectroscopy. **Soil Syst** 4, 1–13. https://doi.org/10.3390/soilsystems4010008

HOSSAIN, M.Z., BAHAR, M.M., SARKAR, B., DONNE, S.W., OK, Y.S., PALANSOORIYA, K.N., KIRKHAM, M.B., CHOWDHURY, S., BOLAN, N., 2020. Biochar and its importance on nutrient dynamics in soil and plant. **Biochar**. https://doi.org/10.1007/s42773-020-00065-z

INSTITUTO BRASILEIRO DE GEOGRAFIA E ESTATÍSTICA (IBGE). Estatística da Produção Pecuária. **IBGE**, 2022.

IPPOLITO, J.A., CUI, L., KAMMANN, C., WRAGE-MÖNNIG, N., ESTAVILLO, J.M., FUERTES-MENDIZABAL, T., CAYUELA, M.L., SIGUA, G., NOVAK, J., SPOKAS, K., BORCHARD, N., 2020. Feedstock choice, pyrolysis temperature and type influence biochar characteristics: a comprehensive meta-data analysis review. **Biochar.** https://doi.org/10.1007/s42773-020-00067-x

JAAFAR, N.M., CLODE, P.L., ABBOTT, L.K., 2015. Soil Microbial Responses to Biochars Varying in Particle Size, Surface and Pore Properties, **Pedosphere.**

JAAFAR, N.M., CLODE, P.L., ABBOTT, L.K., 2014. Microscopy observations of habitable space in biochar for colonization by fungal hyphae from soil. **J Integr Agric** 13, 483–490. https://doi.org/10.1016/S2095-3119(13)60703-0

KEILUWEIT, M., NICO, P.S., JOHNSON, M., KLEBER, M., 2010. Dynamic molecular structure of plant biomass-derived black carbon (biochar). **Environmental Science and Technology** 44, 1247–1253. https://doi.org/10.1021/es9031419

KOCSIS, T., RINGER, M., BIRÓ, B., 2022. Characteristics and Applications of Biochar in Soil–Plant Systems: A Short Review of Benefits and Potential Drawbacks. **Applied Sciences** (Switzerland). https://doi.org/10.3390/app12084051

LAVAKUSH, YADAV, J., VERMA, J.P., JAISWAL, D.K., KUMAR, A., 2014. Evaluation of PGPR and different concentration of phosphorus level on plant growth, yield and nutrient content of rice (Oryza sativa). **Ecol Eng** 62, 123–128. https://doi.org/10.1016/j.ecoleng.2013.10.013

LEHMANN, J., RILLIG, M.C., THIES, J., MASIELLO, C.A., HOCKADAY, W.C., CROWLEY, D., 2011. Biochar effects on soil biota - A review. **Soil Biol Biochem**. https://doi.org/10.1016/j.soilbio.2011.04.022

MARRA, L.M., SOUSA SOARES, C.R.F., DE OLIVEIRA, S.M., FERREIRA, P.A.A., SOARES, B.L., DE CARVALHO, R.F., DE LIMA, J.M., DE MOREIRA, F.M.S., 2012. Biological nitrogen fixation and phosphate solubilization by bacteria isolated from tropical soils**. Plant Soil** 357, 289–307. https://doi.org/10.1007/s11104-012-1157-z

MARTINS DA COSTA, E., DE LIMA, W., OLIVEIRA-LONGATTI, S.M., DE SOUZA, F.M., 2015. Phosphate-solubilising bacteria enhance Oryza sativa growth and nutrient accumulation in an oxisol fertilized with rock phosphate. **Ecol Eng** 83, 380–385. https://doi.org/10.1016/j.ecoleng.2015.06.045

ONI, B.A., OZIEGBE, O., OLAWOLE, O.O., 2019. Significance of biochar application to the environment and economy. **Annals of Agricultural Sciences**. https://doi.org/10.1016/j.aoas.2019.12.006

PAVINATO, P.S., CHERUBIN, M.R., SOLTANGHEISI, A., ROCHA, G.C., CHADWICK, D.R., JONES, D.L., 2020. Revealing soil legacy phosphorus to promote sustainable agriculture in Brazil. **Sci Rep** 10. https://doi.org/10.1038/s41598-020-72302-1

RITZ, C.W., MERKA, W.C., 2013. Maximizing Poultry Manure Use Through Nutrient Management **Planning. Bulletin** 1245, University of Georgia. https://secure.caes.uga.edu/extension/publications/files/pdf/B%201245_3.PDF

REHMAN, A., NAWAZ, S., ALGHAMDI, H.A., ALRUMMAN, S., YAN, W., NAWAZ, M.Z., 2020. Effects of manure-based biochar on uptake of nutrients and water holding capacity of different types of soils. **Case Studies in Chemical and Environmental Engineering** 2. https://doi.org/10.1016/j.cscee.2020.100036

SANTOS, H. G. DOS, 2018. Sistema brasileiro de classificação de solos. 5 ed. Brasilia: **EMBRAPA.**

SARVI, M., HAGNER, M., VELMALA, S., SOINNE, H., UUSITALO, R., KESKINEN, R., YLIVAINIO, K., KASEVA, J., RASA, K., 2021. Bioavailability of phosphorus in granulated and pyrolyzed broiler manure. **Environ Technol Innov** 23. https://doi.org/10.1016/j.eti.2021.101584

SATOSHI HIGASHIKAWA, F., ALBERTO SILVA, C., BETTIOL, W., 2010. Researcher of the Embrapa Environment, Jaguariúna (SP). Fábio Satoshi Higashikawa et al. **R. Bras. Ci. Solo**.

SHARMA, S.B., SAYYED, R.Z., TRIVEDI, M.H., GOBI, T.A., 2013. Phosphate solubilizing microbes: Sustainable approach for managing phosphorus deficiency in agricultural soils. **Springerplus.** https://doi.org/10.1186/2193-1801-2-587

SHEN, J., YUAN, L., ZHANG, J., LI, H., BAI, Z., CHEN, X., ZHANG, W., ZHANG, F., 2011. Phosphorus dynamics: From soil to plant. **Plant Physiol** 156, 997–1005. https://doi.org/10.1104/pp.111.175232

TOMCZYK, A., SOKOŁOWSKA, Z., BOGUTA, P., 2020. Biochar physicochemical properties: pyrolysis temperature and feedstock kind effects. **Rev Environ Sci Biotechnol**. https://doi.org/10.1007/s11157-020-09523-3

TSAI, C.C., CHANG, Y.F., 2021. Quality evaluation of poultry litter biochar produced at different pyrolysis temperatures as a sustainable management approach and its impact on soil carbon mineralization. **Agronomy** 11. https://doi.org/10.3390/agronomy11091692

XU, G., ZHANG, Y., SHAO, H., SUN, J., 2016. Pyrolysis temperature affects phosphorus transformation in biochar: Chemical fractionation and 31P NMR analysis. **Science of the Total Environment** 569–570, 65–72. https://doi.org/10.1016/j.scitotenv.2016.06.081

ZHANG, J., LIU, J., LIU, R., 2015. Effects of pyrolysis temperature and heating time on biochar obtained from the pyrolysis of straw and lignosulfonate. **Bioresource Technology** 176, 288–291. https://doi.org/10.1016/j.biortech.2014.11.011

ZHAO, L., ZHENG, W., MAŠEK, O., CHEN, X., GU, B., SHARMA, B.K., CAO, X., 2017. Roles of Phosphoric Acid in Biochar Formation: Synchronously Improving Carbon Retention and Sorption Capacity. **Journal of Environmental Quality** 46, 393–401. https://doi.org/10.2134/jeq2016.09.0344

CHAPTER I

Magnesium-enriched poultry manure enhances phosphorus bioavailability in biochars

Submitted to Chemosphere Journal

Aline do Amaral Leite[1]; Leônidas Carrijo Azevedo Melo[1]; Luis Carlos Colocho Hurtarte[2]; Lucia Zuin[3]; Cristiano Dela Piccolla[4]; Don Werder[5]; Itamar Shabtai[6]; Johannes Lehmann[7,8,9*]

[1]Federal University of Lavras/UFLA - Soil Science Dept., 37200-900, Lavras, Brazil.

[2]European Synchrotron radiation Facility/ESRF – Grenoble, France.

[3]Canadian Light Source/CLS – Saskatoon, Canada.

[4]University of Western Santa Catarina/UNOESC, Brazil.

[5]Cornell Center for Materials Research, Cornell University, Ithaca, NY 14850, USA.

[6]Department of Environmental Science and Forestry, The Connecticut Agricultural. Experiment Station, New Haven, CT, 06511, USA.

[7]Soil and Crop Sciences, School of Integrative Plant Science, Cornell University, Ithaca, NY 14850, USA.

[8]Department of Global Development, Cornell University, Ithaca, NY 14850, USA.

[9]Cornell Atkinson Center for Sustainability, Cornell University, Ithaca, NY 14850, USA

[*]Corresponding author: cl273@cornell.edu

Highlights

1. Phosphorus availability increases in Mg-enriched biochar up to high pyrolysis temperatures
2. OH^- anions provided with $Mg(OH)_2$ could be a mechanism by which Mg-doped biochars have higher P availability
3. Adding Mg to poultry manure decreased the formation of Ca-P minerals in low temperatures

Abstract
Pyrolysis of calcium-rich feedstock (e.g., poultry manure) generates semi-crystalline and crystalline phosphorus (P) species, compromising its short-term availability to plants. However, enriching poultry manure with magnesium (Mg) before pyrolysis may improve the ability of biochar to supply P. This study investigated how increasing the Mg/Ca ratio and pyrolysis temperature of poultry manure affected its P availability and speciation. Mg enrichment by ~2.1% increased P availability (extracted using 2% citric and formic acid) by 20% in Mg-biochar at pyrolysis temperatures up to 600 °C. Linear combination fitting of P K-edge XANES of biochar, and Mg/Ca stoichiometry, indicate that P species, mainly Ca-P and Mg-P, are altered after pyrolysis. At 300 °C, adding Mg as magnesium hydroxide [$Mg(OH)_2$] created $MgNH_4PO_4$ (18%) and $Mg_3(PO_4)_2.8H_2O$ (23%) in the biochar, while without addition of Mg $Ca_3(PO_4)_2$ (11%) predominated, both differing only for pyrophosphate, 33 and 16%, respectively. Similarly, the P $L_{2,3}$ edge XANES data of biochar made with Mg were indicative of either $MgHPO_4.3H_2O$ or $Mg_3(PO_4)_2.8H_2O$, in comparison to $CaHPO_4.2H_2O$ or $Ca_3(PO_4)_2$ without Mg. More importantly, hydroxyapatite [$Ca_5(PO_4)_3(OH)$] was not identified with Mg additions, while it was abundant in biochars produced without Mg both at 600 (12%) and 700 ºC (32%). The presence of Mg formed Mg-P minerals that could enhance P mobility in soil more than Ca-P, and may have resulted in greater P availability in Mg-enriched biochars. Thus, a relatively low Mg enrichment can be an approach for designing and optimize biochar as a P fertilizer from P-rich excreta, with the potential to improve P availability and contribute to the sustainable use of organic residues.

Key words: linear combination; P speciation; P extractions; nutrient recycling.

1. Introduction

Phosphorus (P) is a non-renewable plant nutrient that requires efficient management to ensure its supply for global agriculture. To reduce mining of P resources, adding new P to agroecosystems, and, consequently, polluting the environment and causing P scarcity, acquiring an efficient cycle in agricultural systems is mandatory (Tilman et al., 2001). In tropical soils, P is one of the most limiting nutrients. Therefore, soils receive large amounts of P fertilization with soluble phosphate fertilizers (Roy et al., 2016) to compensate for strong adsorption to iron and aluminum oxides and low-activity clay minerals (Abdala et al., 2012; Lopes and Guilherme, 2016; Roy et al., 2016). One proposed solution is to use P from excreta, thereby on the one hand reducing environmental pollution, and on the other hand recycling phosphate fertilizer resources. However, comparatively little information is available on high-performance P fertilizers made from wastes and specifically excreta.

Producing P-rich biochars through pyrolysis may enhance plant P use efficiency in P fixing soils as compared to highly water-soluble P sources (Lustosa Filho et al., 2019). Biochar is a byproduct obtained by thermochemical decomposition of organic feedstocks within a range of pyrolysis temperatures typically between 400 and 800 °C and under low or no oxygen conditions (Ippolito et al., 2015). For woody feedstocks, the resulting carbon-rich product improves soil physical and chemical properties, such as increased soil pH, greater cation exchange capacity, and greater water-holding capacity (Glaser et al., 2002; Ippolito et al., 2015; Joseph et al., 2021). Accordingly, many studies report its use as a soil conditioner rather than as a fertilizer with high agronomic performance. Animal-based organic waste is one of the most promising feedstocks for production of biochars and are mainly used for their value as nutrient amendments. These wastes are extensively generated as they are a part of the protein food chain (Akdeniz, 2019), and need to be processed prior to proper land application. Poultry manure is generated in large amounts and is rich in plant nutrients, especially P, with P contents ranging from 1.2-1.8% (dry weight basis) (Darby et al., 2016; Suleiman et al., 2018). Its transformation into biochar can be an efficient way to sanitize the manure, while maintaining or even increasing plant availability of P (Carneiro et al., 2018; Rehman et al., 2020). Transforming animal waste into biochar has proven to be an effective method to mitigate environmental contamination not only of pathogens but also of hormones, antibiotics, microplastics, PFAS etc. (Kyakuwaire et al., 2019; Sauvé et al., 2016). It is less known

whether and under what conditions pyrolysis is also effective in producing a high-efficiency fertilizer (Buss et al., 2020).

The most important parameters controlling the physicochemical and morphological properties of biochars are changes in highest heating temperature and holding time (Enders et al., 2012; Ippolito et al., 2020). The chemical composition of poultry manure is to a large extent dominated by calcium carbonate that is present in poultry diets resulting in a high Ca concentration in manure and consequently a low Mg/Ca ratio (Higashikawa et al., 2010). Its conversion into biochar might form stable Ca-P minerals, and a significant P fraction would become unavailable to plants (Bruun et al., 2017). However, because Mg is a smaller ion than Ca, its incorporation in the manure may cause structural changes, such as destabilization and decomposition of the structure including P species during the heating treatment process (Farzadi et al., 2014; Kannan et al., 2005). A partial substitution of Ca by Mg in synthetic hydroxyapatite production strongly inhibits the crystallinity of phosphates after thermal degradation (Cao and Harris, 2008; Hilger et al., 2020). Little information is available as to the effect of Mg on the water solubility and plant availability of P in biochar made from P-rich excreta or specifically poultry manure.

Therefore, the objectives of this study were (1) to determine how increasing Mg/Ca ratios and highest heating temperature affect biochar-P solubility and crystallinity; (2) to assess changes in P forms in biochar with Mg enrichment, and (3) to elucidate the mechanisms controlling P availability in Mg-enriched biochar and its potential as a fertilizer. We hypothesize that (1) higher ratios of Mg/Ca results in higher P solubility in biochar relevant to plant P uptake; and (2) the addition of Mg decreases the formation of tricalcium phosphate and reduces proportions of crystalline P forms.

2. Materials and methods

2.1. Biomass and Pyrolysis Conditions

Poultry manure was obtained from the experimental poultry farm at Cornell University collected over the course of several days, using commercial feed containing mostly corn, soybean, wheat, calcium carbonate, salt, choline chloride, yeast extract and mono-dicalcium phosphate [$Ca(H_2PO_4)_2$]. Poultry manure feedstock was oven-dried at 70 ºC until constant mass, ground, and sieved (< 850 µm) before pyrolysis. All biochars were produced in an adapted laboratory-scale muffle furnace, and the process was performed with a heating rate of 10 ºC min^{-1} to their target

temperature (300 ºC, 500 ºC, 600 °C, or 700 ºC), with a holding time of 30 min and left to slowly cool down to room temperature. At the end of each cycle, the biochar yield was recorded.

2.2. Feedstock modification

After drying, the poultry manure was pyrolyzed to produce biochar. Before pyrolysis, some of the poultry manure was pre-treated with magnesium hydroxide [$Mg(OH)_2$] to generate Mg-enriched biochar. This source of Mg was selected after tests with other sources (i.e., chloride and sulfate), as it contained no interfering counter-ions (Table S1). Briefly, $Mg(OH)_2$ was mixed with the manure to achieve Mg/Ca ratios of 0.08, 0.10, 0.12, 0.16 and 0.20, soaked in deionized water (1:10, solid-liquid ratio), and stirred with a magnetic ball for 30 min. The mixture was oven-dried at 70 ºC (until constant mass) (Zhang et al., 2012).

2.3. Characterization of feedstock and biochars

All samples were crushed with a mortar and pestle and sieved to a thin powder (< 0.25 μm) prior to analyses. Electrical conductivity (EC) and pH were measured in a suspension of 1:20 (w:v) ratio in deionized water, which was first shaken for 90 min on a reciprocal shaker, and measured using a pH and an EC meter (Rajkovich et al., 2012).

Biochars and manure samples were analyzed for total Ca, Mg, and P contents according to Enders and Lehmann (2012). Briefly, 0.20 g of each sample was ashed in a small muffle furnace for eight hours at 500 °C. It was then digested in concentrated nitric acid (70%) at 120 °C, and for the final digestion step, hydrogen peroxide (30%) was added to accelerate the oxidation of organic carbon. Finally, the samples were diluted to a 2% nitric acid (v/v) solution. Contents were filtered, and elements were measured by inductively coupled plasma spectrometry (ICP, Thermo iCAP 6500 series, Thermo Fisher Scientific, Massachusetts, USA).

Total carbon, hydrogen, oxygen and nitrogen were determined on a Thermo Delta V isotope ratio mass spectrometer (IRMS) interfaced with an NC2500 elemental analyzer. Standards were calibrated against international reference materials provided by the International Atomic Energy Association (IAEA). Ash content from biochars was determined by oven drying (105 °C), and then, heating the samples in open crucibles at 750 °C for 6 hours. The specific and external surface area (BET) and the total pore volume (TPV) were determined by BET-N_2 and the CO_2 sorption

techniques. The surface morphological structures, images, and elemental mapping were obtained with high-resolution scanning electron microscopy (MIRA3 FESEM, Tescan, Pennsylvania, USA), equipped with energy-dispersive spectroscopy (EDS), and the EDS spectra collected on a Bruker 6-60 XFlash detector (Bruker, Massachusetts, USA) after mounting samples on a standard SEM stub using carbon tape. The surface functional groups composition was studied using FTIR spectroscopy (Vertex V80V Vacuum FTIR system, Bruker, Massachusetts, USA) in attenuated total reflectance (ATR) mode. The samples were placed in the sample holder and spectra were collected with a spectral range of 4000−600 cm^{-1}, with a resolution of 4 cm^{1}, averaged over of 64 scans, and processed for baseline correction using OPUS v7.2 (Bruker, Massachusetts, USA).

2.4. Phosphorus extractions

Poultry manure and biochar samples were analyzed for plant-available P using 2% formic acid and 2% citric acid extractions at a ratio of 1:100 (w/v). The samples were shaken with the extractant for 30 min and filtered through qualitative filter paper (Wang et al., 2012). Water-soluble P was extracted by shaking the samples with deionized water for 16 h, at a ratio of 1:150 (w/v), and filtering through qualitative filter paper (Zwetsloot et al., 2015). For all extractions, P concentration was determined using the molybdenum blue method, adapted from Murphy and Riley (1962). Briefly, P concentration in samples was determined by UV-vis spectrophotometry (Shimadzu, Kyoto, Japan) measuring the intensity of the color from the formation of a phospho-molybdic complex (660 nm) produced by the reaction of ammonium molybdate and ascorbic acid according to P concentration in samples.

2.5. Kinetics of P release

Samples of pyrolyzed and unpyrolyzed manure, with and without $Mg(OH)_2$ addition, were selected to determine the kinetics of P release in water. Briefly, samples were mixed with deionized water in a proportion of 1/200 ratio (w/v) and then shaken at 120 rpm for 240 h, and sampled after 0.25, 0.5, 1, 6, 12, 24, 48, 72, 120, and 240 h. The samples were filtered through qualitative filter paper and analyzed for P using the molybdenum blue method (Murphy and Riley, 1962). The P release kinetics was determined by the changes in P concentrations over the sampling time and then fitted to the following models: parabolic diffusion model, Elovich equation, power function, first order, and second-order functions (Carneiro et al., 2021; Liang et al., 2014). The fit of each

mathematical model was based on its standard error of the estimative (SE) (Carneiro et al., 2021; Shariatmadari et al., 2006), and the best models were chosen based on the Akaike information criterion (AIC) (Akaike, 1974).

2.6. X-ray absorption near edge spectroscopy (XANES)

The P K-edge XANES analysis was carried out at the IDEAS beamline at the Canadian Light Source (CLS) (Saskatoon, Canada). Fluorescence spectra were collected under vacuum using a Vortex ME4 SDD with FalconX electronics. Samples were loaded in sample holders in the pre-chamber. Information for reference P compounds was obtained from the following sources: magnesium phosphate dibasic ($MgHPO_4.3H_2O$, CAS 7782-75-4, Sigma Aldrich), tricalcium phosphate and calcium phosphate dibasic [$Ca_3(PO_4)_2$ and $CaHPO_4.2H_2O$, respectively, (dela Piccolla et al., 2021)], trimagnesium phosphate, struvite, octacalcium phosphate, pyrophosphate, lecithin, hydroxyapatite and phosphate adsorbed on Pahokee peat [$Mg_3(PO_4)_2.8H_2O$, $MgNH_4PO_4$, $Ca_8H_2(PO_4)_6.5H_2O$, P_2O_7, organic-complexed P-Fe, 1200 mmol Kg^{-1} of Fe and $Ca_{10}(PO_4)_6(OH)_2$, respectively, (Beauchemin et al., 2003; Hesterberg et al., 2017)]. Samples were collected in the energy range of 2085 to 2245 eV, scanned twice, and checked for reproducibility. The E_0 was set to 2151 eV and energy step sizes were 5 eV from 2085 to 2135 eV, 0.2 eV from 2135 to 2175 eV, 2 eV from 2175 to 2245 eV. The program Athena v0.9.26 (Ravel and Newville, 2005) was used for data processing and analysis of the P K-edge XANES spectra. Data were normalized, pre-edge and post-edge energy regions were set to -65 to -10 eV and 30 to 60 eV, respectively. Linear combination fitting was performed over the spectral region and above the P adsorption edge (2145 – 2180 eV). Reported fits were obtained using a modified standard elimination procedure (Hesterberg et al., 2017; Manceau et al., 2012), progressively reducing the number and combinations of standards until reaching a higher accuracy model (coefficients > 5% and R factor <0.05). For the final set, a maximum of five standards was allowed for each fit, and an energy shift of up to ± 0.5 eV was allowed for the standards individually.

P $L_{2,3}$-edge XANES analyses were carried out at the Variable Line Spacing Plane Grating Monochromator (VLS-PGM) beamline at the Canadian Light Source. Despite the similarities with K-edge XANES, scanning the absorption from $L_{2,3}$-edge provides more detailed information on species and mineral ordering because of more possible electron transitions and distinguishable features (Kruse et al., 2009; Liu et al., 1992). However, both techniques complement each other.

While K-edge provides information on bulk properties of the samples, L-edge, due to its low energy and, thus, lower penetration of the incident beam, is restricted to the surface of the analyzed sample (Bruun et al., 2017). The spectra were collected in total fluorescence yield mode (FLY), using a microchannel plate detector and total electron yield (TEY) mode measuring the sample drain current. For normalization purpose, the incident beam current was measured with a Ni mesh located upstream the sample. Scans were performed in triplicates from 130 to 155 eV, with step sizes of 0.1 eV and 1s of dwell time. Merged data were subtracted from a linear background adjusted at an energy level between 130 to 135 eV, followed by extended multiplicative scatter correction and normalization to the peak at 139 eV using Unscrambler X software v10.5.1 (CAMO Software AS, Oslo, Norway). For consistently determining peak positions, peaks were found using Origin Pro v9.90 (Originlab Corp, Massachusetts, USA).

2.7. X-ray Diffraction (XRD)

Poultry manure and biochar samples were analyzed by X-ray diffraction analysis (XRD) to detect crystalline phases. This technique allows the identification of the degree of crystallinity of the samples. Due to the crystallite size of the samples, XRD analyses were carried out at the beamline ID13 of the European Synchrotron Radiation Facility (ESRF). The beamline ID13 is an undulator beamline dedicated to high-lateral-resolution diffraction and scattering experiments using focused monochromatic X-ray beams (Riekel et al., 2010). Samples were ground, sieved to form a powder suspension, deposited on a SiN3 membrane, and air-dried. The samples were examined by light microscopy to locate regions of interest, consisting of isolated microparticles of biochar. Samples are mounted vertically, perpendicular to the X-ray beam. The energy of the incident beam was chosen around 13.0 keV. The beam was focused to ~2 × 2 μm^2 (flux ~2 × 1012 phs^{-1}, at I = 128 mA electron beam current; attenuated to ~1011 ph s^{-1} by detuning the undulator) using a compound refractive lens set-up (CRL) mounted in a transfocator. X-ray powder diffraction (XRPD) maps were obtained by raster-scanning the samples and collecting 2D XRPD patterns, in transmission, with a Dectris EIGER 4 M single photon counting detector that acquires frames with 2070 × 2167 pixels (75 × 75 μm^2 pixel size) at a rate up to 750 Hz. Azimuthal integration and calculation of crystalline phases by linear fits were performed using dedicated Jupyter Notebooks. For both analytical configurations, the synchrotron diffraction data has been corrected for attenuation effects and processed using the software package PyMCA, region of interest (ROI)

imaging was also used to extract averages and statistical analyses (Solé et al., 2007). Crystalline phases were identified using Match! v2 (Crystal Impact, Bonn, Germany), compared with minerals available at the open crystallography database (COD). The degree of crystallinity was calculated using Origin Pro v9.90 and X'Pert Highscore Plus v3.0.0 (Panalytical, Malvern, UK). The degree of crystallinity of the samples was defined based on the average crystallite size and degree of crystallinity, considering the calculated areas under the peaks and the width at half-height of the diffraction peak.

3. Data analysis

The collected data were checked for normality by the Shapiro–Wilk's test prior to other data analyses. Data were submitted to analysis of variance, and the means of the treatments were clustered by the Scott Knott test ($p \leq 0.05$) to avoid overlapping average results (Scott and Knott, 1974). Data from the kinetics of P release were fitted to nonlinear models using the *nlstools* package (Baty et al., 2015).

4. Results

4.1. Phosphorus availability

The extractable P portion from unpyrolyzed poultry manure was, on average, 25% lower than in any biochar regardless of Mg/Ca ratio (Figure 1). Comparing pyrolysis temperatures, at the lowest (300 °C) and highest (700 °C), the range of formic and citric-P was higher than unpyrolyzed biomass, 27 and 23% for biochar (Mg/Ca of 0.08), and 46 and 17% for Mg-biochar (Mg/Ca ratio of 0.16), respectively (Figure 1 a and b). Across pyrolysis temperatures ranging from 300 to 600 °C, adding Mg resulted in higher P availability (except for a Mg/Ca ratio of 0.2) (Figure S2). At 300 °C, citric and formic acid extracted about 16.8 and 16.7 g P kg^{-1} biochar, representing approximately 96 and 94% of the total P when Mg was added. The extractions were significantly lower for biochar without Mg additions, about 14.4 and 13.6 g kg^{-1}, representing about 73 and 70% of total P. With increasing pyrolysis temperature, the effect of $Mg(OH)_2$ addition on extractable P is positive up to 600 °C, with formic-P extractable P of 19.6 g kg^{-1} (90% of total P), and of 15.8 g kg^{-1} (68% of total P) with and without added Mg, respectively. At 700 °C, however, the amounts of formic acid-extractable P were very similar, about 69 and 71% of total P, respectively.

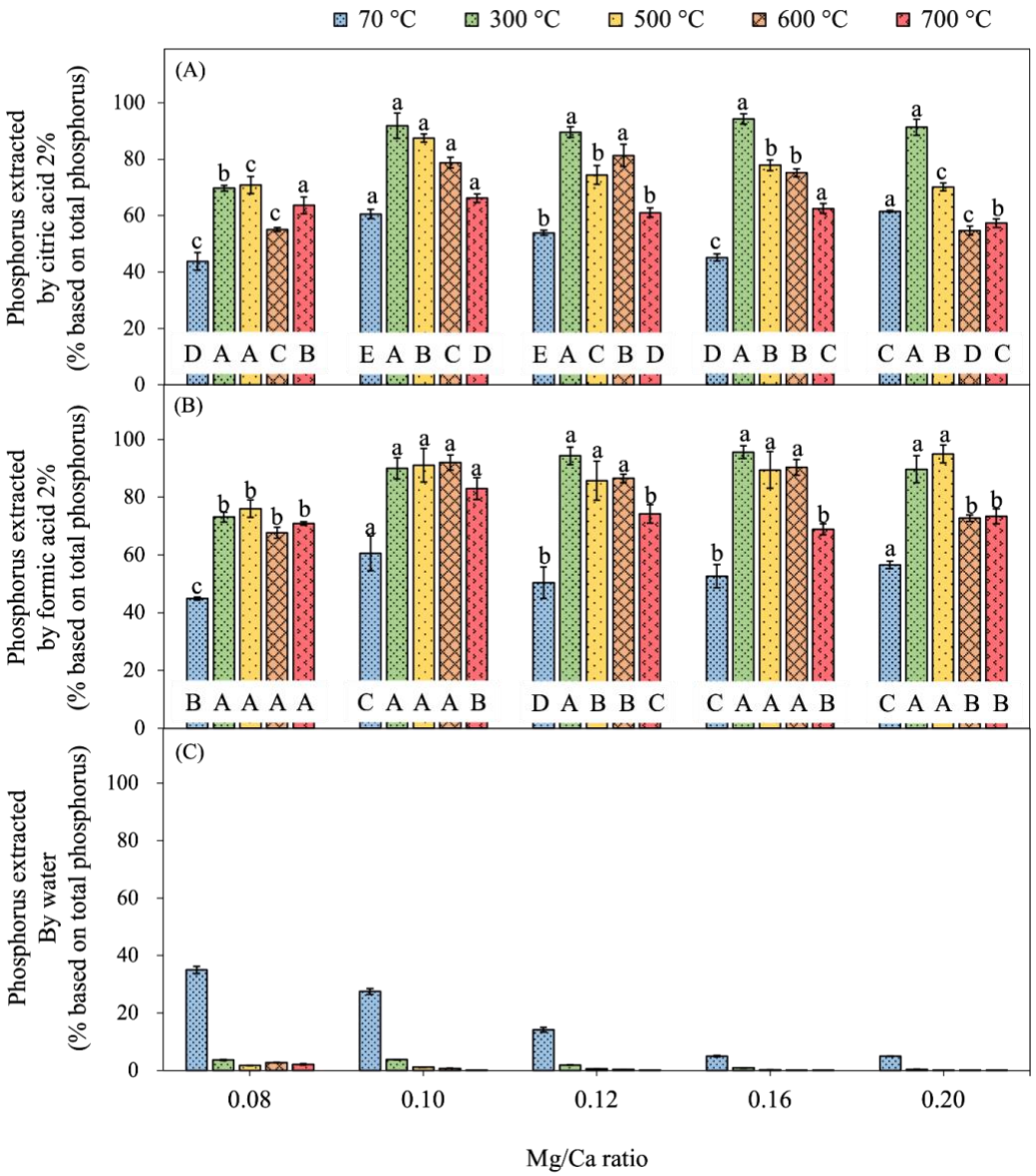

Figure 1. Phosphorus extracted by citric acid 2% (A), formic acid 2% (B) and water (C) as a function of Magnesium hydroxide modified biochars and magnesium and calcium ratios. Lowercase letters compare each temperature in all Mg/Ca ratio, and uppercase letters compare all Mg/Ca ratio in each temperature, the means of the treatments were grouped by the Scott Knot test ($p < 0.05$). Mean values ± standard deviation; n=3. The extractable portion in grams per kilogram and percentage are referenced in Table S2.

Water-extractable P, however, decreased as a function of pyrolysis temperature and even more as a function of Mg addition (Figure 1c). For unpyrolyzed biomass, at a Mg/Ca ratio of 0.08,

water extracted 3.8 g kg^{-1} (35% of total P), and for a Mg/Ca ratio of 0.16, only 0.5 g kg^{-1} (5% of total P). At 300 °C, water-P was even lower for both biochar and Mg-biochar, 0.7 and 0.2 g kg^{-1} (3.7 and 0.9% of total P, respectively).

4.2. Kinetics of phosphorus release

The kinetics of P release from poultry manure pyrolyzed at 300 °C was initially greater than that of unpyrolyzed poultry manure (Figure 2). However, P release from unpyrolyzed poultry manure did not stabilize at the end of the assay (240 h). Most importantly, Mg additions decreased P release, and more so for pyrolyzed than unpyrolyzed manure. Adding Mg to unpyrolyzed manure decreased P release by 36% of total P, from 5.36 to 3.45 g kg^{-1} in 72 h. At 300 °C, Mg addition had the greatest effect, decreasing P release from 67% to 3% of total P over the entire sampling period. In contrast, biochar and Mg-biochar at 500 °C had a low P release of 4.6 and 1% of total P, respectively (fitting parameters in Table S3).

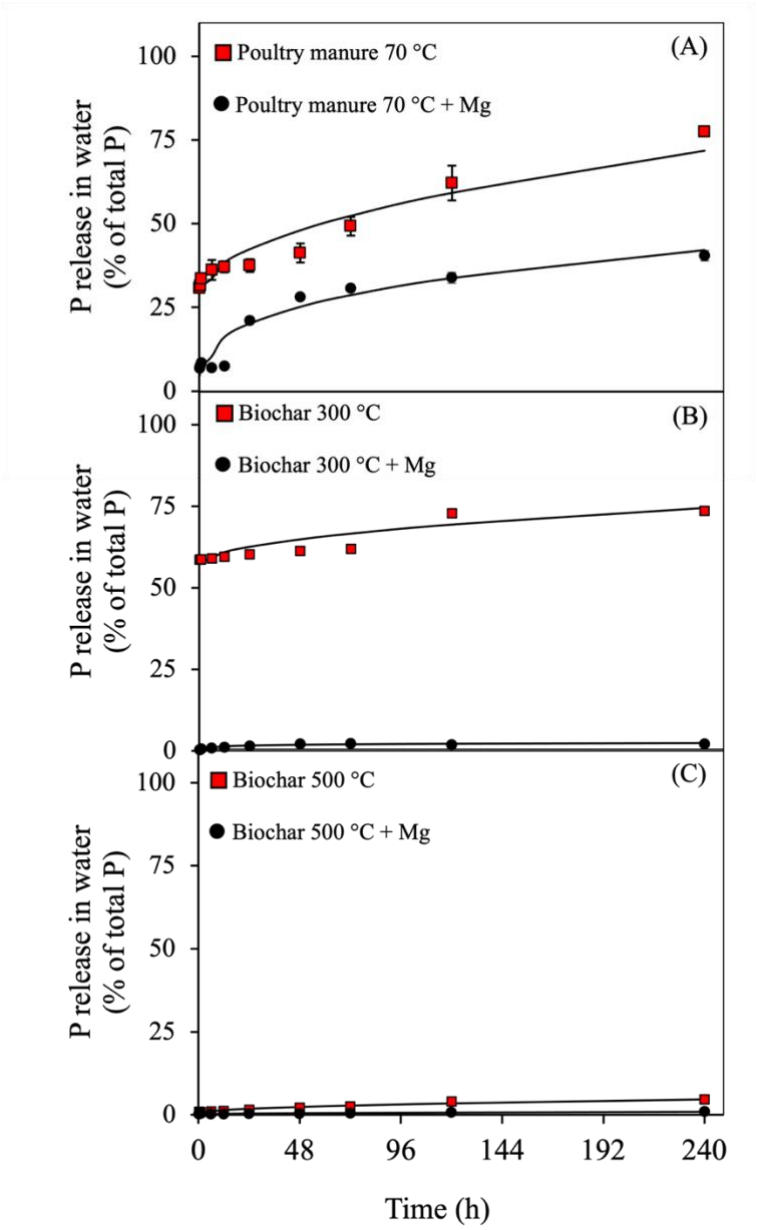

Figure 2. Kinetics of phosphorus release in water of poultry manure and biochars (Mg/Ca: 0.08) and poultry manure and biochars plus magnesium (Mg/Ca: 0.16). Mean value ± standard deviation, n = 3. Poultry manure and biochars at 70, 300 and 500 °C fitted to parabolic diffusion model; poultry manure and biochars plus magnesium at 70, 300 and 500 °C fitted to power function, Elovich equation and parabolic diffusion model, respectively. Parameters of the examined models are shown in Table S3.

4.3. Phosphorus K and $L_{2,3}$ edge XANES spectroscopy

K edge XANES spectra (Figure 3 A and B) and the linear combination fitting of P K-edge XANES of biochar and Mg-biochar data indicates that Ca-P and Mg-P species are mainly altered

after pyrolysis, with few differences whether or not Mg was added to the unpyrolyzed biomasses (70 °C) (Table 1 and Figure S1). The P minerals for biomass were $Mg_3(PO_4)_2.8H_2O$ (35.9 and 41.6%), $CaHPO_4.2H_2O$ (16.6 and 23.9%), P-Fe (12.5 and 9.3%), and organic P as lecithin (35.0 and 25.2%) without and with Mg addition, respectively. The Fe-P only appeared for unpyrolyzed biomasses, and lecithin appeared at up to 300 °C only without Mg additions (9.0%). Also, at all pyrolysis temperatures, biochar and Mg-biochar had similar proportions of $CaHPO_4.2H_2O$ and octacalcium phosphate. However, at 300 °C, only Mg-biochar had $MgNH_4PO_4$ (17.9%) and $Mg_3(PO_4)_2.8H_2O$ (23.0%), while biochar without Mg showed $Ca_3(PO_4)_2$ (10.4%), both differing only for pyrophosphate, 32.9 and 16.0%, respectively. Biochars made at temperatures of 500 and 600 °C had similar P compounds but differed whether or not Mg was added. For biochars made at 500 and 600 °C, biochar without Mg showed pyrophosphate (29.8 and 14.0%) and hydroxyapatite (not identified and 12.5%), while Mg-doped biochar showed $Mg_3(PO_4)_2.8H_2O$ (10.4 and 11.2%). At 700 °C, biochar without Mg showed hydroxyapatite (32.5%) and pyrophosphate (15.7%), and Mg-doped biochar showed $Mg_3(PO_4)_2.8H_2O$ (5.2%).

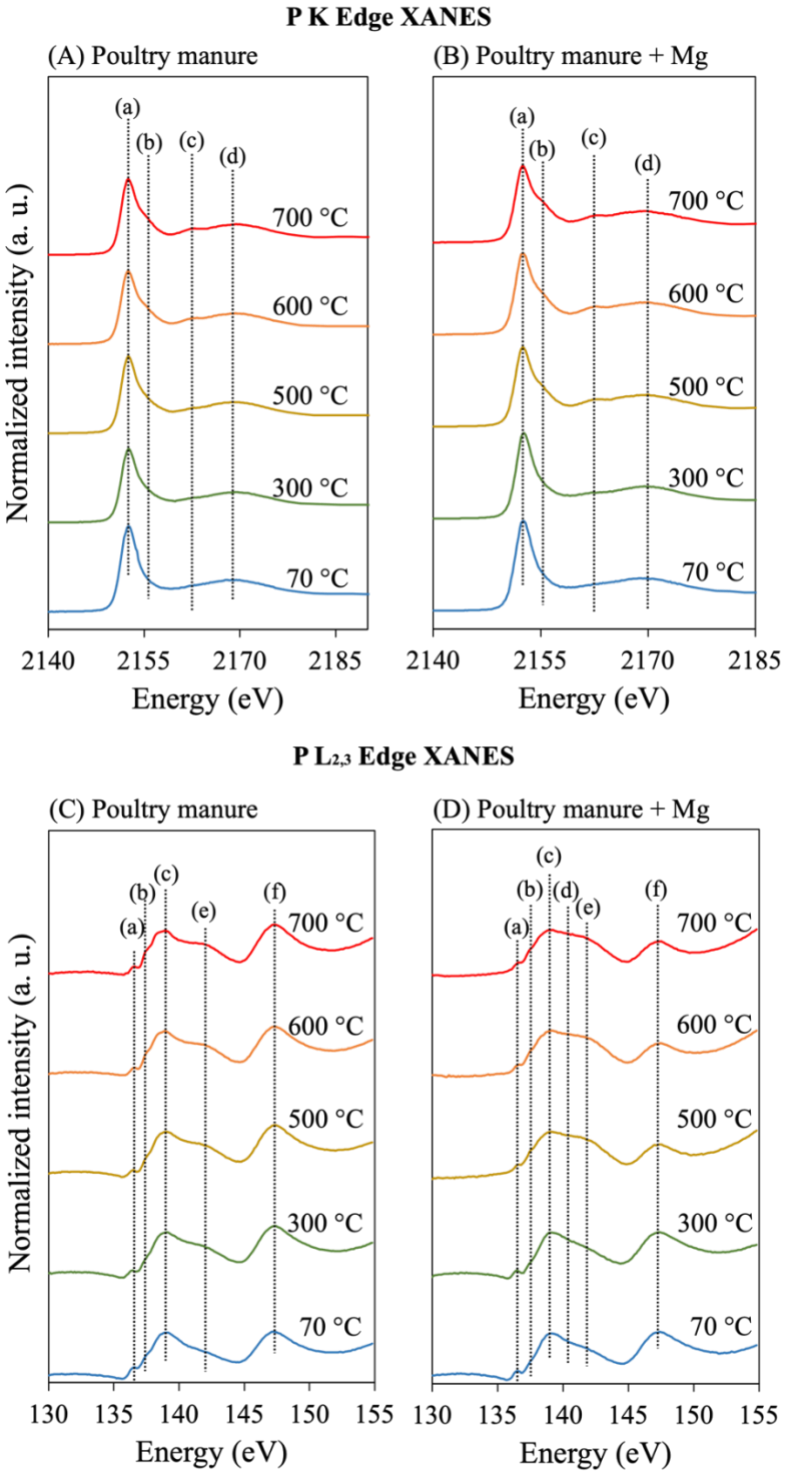

Figure 3. Phosphorus K-edge (A, B) and $L_{2,3}$ edge (C, D) XANES spectra of unmodified (Mg/Ca: 0.08) and $Mg(OH)_2$ added (Mg/Ca: 0.16) poultry manure and biochars. The dotted lines indicate energy levels of spectral features from unique P species. Overlaid linear combination fitting for P

K edge in Figure S1. Energy position for $L_{2,3}$ edge in Table S4. Spectra for P compounds in supplementary in Figure S2.

Table 1. Major phosphorus species determined by linear combination fitting of XANES spectra of standards (Figure S1) to XANES spectra of biochar of different temperatures with and without magnesium enrichment.

Samples	$MgNH_4PO_4$	$Mg_3(PO_4)_2$	$CaHPO_4$	$Ca_3(PO_4)_2$	OCP	HAP	PYP	P-Fe	Lecithin	R factor
		%								
Poultry manure	-	35.9	16.6	-	-	-	-	12.5	35.0	0.0008
Poultry manure 70 °C + Mg	-	41.6	23.9	-	-	-	-	9.3	25.2	0.0008
Biochar 300 °C	-	-	18.4	10.6	29.2	-	32.9	-	9.0	0.0003
Biochar 300 °C + Mg	17.9	23.0	16.9	-	26.4	-	15.8	-	-	0.0004
Biochar 500 °C	-	-	21.7	8.7	39.7	-	29.8	-	-	0.0007
Biochar 500 °C + Mg	-	10.4	23.8	27.6	38.2	-	-	-	-	0.0005
Biochar 600 °C	-	-	23.7	20.7	28.8	12.5	14.3	-	-	0.0005
Biochar 600 °C + Mg	-	11.2	22.0	26.7	40.0	-	-	-	-	0.0005
Biochar 700 °C	-	-	-	12.2	39.6	32.5	15.7	-	-	0.0004
Biochar 700 °C + Mg	-	5.2	22.9	37.3	34.6	-	-	-	-	0.0007

Note: OCP, Octacalcium phosphate; HAP, Hydroxyapatite; PYP, Pyrophosphate; P-Fe, phosphate adsorbed on Pahokee peat

The P $L_{2,3}$ edge XANES data indicate that Mg-biochar presented a shoulder feature at around 139.7 – 140 eV, which could be either $MgHPO_4.3H_2O$ or $Mg_3(HPO_4).8H_2O$ (Figure 3 C and D and Table S4). The biochars without Mg addition do not have this Mg-P feature, and even without Mg, they already have a shoulder with a center at 141.7 – 141.9 eV attributed to $CaHPO_4.2H_2O$ or $Ca_3(PO_4)_2$, more intensely at higher pyrolysis temperatures. These Ca-peaks also appear when Mg is added, but only from 500 °C onwards, with no intense features observed at 300 °C, similar to unpyrolyzed biomass. For all samples, two primary peaks described P features at the energy position at around ~139 and ~147 eV.

4.4 SEM-EDS and BET surface area

The elemental mapping by SEM revealed a uniform distribution of P and Mg (Figure 4A) and concentrated Ca spots on the surface of biochars irrespective of Mg additions. Phosphorus is distributed on the surface similarly to Mg. The biochar has a smooth surface with evenly-spread round features, quantified by EDS spectra to have a high concentration of Ca (Table S5). In contrast, features with different spatial patterns were observed in Mg-biochar, such as cubes, flakes, and blocks (Figure 4B). These patterns have high concentrations of Mg as quantified by EDS (Table S5).

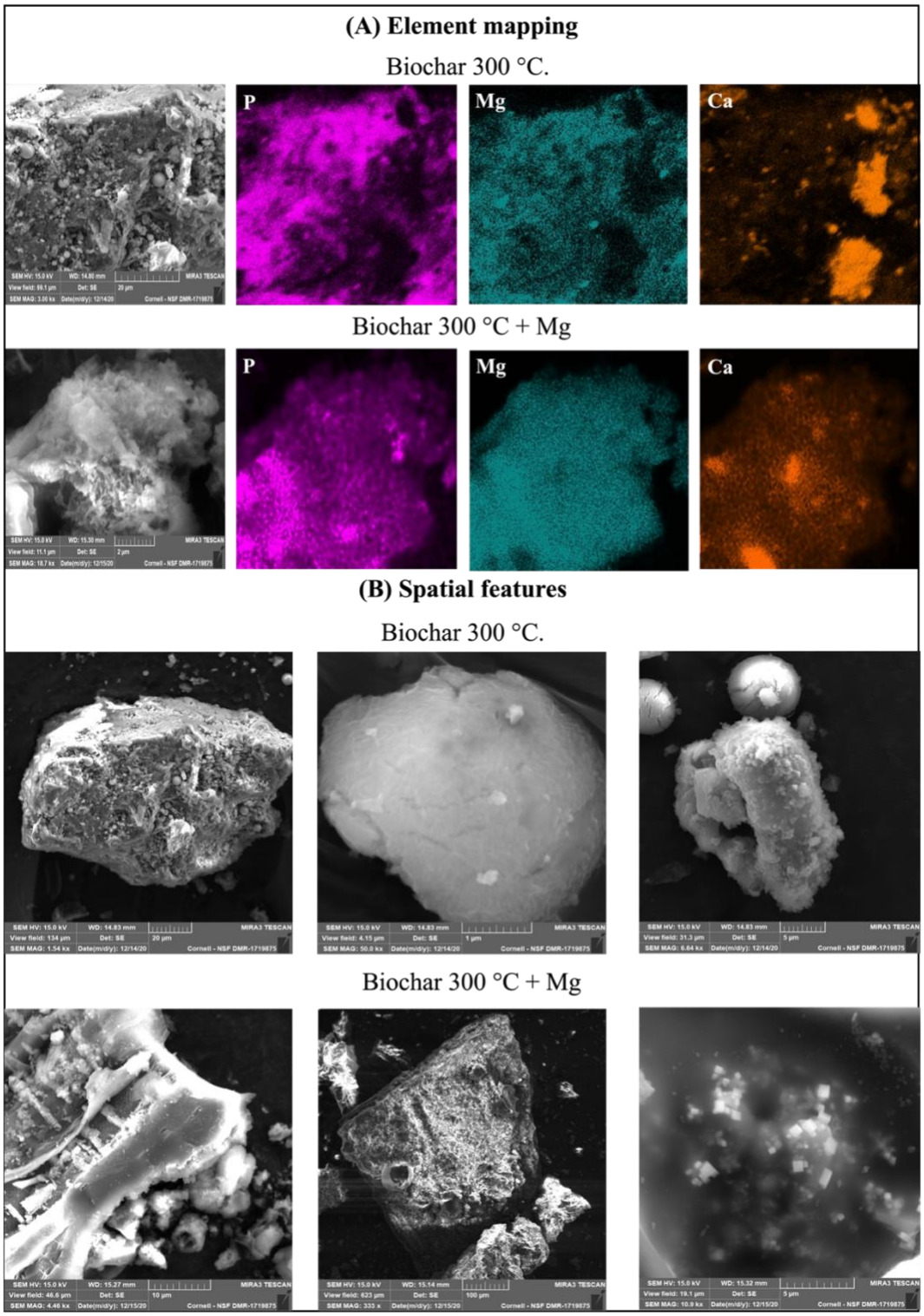

Figure 4. Scanning electron microscopy (SEM) of biochars with and without Mg additions prior to pyrolysis. (A) Images of biochar pyrolyzed at 300 °C with and without Mg addition (B) Spatial features of biochar pyrolyzed at 300 °C with and without Mg addition**.** Energy-dispersive spectroscopy (EDS) elemental quantification in Table S5 and Figure S3.

The BET surface area analysis (Table S6) indicates that biochar and Mg-biochar possess a non-porous and low-porous morphology. The BET surface area decreased by Mg additions from 3.16 and 2.43 m^2/g to a non-porous condition at 500 °C and 600 °C, respectively. The total pore volume decreased by Mg additions from 9.7 and 0.84 $cm^3\ kg^{-1}$ to undetected at 500 °C and 600 °C, respectively. At both low (300 °C) and high (700 °C) pyrolysis temperatures, biochar and Mg-biochar had low porosity and surface area that did not increase after additions of Mg.

4.5. Elemental analysis

Total P concentrations increased in Mg-biochar at high pyrolysis temperatures but decreased at low temperatures (Table 2). For instance, at 300 °C, total P from biochar without Mg addition (Mg/Ca ratio 0.08) decreased from 19.6 to 17.5 $g\ kg^{-1}$ when Mg was added (Mg/Ca ratio 0.16). In contrast, at 700 °C, total P increased from 23.3 to 25.0 $g\ kg^{-1}$, for the same Mg/Ca ratios. Total Mg concentration did not vary substantially as a function of pyrolysis temperature (Table 2). However, on average, the Mg yield was 2-fold higher than its unpyrolyzed biomass for biochar and only 1.3 higher for Mg-biochar.

Table 2. Properties of magnesium hydroxide modified poultry manure and biochar as a function of magnesium and calcium ratios.

Mg/Ca Ratio	T (°C)	pH	EC (ds m^{-1})	Total P (g kg^{-1})	Total Ca (g kg^{-1})	Total Mg (g kg^{-1})	N (mg g^{-1})	C (mg g^{-1})	H (mg g^{-1})	O (mg g^{-1})	H/C (mol mol^{-1})	O/C (mol mol^{-1})	Ash (mg g^{-1})	Biochar Yield (mg g^{-1})
0.08	70	6.5 ± 0.0	4.1 ± 0.1	10.9 ± 0.3	102.7 ± 1.3	6.5 ± 0.1	41.0 ± 0.8	284.5 ± 3.7	45.0 ± 9.0	364.7 ± 12.3	1.9 ± 0.4	1.0 ± 0.0	-	-
	300	10.6 ± 0.1	3.3 ± 0.1	19.6 ± 0.0	164.4 ± 0.4	12.5 ± 0.2	67.5 ± 0.2	391.7 ± 10.7	22.0 ± 2.4	263.0 ± 31.3	0.7 ± 0.1	0.5 ± 0.0	381.6 ± 22.5	570.0 ± 26.5
	500	11.3 ± 0.1	3.7 ± 0.1	21.4 ± 0.5	173.4 ± 6.0	13.2 ± 0.3	33.8 ± 0.2	335.4 ± 2.4	8.5 ± 0.1	264.8 ± 1.0	0.3 ± 0.0	0.6 ± 0.0	477.4 ± 30.5	503.3 ± 5.8
	600	11.7 ± 0.0	4.1 ± 0.2	23.1 ± 2.6	169.1 ± 0.6	13.3 ± 0.1	25.5 ± 0.2	296.5 ± 8.0	6.3 ± 0.7	253.0 ± 1.5	0.3 ± 0.0	0.6 ± 0.0	473.1 ± 4.6	486.7 ± 05.8
	700	11.9 ± 0.0	4.8 ± 0.1	23.3 ± 0.8	178.5 ± 0.9	13.5 ± 0.4	27.0 ± 1.2	313.4 ± 12.3	3.6 ± 0.7	226.1 ± 19.2	0.1 ± 0.0	0.5 ± 0.1	490.3 ±14.5	470.0 ± 10.0
0.10	70	6.4 ± 0.1	4.4 ± 0.1	11.1 ± 0.4	103.9 ± 3.9	9.9 ± 0.0	60.7 ± 6.1	330.0 ± 32.4	40.8 ± 4.7	360.7 ± 20.5	1.5 ± 0.0	0.8 ± 0.0	-	-
	300	11.5 ± 0.0	5.6 ± 0.1	20.1 ± 0.2	167.5 ± 1.3	15.1 ± 0.1	43.5 ± 9.3	301.8 ± 43.6	13.7 ± 0.1	266.3 ± 1.0	0.6 ± 0.1	0.7 ± 0.1	423.9 ± 22.5	566.7 ± 5.8
	500	11.2 ± 0.1	5.8 ± 0.0	23.5 ± 0.9	171.8 ± 2.9	16.8 ± 0.1	30.4 ± 0.0	317.0 ± 6.1	7.5 ± 0.1	247.6 ± 2.7	0.3 ± 0.0	0.6 ± 0.0	534.8 ± 18.4	500.0 ± 20.0
	600	12.4 ± 0.1	7.2 ± 0.0	25.1 ± 0.6	180.8 ± 4.0	17.2 ± 0.3	21.9 ± 2.9	243.4 ± 15.8	4.4 ± 0.1	260.6 ± 6.8	0.2 ± 0.0	0.8 ± 0.0	545.6 ± 14.1	470.0 ± 10.0
	700	12.6 ± 0.0	8.4 ± 0.0	27.3 ± 0.1	195.5 ± 0.2	18.4 ± 0.3	27.0 ± 4.4	257.7 ± 31.5	3.8 ± 0.1	246.3 ± 4.4	0.2 ± 0.0	0.7 ± 0.1	593.2 ± 16.6	416.7 ± 5.8
0.12	70	9.0 ± 0.0	4.9 ± 0.0	10.9 ± 0.3	109.5 ± 2.5	13.2 ± 0.1	33.4 ± 3.5	266.3 ± 20.6	37.2 ± 1.9	352.9 ± 3.8	1.7 ± 0.2	1.0 ± 0.1	-	-
	300	9.8 ± 0.25	3.1 ± 0.2	19.5 ± 0.6	166.2 ± 2.5	19.2 ± 0.1	38.8 ± 4.7	300.5 ± 22.0	13.7 ± 0.6	275.9 ± 4.2	0.6 ± 0.1	0.7 ± 0.0	455.9 ± 17.0	600.0 ± 20.0
	500	11.3 ± 0.1	4.6 ± 0.3	24.2 ± 0.1	176.8 ± 1.3	21.3 ± 0.1	15.9 ± 2.0	239.2 ± 12.7	6.6 ± 0.4	246.3 ± 6.0	0.3 ± 0.0	0.8 ± 0.1	573.8 ± 5.6	513.3 ± 15.3
	600	11.5 ± 0.1	5.6 ± 0.3	22.4 ± 0.7	189.7 ± 6.0	20.7 ± 0.6	14.2 ± 0.7	248.0 ± 13.2	4.8 ± 0.7	259.7 ± 2.6	0.2 ± 0.0	0.8 ± 0.0	537.1 ± 11.4	480.0 ± 34.6
	700	12.0 ± 0.0	5.5 ± 0.1	25.9 ± 0.5	180.0 ± 2.3	23.7 ± 0.3	22.7 ± 1.0	250.0 ± 3.7	4.1 ± 0.4	258.1 ± 1.7	0.2 ± 0.0	0.8 ± 0.0	534.3 ± 8.1	493.3 ± 5.8
0.16	70	9.3 ± 0.0	5.7 ± 0.2	11.2 ± 0.1	106.1 ± 0.4	20.8 ± 0.1	45.3 ± 4.0	309.2 ± 18.9	38.0 ± 0.5	366.5 ± 4.7	1.5 ± 0.1	0.9 ± 0.0	-	-
	300	11.1 ± 0.0	4.5 ± 0.2	17.5 ± 0.6	158.5 ± 4.5	25.5 ± 0.3	38.2 ± 0.9	296.7 ± 7.5	17.6 ± 2.8	302.9 ± 9.6	0.7 ± 0.1	0.8 ± 0.0	456.2 ± 10.2	586.7 ± 25.2
	500	12.1 ± 0.0	6.1 ± 0.2	21.9 ± 0.1	178.0 ± 1.3	27.5 ± 0.0	17.5 ± 0.5	231.9 ± 3.3	5.0 ± 0.1	271.6 ± 5.7	0.3 ± 0.0	0.9 ± 0.0	501.8 ± 5.6	503.3 ± 5.8
	600	12.0 ± 0.0	5.5 ± 0.2	21.4 ± 0.5	170.4 ± 5.3	27.1 ± 0.5	21.5 ± 1.5	272.7± 11.8	5.8 ± 0.4	264.2 ± 1.8	0.3 ± 0.0	0.7 ± 0.0	565.7 ± 1.9	503.3 ± 15.3
	700	12.2 ± 0.0	7.4 ± 0.1	25.0 ± 0.1	206.1 ± 0.1	28.5 ± 0.0	13.3 ± 0.3	1551 ± 1.7	3.3 ± 1.0	244.4 ± 7.5	0.3 ± 0.1	1.2 ± 0.0	644.6 ± 29.8	460.0 ± 26.5
0.20	70	10.1 ± 0.0	6.1 ± 0.0	8.7 ± 0.2	79.2 ± 7.4	28.6 ± 0.2	47.5 ± 2.0	246.0 ± 3.1	39.0 ± 1.9	364.9 ± 3.8	1.9 ± 0.1	1.1 ± 0.0	-	-
	300	11.3 ± 0.0	4.8 ± 0.0	16.9 ± 0.3	126.1 ± 0.7	29.4 ± 0.0	33.8 ± 3.1	223.2 ± 1.4	15.8 ± 0.7	263.0 ± 13.9	0.8 ± 0.0	0.9 ± 0.0	566.6 ± 9.8	596.7 ± 25.2
	500	12.1 ± 0.1	4.9 ± 0.0	17.8 ± 0.3	149.7 ± 3.6	29.5 ± 0.0	10.4 ± 0.1	161.4 ± 4.2	4.9 ± 0.3	216.7 ± 0.4	0.4 ± 0.0	1.0 ± 0.0	648.7 ± 15.4	503.3 ± 11.5
	600	12.2 ± 0.1	5.3 ± 0.2	19.3 ± 1.3	154.8 ± 1.6	29.5 ± 0.1	9.3 ± 1.1	137.7 ± 5.1	3.3 ± 0.2	207.3 ± 3.5	0.3 ± 0.0	1.1 ± 0.1	682.3 ± 3.2	483.3 ± 11.5
	700	12.4 ± 0.0	6.4 ± 0.0	20.4 ± 0.2	163.8 ± 1.9	29.5 ± 0.0	11.6 ± 0.2	126.1 ± 0.7	2.5 ± 0.3	188.7 + 3.1	0.2 ± 0.0	1.1 ± 0.0	745.9 ± 17.3	450.0 ± 10.0

Mean values ± standard deviation; (pH, EC, Ash, Biochar yield, n=3; Total Ca, P, Mg, N, C, H and O, n = 2).

4.6. C, H, N and O content

The biochars had low C and N contents regardless of their Mg/Ca ratios (Table 2). At 300 °C, the C content of biochar (Mg/Ca ratio 0.16) decreased from 39% to 29% when adding Mg (Mg/Ca ratio 0.16), and at 700 °C, the C content decreased from 31% to 15%. The total N decreased during pyrolysis more than the total C content by the addition of Mg (Mg/Ca ratio of 0.16), from 7% to 4% at 300 ºC and from 3% to 1% at 700 °C. The H/C ratio declined as a function of pyrolysis temperature, but no substantial changes were observed as a result of Mg additions. The H/C ratios remained between 0.6 and 0.7 at 300 °C and between 0.2 and 0.3 at 600 °C. In contrast, the O/C ratio varied only as a function of Mg addition, remaining between 0.5 and 0.6, for the Mg/Ca ratio of 0.08 and between 0.8 and 1.2, for Mg/Ca 0.16.

4.7. X-ray diffraction and FTIR spectra

Regardless of Mg enrichment, the higher intensities of the crystalline phases for poultry manure and biochar were identified at the following 2θ positions: calcite ($CaCO_3$ – 18 and 24°), cristobalite (SiO_2 – 9 and 13°), and periclase (MgO – 26°), with a d-spacing of 4.89 and 3.68 [Å], 10.1 and 6.77 [Å], and 3.40 [Å], respectively (Figure 5A). The crystallite size (in nm) and degree of crystallinity (in %) of unpyrolyzed poultry manure were, on average, 0.27 nm and 57%, which increased to 0.31 nm and 66% when pyrolyzed (Table S7) (300 °C). After pyrolyzing, the crystallite size of MgO in Mg-doped biochar increased by 25%.

The highest peak intensities in the FTIR spectra were observed between 1625 and 600 cm^{-1} (Figure 5B). With pyrolysis, peak intensity decreased at 3190 and 2914 cm^{-1}, assigned to aromatic and aliphatic C-H stretching, respectively, irrespective of Mg addition (Liang et al., 2018; Wang et al., 2014). At 70 °C, $Mg(OH)_2$ addition increased peak intensity at 1625 and 1579 cm^{-1}, corresponding to aromatic C=C, and at 1407 cm^{-1}, corresponding to C-O stretching and carbonates (Bekiaris et al., 2016; Domingues et al., 2017; Farah Nadia et al., 2015). At 300 °C, Mg additions increased intensity at 1579 and 1026, corresponding to C=C and P-O or Mg-O bond, and decreased intensity at 873 and 705, corresponding to P-O-P or P=O stretching (Bekiaris et al., 2016; Li et al., 2016; Nardis et al., 2021). Intensity at 873 cm^{-1} corresponds to Ca-P, and intensity at 1026 cm^{-1} is attributed to P-O bond stretching in Ca-P or Mg-P minerals (Figure S4). At 500 and 700 °C, Mg additions increased intensity at peaks 1407, 1026 and 873 cm^{-1}.

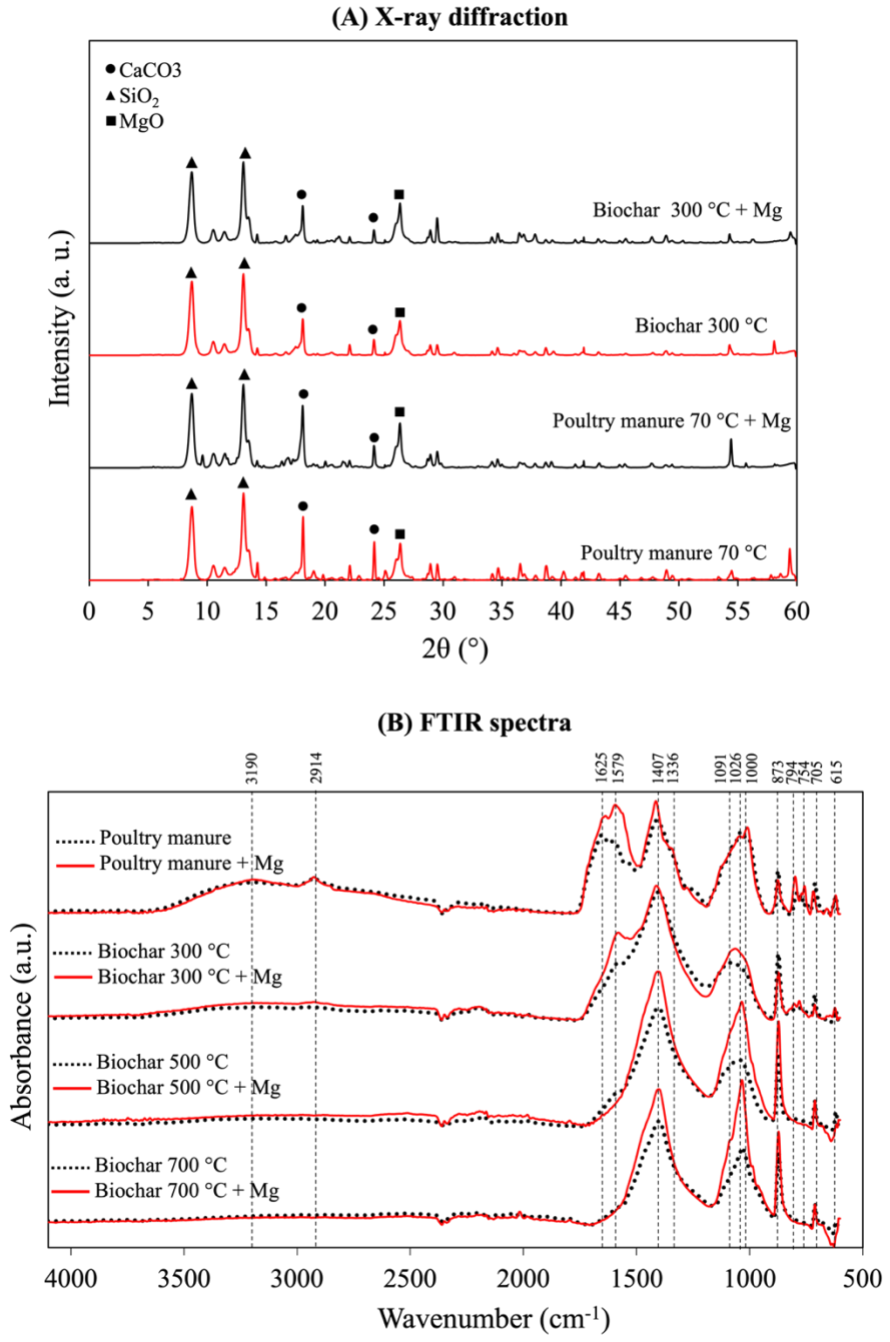

Figure 5. X-ray diffraction and Fourier transform infrared spectroscopy (FTIR) spectra and spectral bands of unmodified (Mg/Ca: 0.08) and Mg added (Mg/Ca: 0.16) poultry manure and biochars. XRD peaks position, crystallite size and area under peaks in Table S7. FTIR peaks assignments in Table S8.

5. Discussion

5.1. Magnesium enrichment increases phosphorus availability on biochar

Phosphorus availability assessed by citric and formic acid extraction increases with Mg addition, up to a pyrolysis temperature of 600 °C (Figure 1). With pyrolysis, enhanced P availability seems to be consistent with precipitation of Mg minerals determined by P K and $L_{2,3}$-edge [$MgNH_4PO_4$ and $Mg_3(PO_4)_2.8H_2O$] (Table 1 and S4). At the highest examined pyrolysis temperatures (700 °C) Mg-P minerals are reduced. This is consistent with previous studies where Mg-P may gradually decompose as the temperature rises, probably due to instability at high temperatures. Also, the decomposition of struvite at temperatures higher than 300 ºC may explain the decrease in total N in these Mg-biochars, probably due to the evolution of volatiles (Ramlogan and Rouff, 2016).

The greater P availability plateaued at a Mg/Ca ratio of 0.10 and even decreases at 0.16, and not only Mg-P minerals were formed in Mg-biochar. As observed by SEM-EDS quantification analysis at 300 ºC (Table S5), Mg-biochar has several features (blocks and flakes) of high Mg concentration, which was confirmed by the presence of MgO particles in the form of nano-flakes within the biochar matrix in prior studies (Wu et al., 2019; Zhang et al., 2012), and confirmed by the increase in MgO crystallite size in Mg-biochar in our study (Table S7). These Mg-rich spatial features could explain why increasing Mg/Ca ratios do not increase P availability from a certain amount of Mg onwards, as a low or no difference was observed for the highest Mg/Ca ratios to biochar without Mg addition (Figure 1), thus restricting P and Mg reaction to some extent. Moreover, the success of Mg addition to increase P availability could be influenced by other factors such as P concentration in poultry manure (~11 g P kg^{-1}) and biochar (25 g P kg^{-1}) (Table 2). Therefore, the increase in P availability was affected by the P/Mg ratio. The SEM mapping of P and Mg show both Mg and P evenly distributed on the surface (Figure 4A). This spatial correlation between Mg and P has already been reported for poultry manure at low pyrolysis temperature (300 ºC); at high pyrolysis temperatures, however, this correlation decreases in favor of a higher correlation between Ca and P (Bruun et al., 2017).

Phosphorus availability in unpyrolyzed poultry manure was lower compared to that in biochar (Table S2), which could be related to the larger amount of organic P present in manure, e.g., DNA, phytates, and lecithin (Uchimiya and Hiradate, 2014), while biochars usually lack organic P forms as a result of thermal treatment (Zwetsloot et al., 2015). Moreover, as observed by

P K-edge XANES analysis, the unpyrolyzed poultry manure had around 35% of organic-complexed lecithin (Table 1). After pyrolysis, organic P decreased as expected, present only at a low proportion at 300 ºC (Table 1).

Water-extractable P mainly decreased as a result of pyrolysis and to a minor extent as pyrolysis temperature increased (Figure 1, Table S2), which is explained by the formation of less soluble P minerals after thermal degradation, already at the lowest temperature. Regardless of pyrolysis temperature or indeed because of pyrolyzing at the lowest temperature, it decreased as a function of Mg enrichment. Lower water solubility could have resulted from the OH^- anions provided with $Mg(OH)_2$ additions, and that could also be part of the mechanisms by which Mg-doped biochars have higher P availability assessed by citric and formic acid extractions, since these anions can also react with Ca^{2+} ions, preventing Ca-P precipitation and crystallization with heat treatment.

The kinetics of P release confirms the lower water solubility of P with Mg additions to both pyrolyzed and unpyrolyzed poultry over ten days (Figure 2). Most of the P from biochar without Mg is released within ten days, getting close to what is determined to be plant available using citric and formic acid extraction (Figure 2). In comparison, Mg-doped biochar and Mg-doped unpyrolyzed manure had a lower P release rate even after ten days. However, the lower P availability in water does not correlate with P fertilizer potential from these sources, as plants may improve P dissolution and absorption through several mechanisms (Morgan and Connolly, 2013), primarily through rhizosphere acidification. Besides, P sources with low water-soluble P are less susceptible to strong adsorption to soil minerals and, therefore, might have a sustained P release over the plant growth cycle (Hart et al., 2004), which is desirable in tropical soils due to its high P adsorption capacity.

5.2. Magnesium enrichment decreases the formation of highly crystalline calcium phosphates

Adding Mg to poultry manure biomass prevented or decreased the formation of Ca-P minerals (Table 1). As suggested by P K-edge XANES analysis, Mg-doped biochar has lower proportions of pyrophosphate (low temperature) and no detectable hydroxyapatite (high temperature), a highly crystalline P compound (Table 1). Previous studies have reported that the partial substitution of Ca by Mg (a smaller ion) inhibits the crystallinity of synthetic hydroxyapatite via inhibiting crystal growth propagation during thermal degradation (Cao and Harris, 2008; Hilger

et al., 2020). Thus, the data from this study confirms that this also happens in manure biochar, and it may be the main mechanism involved in the greater P availability.

Besides being a smaller ion and causing structural changes, Mg has a larger hydrated ionic radius than Ca, a reason why Mg-P minerals could enhance P mobility in soil more than Ca-P. An increase in P solubility in calcareous soil due to an increase in Mg/Ca ratios on the exchange complex has already been reported (Manimel Wadu et al., 2013), making the enrichment of manure and its biochar with Mg a promising approach also for high-pH soils. However, further studies on Mg/Ca ratios on P availability are still necessary for both acidic and alkaline soils.

Besides forming Mg-P minerals, adding Mg did not entirely prevent P from binding to Ca, as we still observed increasing proportions of $CaHPO_4.2H_2O$, $Ca_3(PO_4)_2$, and octacalcium phosphate (Table 1) with increasing pyrolysis temperatures. High Ca concentrations can result from poultry diets. At the highest examined pyrolysis temperature of 700 °C, the proportions of $CaHPO_4.2H_2O$ and $Ca_3(PO_4)_2$ decrease in favor of hydroxyapatite formation (Table 1), a process that does not occur with Mg additions. For Mg-doped biochar, the abundance of $CaHPO_4.2H_2O$ as shown by decreasing intensity of the FTIR peak 873 cm^{-1} at 300 °C (Figure 5A). At the same temperature, the intensity of the peak at 1026 cm^{-1} decreased, which could either be $Ca_3(PO_4)_2$ or $Mg_3(PO_4)_2$ minerals, as they have similar features (Figure S4). However, no features for $Ca_3(PO_4)_2$ were observed for Mg-doped biochar at 300 °C in the K and $L_{2,3}$-edge XANES spectra, and the peak at 1026 cm^{-1} is therefore likely caused by $Mg_3(PO_4)_2$. Thus, Mg-P precipitation at low pyrolysis temperatures may have been responsible for preventing hydroxyapatite formation at higher temperatures.

At 500 and 700 °C, however, Mg-biochar had increased peak intensities at both 1026 and 873 cm^{-1} (Table S8), consistent with increases in Ca-P or Mg-P compounds, likely to be P-Ca compounds as determined by P K and $L_{2,3}$-edge XANES. This indicated that pyrolyzing at temperatures above 700 °C would probably no longer have a positive effect of Mg on P availability or crystallinity.

Regarding the abundance of minerals without P, calcite is observed, which is consistent with this type of material (Domingues et al., 2017). The presence of cristobalite (SiO_2) and periclase (MgO) (Figure 5B) was also observed in studies with poultry litter biochar (Domingues et al., 2017; Lustosa Filho et al., 2017; Yuan et al., 2011). The increase in crystallite size of MgO is compatible with a Mg enrichment (Table S7). In response to the thermal treatment, the degree

of crystallinity of biochar was higher than in the original manure, indicating a decrease in its amorphous and aliphatic structure, consequently increasing its aromaticity, resulting in a higher-order material with lower reactivity (Lu et al., 2002; Xie et al., 2019). However, no significant changes were observed in the general degree of crystallinity in biochar with or without Mg addition, except for higher crystallinity observed for MgO (Table S7 and Figure S5).

Conclusion

The enrichment of poultry manure biomass with magnesium hydroxide for biochar production increased phosphorus availability through the increase of Mg-P compounds at lower pyrolysis temperature and consequently less proportions of hydroxyapatite at higher pyrolysis temperature. The resulting low water solubility of P can improve management for this and other Ca-rich manure (e.g., pig manure or dairy manure). For biochar, pyrolysis of Mg-enriched manure biomass can reduce the volume required for application, and the higher P availability can increase the efficiency of phosphate fertilization. For future research, it is necessary to study the effects of microbial solubilization and subsequent plant uptake from Mg-enriched biochar.

Credit author statement

Conceptualization: AdAL, LCAM, JL. Methodology: AdAL, LCAM, JL. Laboratory Analysis: AdAL. Validation: AdAL, LCAM, JL. Investigation: AdAL, LCAM, JL. Formal analysis: All authors. Visualization: All authors. Writing - original draft: AdAL. Resources: JL. Supervision: LCAM, JL. Project administration LCAM, JL. Funding acquisition: JL Writing - review & editing: All authors.

Declaration of competing interest

The authors declare that no known competing financial interests or personal relationships that could have influenced the work reported in this paper.

Acknowledgments

This work was funded in part by USDA-NIFA (2019-67021-29945), USDA-Hatch (2018-19-204). The first author received a scholarship from the Improvement of Higher Education Personnel (CAPES - Proex 88887.358193/2019-00, and CAPES - PrInt 88887.465631/2019-00). The XRD

experiments were performed on beamline ID13 at the European Synchrotron Radiation Facility (ESRF), Grenoble, France. We are grateful to Manfred Burghammer for providing assistance in beamline ID13. Part of the research described in this paper was performed through the MAPLE project, a collaboration between the Canadian Light Source (CLS) and the Brazilian Synchrotron Light Laboratory (LNLS-CNPEM). Canadian Light Source, a national research facility of the University of Saskatchewan is supported by the Canada Foundation for Innovation (CFI), the Natural Sciences and Engineering Research Council (NSERC), the National Research Council (NRC), the Canadian Institutes of Health Research (CIHR), the Government of Saskatchewan, and the University of Saskatchewan. The Brazilian Synchrotron Light Laboratory, part of the Brazilian Center for Research in Energy and Materials (CNPEM), is a private non-profit organization under the supervision of the Brazilian Ministry for Science, Technology, and Innovations (MCTI). The authors thank Dr D. Muir for the support at the IDEAS beamline. The authors thank Dr Dean Hesterberg for the support with P K-edge XANES analysis and phosphate standards. This work also made use of the Cornell Center for Materials Research Facilities supported by the National Science Foundation under Award Number DMR-1719875. We thank Shannan Sweet, Ivan Ribeiro, Annette Dathe, Jefferson Carneiro, Barbara Nardis and Akio Enders, for help with sample analyses.

References

Abdala, D.B., Ghosh, A.K., da Silva, I.R., de Novais, R.F., Alvarez Venegas, V.H., 2012. Phosphorus saturation of a tropical soil and related P leaching caused by poultry litter addition. Agric Ecosyst Environ 162, 15–23. https://doi.org/10.1016/j.agee.2012.08.004

Akaike, H., 1974. A New Look at the Statistical Model Identification. IEEE Trans Automat Contr 19, 716–723. https://doi.org/10.1109/TAC.1974.1100705

Akdeniz, N., 2019. A systematic review of biochar use in animal waste composting. Waste Management. https://doi.org/10.1016/j.wasman.2019.03.054

Baty, F., Ritz, C., Charles, S., Brutsche, M., Flandrois, J.-P., Delignette-Muller, M.-L., 2015. A Toolbox for Nonlinear Regression in R: The Package nlstools, JSS Journal of Statistical Software.

Beauchemin, S., Hesterberg, D., Chou, J., Beauchemin, M., Simard, R.R., Sayers, D.E., 2003. Speciation of Phosphorus in Phosphorus-Enriched Agricultural Soils Using X-Ray Absorption Near-Edge Structure Spectroscopy and Chemical Fractionation. J Environ Qual 32, 1809–1819. https://doi.org/10.2134/jeq2003.1809

Bekiaris, G., Peltre, C., Jensen, L.S., Bruun, S., 2016. Using FTIR-photoacoustic spectroscopy for phosphorus speciation analysis of biochars. Spectrochim Acta A Mol Biomol Spectrosc 168, 29–36. https://doi.org/10.1016/j.saa.2016.05.049

Bruun, S., Harmer, S.L., Bekiaris, G., Christel, W., Zuin, L., Hu, Y., Jensen, L.S., Lombi, E., 2017. The effect of different pyrolysis temperatures on the speciation and availability in soil of P in biochar produced from the solid fraction of manure. Chemosphere 169, 377–386. https://doi.org/10.1016/j.chemosphere.2016.11.058

Buss, W., Bogush, A., Ignatyev, K., Mašek, O., 2020. Unlocking the Fertilizer Potential of Waste-Derived Biochar. ACS Sustain Chem Eng 8, 12295–12303. https://doi.org/10.1021/acssuschemeng.0c04336

Cao, X., Harris, W., 2008. Carbonate and magnesium interactive effect on calcium phosphate precipitation. Environ Sci Technol 42, 436–442. https://doi.org/10.1021/es0716709

Carneiro, J.S. da S., Ribeiro, I.C.A., Nardis, B.O., Barbosa, C.F., Lustosa Filho, J.F., Melo, L.C.A., 2021. Long-term effect of biochar-based fertilizers application in tropical soil: Agronomic efficiency and phosphorus availability. Science of the Total Environment 760. https://doi.org/10.1016/j.scitotenv.2020.143955

Carneiro, J.S.D.S., Lustosa Filho, J.F., Nardis, B.O., Ribeiro-Soares, J., Zinn, Y.L., Melo, L.C.A., 2018. Carbon Stability of Engineered Biochar-Based Phosphate Fertilizers. ACS Sustain Chem Eng 6, 14203–14212. https://doi.org/10.1021/acssuschemeng.8b02841

Darby, I., Xu, C.Y., Wallace, H.M., Joseph, S., Pace, B., Bai, S.H., 2016. Short-term dynamics of carbon and nitrogen using compost, compost-biochar mixture and organo-mineral biochar. Environmental Science and Pollution Research 23, 11267–11278. https://doi.org/10.1007/s11356-016-6336-7

dela Piccolla, C., Hesterberg, D., Muraoka, T., Novotny, E.H., 2021. Optimizing pyrolysis conditions for recycling pig bones into phosphate fertilizer. Waste Management 131, 249–257. https://doi.org/10.1016/j.wasman.2021.06.012

Domingues, R.R., Trugilho, P.F., Silva, C.A., de Melo, I.C.N.A., Melo, L.C.A., Magriotis, Z.M., Sánchez-Monedero, M.A., 2017a. Properties of biochar derived from wood and high-nutrient biomasses with the aim of agronomic and environmental benefits. PLoS One 12. https://doi.org/10.1371/journal.pone.0176884

Enders, A., Hanley, K., Whitman, T., Joseph, S., Lehmann, J., 2012. Characterization of biochars to evaluate recalcitrance and agronomic performance. Bioresour Technol 114, 644–653. https://doi.org/10.1016/j.biortech.2012.03.022

Enders, A., Lehmann, J., 2012. Comparison of Wet-Digestion and Dry-Ashing Methods for Total Elemental Analysis of Biochar. Commun Soil Sci Plant Anal 43, 1042–1052. https://doi.org/10.1080/00103624.2012.656167

Farah Nadia, O., Xiang, L.Y., Lie, L.Y., Chairil Anuar, D., Mohd Afandi, M.P., Azhari Baharuddin, S., 2015. Investigation of physico-chemical properties and microbial

community during poultry manure co-composting process. J Environ Sci (China) 28, 81–94. https://doi.org/10.1016/j.jes.2014.07.023

Farzadi, A., Bakhshi, F., Solati-Hashjin, M., Asadi-Eydivand, M., Osman, N.A.A., 2014. Magnesium incorporated hydroxyapatite: Synthesis and structural properties characterization. Ceram Int 40, 6021–6029. https://doi.org/10.1016/j.ceramint.2013.11.051

Glaser, B., Lehmann, J., Zech, W., 2002. Ameliorating physical and chemical properties of highly weathered soils in the tropics with charcoal - A review. Biol Fertil Soils. https://doi.org/10.1007/s00374-002-0466-4

Hart, M.R., Quin, B.F., Nguyen, M.L., 2004. Phosphorus Runoff from Agricultural Land and Direct Fertilizer Effects: A Review. J Environ Qual 33, 1954–1972. https://doi.org/10.2134/jeq2004.1954

Hesterberg, D., McNulty, I., Thieme, J., 2017. Speciation of Soil Phosphorus Assessed by XANES Spectroscopy at Different Spatial Scales. J Environ Qual 46, 1190–1197. https://doi.org/10.2134/jeq2016.11.0431

Higashikawa, F.S., Silva, C.A., Bettiol, W., 2010. Chemical and physical properties of organic residues. Rev Bras Cienc Solo 34, 1743–1752. https://doi.org/10.1590/s0100-06832010000500026

Hilger, D.M., Hamilton, J.G., Peak, D., 2020. The influences of magnesium upon calcium phosphate mineral formation and structure as monitored by x-ray and vibrational spectroscopy. Soil Syst 4, 1–13. https://doi.org/10.3390/soilsystems4010008

Ippolito, J.A., Cui, L., Kammann, C., Wrage-Mönnig, N., Estavillo, J.M., Fuertes-Mendizabal, T., Cayuela, M.L., Sigua, G., Novak, J., Spokas, K., Borchard, N., 2020. Feedstock choice, pyrolysis temperature and type influence biochar characteristics: a comprehensive meta-data analysis review. Biochar. https://doi.org/10.1007/s42773-020-00067-x

Ippolito, J.A., Spokas, K.A., Novak, J.M., Lentz, R.D. and Cantrell, K.B., 2015. Biochar elemental composition and factors influencing nutrient retention. Lehmann J, Joseph S (Eds.) Biochar for environmental management: Science, technology and implementation, 139-163.

Joseph, S., Cowie, A.L., van Zwieten, L., Bolan, N., Budai, A., Buss, W., Cayuela, M.L., Graber, E.R., Ippolito, J.A., Kuzyakov, Y., Luo, Y., Ok, Y.S., Palansooriya, K.N., Shepherd, J., Stephens, S., Weng, Z., Lehmann, J., 2021. How biochar works, and when it doesn't: A review of mechanisms controlling soil and plant responses to biochar. GCB Bioenergy. https://doi.org/10.1111/gcbb.12885

Kannan, S., Lemos, I.A.F., Rocha, J.H.G., Ferreira, J.M.F., 2005. Synthesis and characterization of magnesium substituted biphasic mixtures of controlled hydroxyapatite/β-tricalcium phosphate ratios. J Solid State Chem 178, 3190–3196. https://doi.org/10.1016/j.jssc.2005.08.003

Kruse, J., Leinweber, P., Eckhardt, K.U., Godlinski, F., Hu, Y., Zuin, L., 2009. Phosphorus L2,3-edge XANES: Overview of reference compounds. J Synchrotron Radiat 16, 247–259. https://doi.org/10.1107/S0909049509000211

Kyakuwaire, M., Olupot, G., Amoding, A., Nkedi-Kizza, P., Basamba, T.A., 2019. How safe is chicken litter for land application as an organic fertilizer? A review. Int J Environ Res Public Health 16. https://doi.org/10.3390/ijerph16193521

Li, R., Wang, J.J., Zhou, B., Awasthi, M.K., Ali, A., Zhang, Z., Lahori, A.H., Mahar, A., 2016. Recovery of phosphate from aqueous solution by magnesium oxide decorated magnetic biochar and its potential as phosphate-based fertilizer substitute. Bioresour Technol 215, 209–214. https://doi.org/10.1016/j.biortech.2016.02.125

Liang, X., Jin, Y., He, M., Niyungeko, C., Zhang, J., Liu, C., Tian, G., Arai, Y., 2018. Phosphorus speciation and release kinetics of swine manure biochar under various pyrolysis temperatures. Environmental Science and Pollution Research 25, 25780–25788. https://doi.org/10.1007/s11356-017-0640-8

Liang, Y., Cao, X., Zhao, L., Xu, X., Harris, W., 2014. Phosphorus Release from Dairy Manure, the Manure-Derived Biochar, and Their Amended Soil: Effects of Phosphorus Nature and Soil Property. J Environ Qual 43, 1504–1509. https://doi.org/10.2134/jeq2014.01.0021

Liu, Z.F., Cutler, J.N., Bancroft, G.M., Tan, K.H., Cave11, R.G., Tse, J.S., 1992. Crystal field splittings of continuum d orbitals. A comparative study on the L2,3 edge X-ray absorption spectra of Si, P and S compounds, Chemical Physics.

Lopes, A.S., Guimarães Guilherme, L.R., 2016. A career perspective on soil management in the Cerrado region of Brazil, in: Advances in Agronomy. Academic Press Inc., pp. 1–72. https://doi.org/10.1016/bs.agron.2015.12.004

Lu, L., Kong, C., Sahajwalla, V., Harris, D., 2002. Char structural ordering during pyrolysis and combustion and its influence on char reactivity. Fuel 81, 1215–1225. https://doi.org/10.1016/S0016-2361(02)00035-2

Lustosa Filho, J.F., Barbosa, C.F., Carneiro, J.S. da S., Melo, L.C.A., 2019. Diffusion and phosphorus solubility of biochar-based fertilizer: Visualization, chemical assessment and availability to plants. Soil Tillage Res 194. https://doi.org/10.1016/j.still.2019.104298

Lustosa Filho, J.F., Penido, E.S., Castro, P.P., Silva, C.A., Melo, L.C.A., 2017. Co-Pyrolysis of Poultry Litter and Phosphate and Magnesium Generates Alternative Slow-Release Fertilizer Suitable for Tropical Soils. ACS Sustain Chem Eng 5, 9043–9052. https://doi.org/10.1021/acssuschemeng.7b01935

Manceau, A., Marcus, M.A., Grangeon, S., 2012. Determination of Mn valence states in mixed-valent manganates by XANES spectroscopy. American Mineralogist 97, 816–827. https://doi.org/10.2138/am.2012.3903

Morgan, J. B., Connolly, E. L., 2013. Plant-Soil Interactions: Nutrient Uptake. Nature Education Knowledge 4, 2

Murphy, J., and Riley, J.P., 1962. A Modified Single Solution Method for the Determination of Phosphate in Natural Waters. Analytica Chimica Acta 27, 31-36. http://dx.doi.org/10.1016/S0003-2670(00)88444-5

Manimel Wadu, M.C.W., Michaelis, V.K., Kroeker, S., Akinremi, O.O., 2013. Exchangeable Calcium/Magnesium Ratio Affects Phosphorus Behavior in Calcareous Soils. Soil Science Society of America Journal 77, 2004–2013. https://doi.org/10.2136/sssaj2012.0102

Nardis, B.O., Santana Da Silva Carneiro, J., Souza, I.M.G. de, Barros, R.G. de, Azevedo Melo, L.C., 2021. Phosphorus recovery using magnesium-enriched biochar and its potential use as fertilizer. Arch Agron Soil Sci 67, 1017–1033. https://doi.org/10.1080/03650340.2020.1771699

Rajkovich, S., Enders, A., Hanley, K., Hyland, C., Zimmerman, A.R., Lehmann, J., 2012. Corn growth and nitrogen nutrition after additions of biochars with varying properties to a temperate soil. Biol Fertil Soils 48, 271–284. https://doi.org/10.1007/s00374-011-0624-7

Ramlogan, M. v., Rouff, A.A., 2016. An investigation of the thermal behavior of magnesium ammonium phosphate hexahydrate. J Therm Anal Calorim 123, 145–152. https://doi.org/10.1007/s10973-015-4860-1

Ravel, B., Newville, M., 2005. ATHENA, ARTEMIS, HEPHAESTUS: Data analysis for X-ray absorption spectroscopy using IFEFFIT, in: Journal of Synchrotron Radiation. pp. 537–541. https://doi.org/10.1107/S0909049505012719

Rehman, A., Nawaz, S., Alghamdi, H.A., Alrumman, S., Yan, W., Nawaz, M.Z., 2020. Effects of manure-based biochar on uptake of nutrients and water holding capacity of different types of soils. Case Studies in Chemical and Environmental Engineering 2. https://doi.org/10.1016/j.cscee.2020.100036

Riekel, C., Burghammer, M., Davies, R., 2010. Progress in micro- and nano-diffraction at the ESRF ID13 beamline. IOP Conf Ser Mater Sci Eng 14, 012013. https://doi.org/10.1088/1757-899x/14/1/012013

Roy, E.D., Richards, P.D., Martinelli, L.A., Coletta, L. della, Lins, S.R.M., Vazquez, F.F., Willig, E., Spera, S.A., VanWey, L.K., Porder, S., 2016. The phosphorus cost of agricultural intensification in the tropics. Nat Plants 2. https://doi.org/10.1038/NPLANTS.2016.43

Sauvé, S., Bernard, S., Sloan, P., 2016. Environmental sciences, sustainable development and circular economy: Alternative concepts for trans-disciplinary research. Environ Dev 17, 48–56. https://doi.org/10.1016/j.envdev.2015.09.002

Scott, A.J., Knott, M., 1974. A Cluster Analysis Method for Grouping Means in the Analysis of Variance.

Shariatmadari, H., Shirvani, M., Jafari, A., 2006. Phosphorus release kinetics and availability in calcareous soils of selected arid and semiarid toposequences. Geoderma 132, 261–272. https://doi.org/10.1016/j.geoderma.2005.05.011

Solé, V.A., Papillon, E., Cotte, M., Walter, P., Susini, J., 2007. A multiplatform code for the analysis of energy-dispersive X-ray fluorescence spectra. Spectrochim Acta Part B At Spectrosc 62, 63–68. https://doi.org/10.1016/j.sab.2006.12.002

Suleiman, A.K.A., Lourenço, K.S., Pitombo, L.M., Mendes, L.W., Roesch, L.F.W., Pijl, A., Carmo, J.B., Cantarella, H., Kuramae, E.E., 2018. Recycling organic residues in agriculture

impacts soil-borne microbial community structure, function and N2O emissions. Science of the Total Environment 631–632, 1089–1099. https://doi.org/10.1016/j.scitotenv.2018.03.116

Tilman, D., Fargione, J., Wolff, B., D'Antonio, C., Dobson, A., Howarth, R., Schindler, D., Schlesinger, W.H., Simberloff, D., Swackhamer, D., 2001. Forecasting agriculturally driven global environmental change. Science (1979) 292, 281–284. https://doi.org/10.1126/science.1057544

Uchimiya, M., Hiradate, S., 2014. Pyrolysis temperature-dependent changes in dissolved phosphorus speciation of plant and manure biochars. J Agric Food Chem 62, 1802–1809. https://doi.org/10.1021/jf4053385

Wang, T., Camps-Arbestain, M., Hedley, M., Bishop, P., 2012. Predicting phosphorus bioavailability from high-ash biochars. Plant and Soil 357, 173–187. https://doi.org/10.1007/s11104-012-1131-9

Wang, Y., Yin, R., Liu, R., 2014. Characterization of biochar from fast pyrolysis and its effect on chemical properties of the tea garden soil. J Anal Appl Pyrolysis 110, 375–381. https://doi.org/10.1016/j.jaap.2014.10.006

Wu, L., Wei, C., Zhang, S., Wang, Y., Kuzyakov, Y., Ding, X., 2019. MgO-modified biochar increases phosphate retention and rice yields in saline-alkaline soil. J Clean Prod 235, 901–909. https://doi.org/10.1016/j.jclepro.2019.07.043

Xie, Y., Yang, H., Zeng, K., Zhu, Y., Hu, J., Mao, Q., Liu, Q., Chen, H., 2019. Study on CO2 gasification of biochar in molten salts: Reactivity and structure evolution. Fuel 254. https://doi.org/10.1016/j.fuel.2019.06.022

Yuan, J.H., Xu, R.K., Zhang, H., 2011. The forms of alkalis in the biochar produced from crop residues at different temperatures. Bioresour Technol 102, 3488–3497. https://doi.org/10.1016/j.biortech.2010.11.018

Zhang, M., Gao, B., Yao, Y., Xue, Y., Inyang, M., 2012. Synthesis of porous MgO-biochar nanocomposites for removal of phosphate and nitrate from aqueous solutions. Chemical Engineering Journal 210, 26–32. https://doi.org/10.1016/j.cej.2012.08.052

Zwetsloot, M.J., Lehmann, J., Solomon, D., 2015. Recycling slaughterhouse waste into fertilizer: How do pyrolysis temperature and biomass additions affect phosphorus availability and chemistry? J Sci Food Agric 95, 281–288. https://doi.org/10.1002/jsfa.6716

Supplementary information

Table S1. Total phosphorus, phosphorus extracted by citric acid 2% and formic acid 2% of poultry manure enriched with magnesium sulfate ($MgSO_4$) and magnesium chloride ($MgCl_2$) (means values ± standard deviation; n=3).

Poultry manure enrichment	T (ºC)	Mg/Ca ratio	Total P (g kg^{-1})	Citric acid (g kg^{-1})	Citric acid (% of total P)	Formic acid (g kg^{-1})	Formic acid (% of total P)
$MgSO_4$	70	0.16	10.4 ± 0.2	5.5 ± 0.2	53.3	5.8 ± 0.0	56.3
$MgCl_2$			10.2 ± 0.0	5.4 ± 0.1	53.3	5.9 ± 0.2	58.3
$MgSO_4$	300		19.3 ± 0.7	8.9 ± 0.8	46.3	9.0 ± 0.6	46.5
$MgCl_2$			14.6 ± 0.9	9.5 ± 0.4	65.1	9.5 ± 0.7	65.2
$MgSO_4$	500		18.8 ± 0.4	17.7 ± 0.8	94.1	17.5 ± 0.4	92.8
$MgCl_2$			15.8 ± 0.8	14.4 ± 0.5	90.8	15.1 ± 0.1	95.6

Table S2. Phosphorus extracted by citric acid 2%, formic acid 2% and water as a function of Magnesium hydroxide modified biochars and magnesium and calcium ratios (means values ± standard deviation; n=3).

Mg/Ca Ratio	T (°C)	Citric acid (g kg^{-1})	Citric acid (% of total P)	Formic acid (g kg^{-1})	Formic acid (% of total P)	Water (g kg^{-1})	Water (% of total P)
	70	5.0 ± 0.3	43.8	4.9 ± 0.1	44.9	3.8 ± 0.1	35.0
	300	13.6 ± 0.2	69.8	14.4 ± 0.3	73.1	0.7 ± 0.0	3.7
0.08*	500	14.9 ± 0.7	70.8	16.5 ± 0.6	76.0	0.4 ± 0.0	1.8
	600	12.7 ± 0.2	55.1	15.8 ± 0.5	67.7	0.6 ± 0.0	2.8
	700	14.5 ± 0.7	63.6	16.6 ± 0.1	70.9	0.5 ± 0.0	2.1
	70	6.7 ± 0.2	60.6	7.0 ± 0.7	60.6	3.1 ± 0.1	27.5
	300	19.4 ± 1.0	93.8	17.9 ± 0.7	90.0	0.8 ± 0.0	3.8
0.10	500	21.1 ± 1.4	87.5	22.0 ± 1.4	91.0	0.2 ± 0.0	1.2
	600	19.6 ± 0.5	78.8	23.2 ± 0.7	92.1	0.2 ± 0.0	0.8
	700	17.9 ± 0.4	66.2	22.8 ± 1.0	83.1	0.0 ± 0.0	<LD
	70	5.9 ± 0.1	53.9	6.0 ± 0.6	50.2	1.5 ± 0.1	14.2
	300	17.6 ± 0.4	89.6	18.6 ± 0.6	94.3	0.4 ± 0.0	1.9
0.12	500	17.7 ± 0.8	74.4	20.5 ± 1.6	85.8	0.1 ± 0.0	0.5
	600	18.7 ± 0.9	81.3	19.5 ± 0.3	86.5	0.0 ± 0.0	0.3
	700	16.0 ± 0.4	61.0	19.1 ± 0.8	74.2	0.0 ± 0.0	<LD
	70	5.0 ± 0.1	45.1	5.7 ± 0.5	52.6	0.5 ± 0.0	5.0
	300	16.7 ± 0.3	94.3	16.8 ± 0.4	95.6	0.2 ± 0.0	0.9
0.16	500	17.1 ± 0.4	77.8	20.4 ± 1.4	89.5	0.0 ± 0.0	0.2
	600	16.1 ± 0.3	75.2	19.6 ± 0.5	90.3	0.0 ± 0.0	<LD
	700	15.5 ± 0.4	62.5	17.3 ± 0.5	68.9	0.0 ± 0.0	<LD
	70	5.7 ± 0.5	61.5	4.9 ± 0.1	56.5	0.4 ± 0.0	5.0
	300	15.2 ± 0.5	91.3	15.0 ± 0.8	89.7	0.0 ± 0.0	0.3
0.20	500	12.4 ± 0.2	70.1	16.7 ± 0.6	95.0	0.0 ± 0.0	<LD
	600	10.6 ± 0.3	54.7	14.7 ± 0.2	72.8	0.0 ± 0.0	<LD
	700	11.5 ± 0.3	57.3	14.7 ± 0.5	73.4	0.0 ± 0.0	<LD

<LD: lower than the detection limit.

Table S3. Parameters and standard error of estimative (SE) of the examined models for P release kinetics of unmodified and $Mg(OH)_2$-modified poultry manure and biochars.

Models	Parameters*	Sample information					
		PM 70 °C	PMB 300 °C	PMB 500 °C	$Mg(OH)_2$ - PM 70 °C	$Mg(OH)_2$-300°C	$Mg(OH)_2$ - 500°C
Zero Order	Q_e (g P kg^{-1})	5.222	12.49	1.082	4.144	0.402	0.226
	k_1 (h^{-1})	2.405	9.479	0.015	0.032	0.048	0.012
	SE	1.379	1.106	0.137	0.509	0.041	0.043
	AIC	39.75	35.34	-6.325	19.83	-30.59	-29.33
Second Order	Q_e (g P kg^{-1})	5.453	12.70	1.328	4.832	0.443	0.280
	k_2 [(g P kg^{-1})$^{-1}$]	3.322	25.40	0.016	0.038	0.073	0.012
	SE	1.257	1.013	0.132	0.469	0.036	0.042
	AIC	37.91	33.58	-7.097	18.20	32.73	-29.69
Power Function	a (g P kg^{-1} h^{-1})^b	3.305	11.41	0.136	0.817	0.098	0.042
	b [(g P kg^{-1})$^{-1}$]	0.136	0.033	0.374	0.320	0.288	0.272
	SE	0.686	0.632	0.081	0.322	0.038	0.028
	AIC	25.81	24.15	-16.89	10.70	-31.77	37.87
Elovich	α (g P kg^{-1} h^{-1})	3.499	11.45	0.197	0.902	0.088	0.059
	β [(g P kg^{-1})$^{-1}$]	-0.549	-0.393	-0.113	-0.556	-0.060	-0.017
	SE	0.822	0.656	0.160	0.565	0.037	0.036
	AIC	29.40	24.91	-3.222	21.91	-32.29	-32.65
Parabolic Diffusion	Q_e (g P kg^{-1})	3.128	11.17	0.122	0.663	0.077	0.043
	R (g P kg^{-1})$^{-0.5}$	0.303	0.220	0.062	0.281	0.028	0.010
	SE	0.358	0.330	0.057	0.368	0.056	0.018
	AIC	12.81	11.19	-23.78	13.36	-24.03	-46.04

k_1: first order rate constant; k_2: second order rate constant; a: initial P desorption rate; β: P desorption constant; R: diffusion rate constant; Q_e: amount of P release at equilibrium or maximum P released; SE: tandard error of estimative and AIC: Akaike Information Criterion.

The terms are as follows: Qt (g P kg^{-1}) is the cumulative P release at t time; Qe (g P kg^{1}) is the amount of P release at equilibrium, or maximum P released.

The kinetics of P release for PM was better fitted to the parabolic diffusion model, with the SE and AIC of 0.36 and 12.8, respectively. However, the power function was better suited for Mg-PM, with SE and AIC of 0.32 and 10.7, respectively. PM-BC better fitted the parabolic diffusion model, with SE and AIC of 0.33 and 11.2 (HHT of 300 °C), and SE and AIC of 0.057 and -23.8, (HHT of 500 °C). However, the Mg-PM-BC varied the best-fitted models according to the

pyrolysis temperature. At HHT of 300°C, Mg-PM-BC best fitted the Elovich equation, with SE and AIC of 0.037 and -32.2, respectively, and at HHT of 500°C it best fitted with the parabolic diffusion, SE and AIC of 0.018 and -46.04, respectively (Table S5).

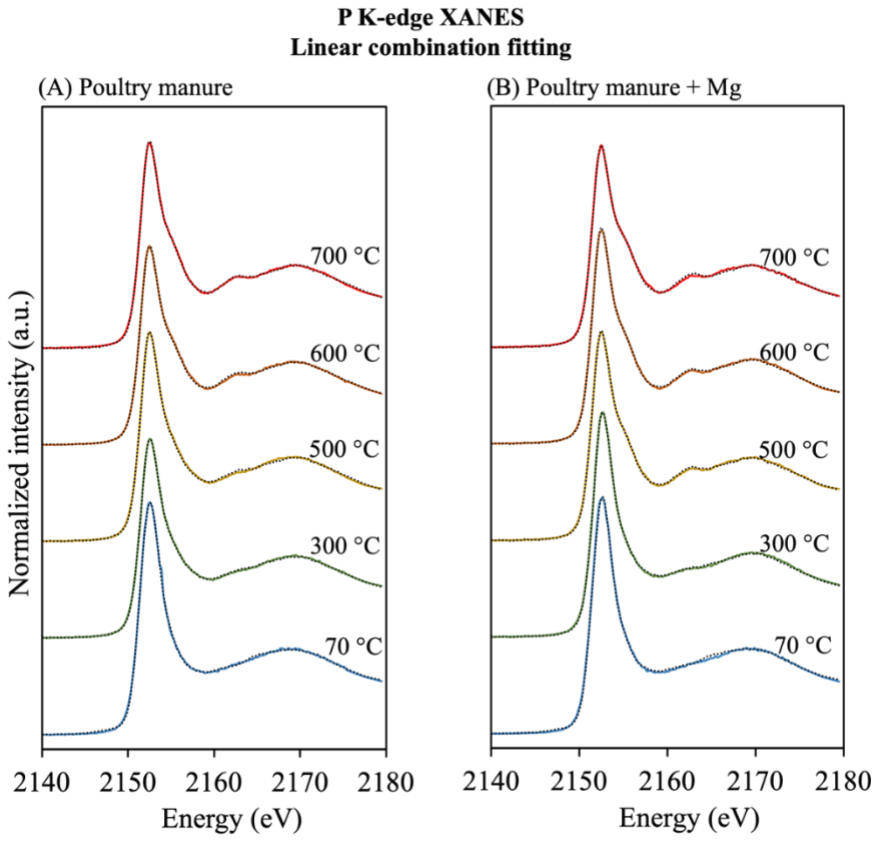

Figure S1. Phosphorus K-edge XANES data and overlaid linear combination fits (Dotted lines). Proportions of phosphorus species in the table 2.

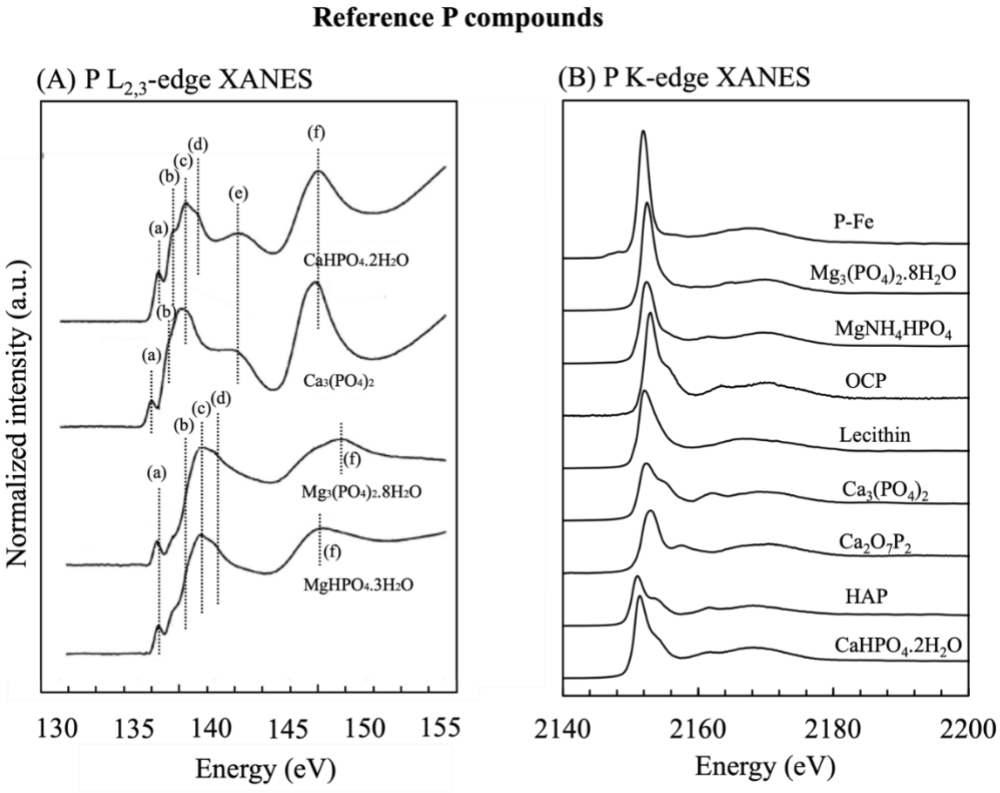

Figure S2. Phosphorus K and $L_{2,3}$-edge XANES spectra for reference phosphorus compounds. (A) The dotted lines indicate energy levels of spectral features from different P species displayed in table S8, Adapted from Kruse et al., 2009. (B) P K-edge XANES spectra for reference compounds adapted from dela Piccolla et al., 2021 and Hesterberg et al., 2017. P-Fe, phosphorus adsorbed on Pahokee peat; OCP, octacalcium phosphate; HAP, Hydroxyapatite.

Table S4. Energy position of P $L_{2,3}$-edge XANES spectra of samples and phosphorus standards (Standards adapted from Kruse et al., 2009).

Samples	Features					
	a	b	c	d	e	f
Poultry manure	136.6	137.3	138.9			147.2
Poultry manure + Mg	136.5	137.4	139.0			147.4
Biochar 300 °C	136.4	137.4	139.0		141.6	147.3
Biochar 300 °C + Mg	136.5	137.4	139.2			147.3
Biochar 500 °C	136.5	137.3	138.9		141.4	147.4
Biochar 500 °C + Mg	136.7	137.4	139.1	139.8	140.8	147.4
Biochar 600 °C	136.6	137.4	138.9		141.8	147.3
Biochar 600 °C + Mg	136.7	137.4	139.1	139.8	141.1	147.5
Biochar 700 °C	136.6	137.4	138.9		141.8	147.4
Biochar 700 °C + Mg	136.6	137.4	139.2	139.9	140.7	147.5

Phosphorus standards	Features					
	a	b	c	d	e	f
$CaHPO_4.2H_2O$	136.4	137.3	138.2	138.9	141.6	146.9
$Ca_3(PO_4)_2$	135.9	136.9	137.9		141.4	146.7
$Mg_3(PO_4)_2.8H_2O$	136.3	138.2	139.2	140.0		148.1
$MgHPO_4.3H_2O$	136.4	138.3	139.1	140.0		147.1

Table S5. Energy-dispersive spectroscopy (EDS) elemental quantification collected from regions of interest (Figure S3) from poultry manure biochar (Mg/Ca ratio 0.08) and magnesium-modified poultry manure biochar (Mg/Ca ratio 0.16).

PM-BC 300°C: round features elemental quantification

Element	Mass [%]	Mass Norm. [%]	Atom [%]	abs. error [%] (1 sigma)	rel. error [%] (1 sigma)
Sodium	3.99	3.99	6.35	0.16	4.08
Magnesium	4.97	4.97	7.48	0.18	3.61
Silicon	5.11	5.11	6.66	0.15	2.97
Potassium	31.94	31.94	29.89	0.81	2.54
Calcium	51.25	51.25	46.79	1.34	2.61
Chlorine	2.74	2.74	2.83	0.07	2.71

Mg-PM-BC 300°C: flakes elemental quantification

Element	Mass [%]	Mass Norm. [%]	Atom [%]	abs. error [%] (1 sigma)	rel. error [%] (1 sigma)
Sodium	6.36	6.36	8.83	0.24	3.72
Magnesium	26.78	26.78	35.15	0.90	3.36
Silicon	2.27	2.27	2.58	0.07	3.27
Phosphorus	4.57	4.57	4.70	0.13	2.95
Chlorine	1.51	1.51	1.36	0.04	2.89
Potassium	39.53	39.53	32.26	1.01	2.56
Calcium	18.99	18.99	15.12	0.51	2.68

Mg-PM-BC 300°C: cubes elemental quantification

Element	Mass [%]	Mass Norm. [%]	Atom [%]	abs. error [%] (1 sigma)	rel. error [%] (1 sigma)
Sodium	3.73	3.73	5.35	0.14	3.75
Magnesium	22.25	22.25	30.18	0.74	3.31
Phosphorus	2.26	2.26	2.40	0.07	2.92
Chlorine	19.44	19.44	18.07	0.51	2.61
Potassium	46.71	46.71	39.38	1.21	2.60
Calcium	5.61	5.61	4.61	0.16	2.80

Note: Imagens and EDS spectra of nodules, cubes and flakes are shown in Figure S2.

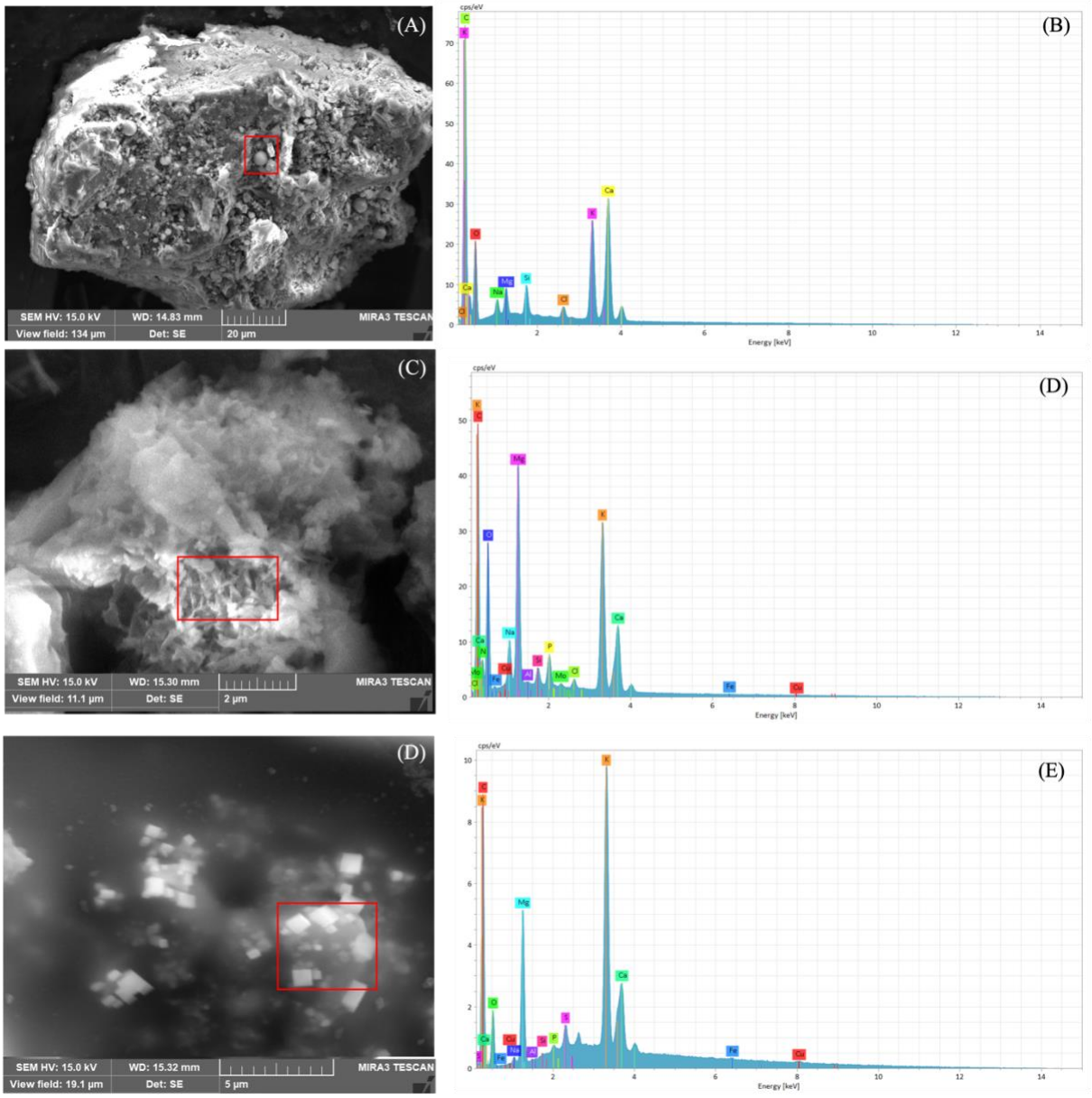

Figure S3. Scanning electron microscopy (SEM) images and Energy dispersive spectroscopy (EDS) spectra of nodules structures of unmodified biochar (Mg/Ca: 0.08) at 300 °C (A and B), and flakes and cubes structures of $Mg(OH)_2$-modified biochar (Mg/Ca: 0.16) at 300 °C (C, D, E and F).

Table S6. The BET (Brunauer-Emmett-Teller) surface area (SA) and total pore volume of raw manure and biochar (Mg/Ca ratio 0.08) and Mg enriched poultry manure and biochar (Mg/Ca ratio 0.16).

Mg/Ca Ratio	**T (°C)**	**BET SA** ($m^2\ g^{-1}$)	**Total Pore Volume ($cm^3\ kg^{-1}$)**
	70	nonporous	-
	300	low porosity	0.86
0.08	500	3.16 ± 0.04	9.71
	600	2.43 ± 0.05	0.84
	700	nonporous	-
	70	nonporous	-
	300	nonporous	-
0.20	500	nonporous	-
	600	nonporous	-
	700	nonporous	-

Table S7. Properties of crystalline phases and respectively peak positions of poultry manure and biochars (300 °C).

Crystalline phase	Peak position [°2θ]	PM	Mg-PM	PM-BC	Mg-PM-BC
		Crystallite size [Å]	Crystallite size [Å]	Crystallite size [Å]	Crystallite size [Å]
SiO_2 – Cristobalite	8.719	188	188	188	188
SiO_2 – Cristobalite	13.063	270	315	315	315
$CaCO_3$ – Calcite	18.101	476	238	317	317
$CaCO_3$ – Calcite	24.15	640	320	320	320
MgO – Periclase	26.214	161	161	120	161
		d-spacing [Å]	d-spacing [Å]	d-spacing [Å]	d-spacing [Å]
SiO_2 – Cristobalite	8.719	10.14664	10.1423	10.13844	10.14177
SiO_2 – Cristobalite	13.063	6.76927	6.78344	6.78283	6.77725
$CaCO_3$ – Calcite	18.101	4.893	4.90662	4.9004	4.90103
$CaCO_3$ – Calcite	24.15	3.68342	3.68416	3.68585	3.68573
MgO – Periclase	26.214	3.39836	3.39861	3.40085	3.3997
		Area under peaks	Area under peaks	Area under peaks	Area under peaks
SiO_2 – Cristobalite	8.719	15.67077	15.93847	16.20692	15.54536
SiO_2 – Cristobalite	13.063	23.01559	19.34183	18.47666	18.82213
$CaCO_3$ – Calcite	18.101	7.82402	8.98561	4.42785	4.85602
$CaCO_3$ – Calcite	24.15	2.67568	1.96428	1.16969	2.15548
MgO – Periclase	26.214	9.50265	10.65638	9.73314	9.99684

Note: PM: Raw poultry manure; Mg-PM: Mg-modified poultry manure; PM-BC: Poultry manure biochar; Mg-PM-BC: Mg-modified poultry manure biochar.

Table S8. Fourier transform infrared spectroscopy (FTIR) spectra band assignments of raw and Mg enriched poultry manure and biochars

Wavenumber, cm^{-1}	**Band assignment**	**References**
3190, 2914	Aromatic and aliphatic C-H stretching	(Liang et al., 2018; Wang et al., 2014)
1625, 1579	C=O, C=C	(Bekiaris et al., 2016; Farah Nadia et al., 2015)
1407, 1336	C-O stretching, Carbonates, C-H_2 bending	(Bekiaris et al., 2016; Domingues et al., 2017; Farah Nadia et al., 2015)
1000, 1026, 1091	P-O Bond, Stretching and bending vibration of Mg-O or Mg-OH	(Bekiaris et al., 2016; Nardis et al., 2021)
873, 794, 754, 705, 615	P-O-P stretching, P-C symmetric, P-O-P, P-O or P=O stretching	(Bekiaris et al., 2016; Li et al., 2016; Nardis et al., 2021)

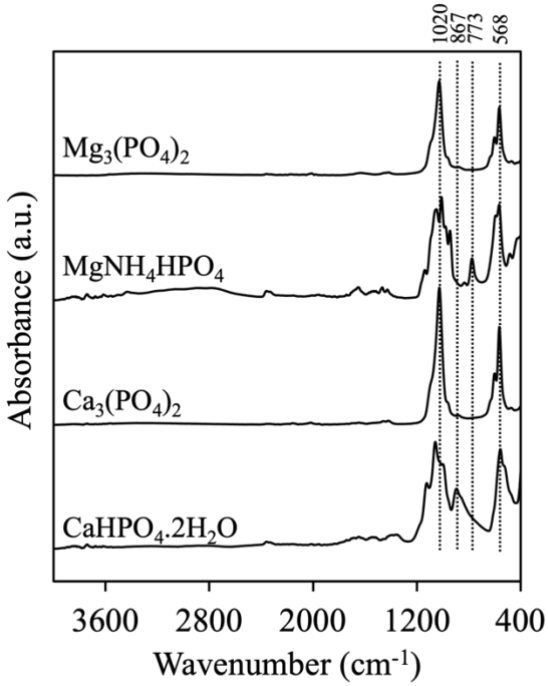

Figure S4. Fourier transform infrared spectroscopy (FTIR) spectra of reference phosphorus compounds.

References

Bekiaris, G., Peltre, C., Jensen, L.S., Bruun, S., 2016. Using FTIR-photoacoustic spectroscopy for phosphorus speciation analysis of biochars. Spectrochim Acta A Mol Biomol Spectrosc 168, 29–36. https://doi.org/10.1016/j.saa.2016.05.049

dela Piccolla, C., Hesterberg, D., Muraoka, T., Novotny, E.H., 2021. Optimizing pyrolysis conditions for recycling pig bones into phosphate fertilizer. Waste Management 131, 249–257. https://doi.org/10.1016/j.wasman.2021.06.012

Domingues, R.R., Trugilho, P.F., Silva, C.A., de Melo, I.C.N.A., Melo, L.C.A., Magriotis, Z.M., Sánchez-Monedero, M.A., 2017. Properties of biochar derived from wood and high-nutrient biomasses with the aim of agronomic and environmental benefits. PLoS One 12. https://doi.org/10.1371/journal.pone.0176884

Farah Nadia, O., Xiang, L.Y., Lie, L.Y., Chairil Anuar, D., Mohd Afandi, M.P., Azhari Baharuddin, S., 2015. Investigation of physico-chemical properties and microbial community during poultry manure co-composting process. J Environ Sci (China) 28, 81–94. https://doi.org/10.1016/j.jes.2014.07.023

Hesterberg, D., McNulty, I., Thieme, J., 2017. Speciation of Soil Phosphorus Assessed by XANES Spectroscopy at Different Spatial Scales. J Environ Qual 46, 1190–1197. https://doi.org/10.2134/jeq2016.11.0431

Kruse, J., Leinweber, P., Eckhardt, K.U., Godlinski, F., Hu, Y., Zuin, L., 2009. Phosphorus L2,3-edge XANES: Overview of reference compounds. J Synchrotron Radiat 16, 247–259. https://doi.org/10.1107/S0909049509000211

Li, R., Wang, J.J., Zhou, B., Awasthi, M.K., Ali, A., Zhang, Z., Lahori, A.H., Mahar, A., 2016. Recovery of phosphate from aqueous solution by magnesium oxide decorated magnetic biochar and its potential as phosphate-based fertilizer substitute. Bioresour Technol 215, 209–214. https://doi.org/10.1016/j.biortech.2016.02.125

Liang, X., Jin, Y., He, M., Niyungeko, C., Zhang, J., Liu, C., Tian, G., Arai, Y., 2018. Phosphorus speciation and release kinetics of swine manure biochar under various pyrolysis temperatures. Environmental Science and Pollution Research 25, 25780–25788. https://doi.org/10.1007/s11356-017-0640-8

Nardis, B.O., Santana Da Silva Carneiro, J., Souza, I.M.G. de, Barros, R.G. de, Azevedo Melo, L.C., 2021. Phosphorus recovery using magnesium-enriched biochar and its potential use as fertilizer. Arch Agron Soil Sci 67, 1017–1033. https://doi.org/10.1080/03650340.2020.1771699

Wang, Y., Yin, R., Liu, R., 2014. Characterization of biochar from fast pyrolysis and its effect on chemical properties of the tea garden soil. J Anal Appl Pyrolysis 110, 375–381. https://doi.org/10.1016/j.jaap.2014.10.006

CHAPTER II

Phosphate-solubilizing bacteria *Pseudomonas* sp. enhances phosphorus availability from Mg-enriched biochar *in vitro,* and P uptake in maize cultivated in soil

To be submitted to Applied soil Ecology Journal

Abstract

Biochar produced from animal manure has been investigated as a P fertilizer for plant cultivation. Thermal degradation into biochar reduces volume, sanitize the material, but transforms organic P into inorganic P, increasing stable pools and decreasing P fertilizer efficiency. Mg modification increases the Mg/Ca ratio in poultry manure and induces the Mg-P reaction during pyrolysis, enhancing P availability. The inoculation of phosphate-solubilizing bacteria (PSB) might also further increase P availability and enhance the efficiency of P fertilization of biochar. The objectives of this study were to evaluate the potential of selected PSB strains in solubilizing P from Ca and Mg phosphates and to evaluate the growth of maize plants in an Oxisol fertilized with biochar and Mg-enriched biochar. First, it was determined the P solubilization *in vitro* from Mg-P and Ca-P phosphates, poultry manure, biochar, and Mg-enriched biochar, and in an *in vivo* experiment shoot dry matter production of maize plants cultivated for 15 and 30 days. We observed that the strain *Pseudomonas* sp. was more efficient in solubilizing P from Mg-P sources ($Mg_3(PO_4)_2$ – 80% of total P added) than Ca-P sources ($Ca_3(PO_4)_2$ – 60% of total P added). And for biochars at 350 °C, this strain also released more P from Mg-biochar (Mg/Ca ratio of 0.15 - 82% of total P added) than unmodified biochar (Mg/Ca ratio of 0.06 – 74% of total P added). In maize, the effect was similar, i.e., higher P concentration in plant shoot tissues was observed with Mg-biochar fertilization and PSB inoculation, representing an increase of 37% in P uptake compared with the unmodified biochar. However, the effect was restricted for biochar produced at 350 °C and at early growth stage (15 days). In addition, and contrary to our hypothesis, neither Mg addition nor PSB inoculation caused an increase in P uptake or plant growth in treatments containing biochar produced at 500 °C. Thus, with the purpose of using poultry manure biochar as P fertilizer, lower pyrolysis temperature (350 °C) is recommended as well as enrichment with Mg and bioaugmentation with PSB, which can be as effective as soluble P fertilizer. More studies are still necessary to better understand the P transformations in biochar produced at higher pyrolysis temperatures (>350 °C), and the potential of Mg enrichment and PSB inoculation on P release.

Keywords: Pyrolysis; bacterial inoculation; maize; P uptake

1. Introduction

Phosphorus (P) is required in relatively low quantities (0.05 to 0.5% of plant dry weight) for plant growth and completion of the life cycle (Johri et al., 2015; Lambers, 2022). In plants, P occurs as organic (e.g., C-O-P bond) and inorganic (e.g., P-O-P bond) (Wieczorek et al., 2022). In soil, plants obtain P as orthophosphates from soil solution ($H_2PO_4^-$ and HPO_4^{2-}), and soil pH regulates their bioavailability (Ullrich-Eberius et al., 1984). In highly weathered soils most P-rich soluble fertilizers are subjected to losses upon contact with soil mineral fraction. The soluble P fraction available to plants can either become unavailable through the adsorption to soil oxidic mineral fraction (Matoso et al., 2022) or precipitation with cations such as Ca^{2+} and Mg^{2+} in alkaline soil and Fe^{2+} and Al^{3+} in acidic soils (Halajnia et al., 2009; Ng et al., 2022). For this reason, usually doses higher than necessary are regularly applied to increase crop productivity, which extends the cost of P fertilization for plant production (Bindraban et al., 2020; Ibrahim et al., 2022). Thus, it is necessary to use secondary P sources to reduce the pressure on P reserves and enhance P fertilization efficiency from alternative sources.

Animal manure (e.g., poultry manure), has been investigated as a P source for land application due to its P concentration (*in natura* ~1.5%), which concentrates after pyrolysis (~3%) (Wang et al., 2015). Besides, the pyrolysis of poultry manure is an alternative for reducing the application volume, stabilizing the carbon fraction, concentrating nutrients, decomposing organic pollutants, and sanitizing the raw material (Buss, 2021; Song and Guo, 2012). However, thermal degradation into biochar also transforms organic P into inorganic P, increasing the proportion of low-availability P fractions (Cui et al., 2019; Li et al., 2018). Furthermore, as poultry manure is a Ca-rich residue low available Ca-P compounds are formed at higher pyrolysis temperature (Li et al., 2018; Wang et al., 2015). Producing novel poultry manure by adding Mg to biomass before pyrolysis could be an alternative for reducing Ca-P phosphates in biochar and modifying P speciation in favor of higher P availability. For instance, adding Mg has already been reported to be a mechanism for decreasing the crystal growth propagation of hydroxyapatite during thermal treatment at high temperatures (> 500 °C) (Farzadi et al., 2014; Hilger et al., 2020; Kannan et al., 2005). Furthermore, Mg modification also increases the Mg/Ca ratio in poultry manure, and that could induce the Mg-P reaction and precipitation in biochar and could provide Mg for plant growth in low-Mg content soils.

The inoculation of phosphate-solubilizing bacteria (PSB) could also be an alternative to increase P availability in soil and, consequently, increase the efficiency of P fertilization (de Zutter et al., 2022). The PSB strains are found naturally in plant root systems, and strains from several bacterial genera, and among them, *Pseudomonas*, *Bacillus* and *Burkholderia*, are reported to be efficient P-solubilizers and can contribute to the cycling of inorganic P in soil (Elias et al., 2016; Yu et al., 2011). Several mechanisms are reported to be involved in the dissolution of inorganic P by these strains, a process known as phosphate solubilization (Alori et al., 2017). Among the mechanisms involved in P solubilization, the production and release of organic acids or media acidification by proton extrusion are reported more often (Adeleke et al., 2017). In addition to P release, organic acids can prevent P from being adsorbed to soil mineral fraction or being precipitated with Al^{3+} and Fe^{2+}, which is desirable to increase P use efficiency in tropical soils (Billah et al., 2019). Moreover, PSB involved in P solubilization may function as a labile P-C fraction, which is released into the soil upon cycling (Bünemann et al., 2004).

Contrasting proportions of P-Ca or P-Mg minerals may alter the capacity of PSB strains to release organic acids and their potential for P solubilization and plant growth. Moreover, it is still unclear whether higher proportions of Mg-P phosphates could change PSB solubilization mechanism and plant growth. Thus, the objectives of this study were (i) to evaluate the potential of selected PSB strains in solubilizing P from Ca and Mg phosphates and quantification of organic acids involved in P solubilization, (ii) to evaluate the potential of the PSB strains in solubilizing P from biochar and Mg-enriched biochar at increasing pyrolysis temperature, and (iii) to evaluate the growth of maize plants and P uptake with fertilization of biochar and Mg-enriched biochar at increasing pyrolysis temperature and bacterial inoculation. We hypothesize that (i) solubilization of P from Ca and Mg phosphates and quantification of organic acids depends more on the strain than on the P source; (ii) PSB strains have a higher potential to release P *in vitro* from Mg-enriched biochar regardless of the pyrolysis temperature and (iii) maize plant growth is higher in treatments containing Mg-enriched biochar and inoculation with PSB strains regardless of the pyrolysis temperature.

2. Materials and methods

2.1 Selected phosphate-solubilizing bacteria

This study evaluated five selected PSB strains belonging to the collection of the Laboratory of Soil biology, Microbiology, and Biologic processes at the Department of Soil Science of the Federal University of Lavras (UFLA), Brazil. The identification of the strains is as follows: *Paraburkholderia fungorum* (UFLA 04-155), *Pseudomonas* sp. (UFPI B5-8A), *Paenibacillus* sp. (UFLA 03-116), *Acinetobacte*r sp. (UFLA 03-09), and *Rhizobium tropici* (CIAT 899). These strains have been previously identified, and details of the origin, solubilization of iron and calcium phosphates both *in vitro* and *in vivo*, plant growth-promoting characteristics, and accession numbers of 16S rRNA gene sequence can be found elsewhere (da Costa et al., 2016; da Silva et al., 2012; Leite et al., 2020; Maria De Oliveira Longatti et al., 2013; Martins da Costa et al., 2015).

2.2 Growth condition and inoculation of phosphate-solubilizing bacteria

For all incubation experiments where PSB was inoculated, the bacterial strains followed the growth conditions and standardization of inoculum from methods of previous studies (Marra et al., 2012; Martins da Costa et al., 2015). Briefly, the strains were grown in Petri dishes containing Yeast Malt Agar (YMA) medium until colonies were isolated. Then, the strains were inoculated into liquid Yeast Malt (YM) medium and incubated under stirring (110 rpm) at room temperature (25 ºC) to achieve $1x10^9$ mL^{-1} of unit forming colonies (UFC) (~3 days).

2.3 Inoculation of PSB for solubilization of Calcium and Magnesium phosphates

For Ca and Mg phosphate solubilization, the National Botanical Research Institute's phosphate growth medium (NBRIP) (Nautiyal, 1999) was prepared to contain the following components per liter of solution: glucose ($C_6H_{12}O_6$ - 10 g), magnesium chloride hexahydrate ($MgCl_2 \cdot 6H_2O$ – 5 g), magnesium sulfate heptahydrate ($MgSO_4 \cdot 7H_2O$ – 0.25 g), potassium chloride (KCl – 0.2) and ammonium sulfate [$(NH_4)_2SO_4$ – 0.1 g]. The reference Ca-P and Mg-P standards chosen to supplement the NBRIP medium (1000 mg L^{-1} of P) are as indicated: trimagnesium phosphate [$(Mg_3(PO_4)_2$], magnesium phosphate dibasic ($MgHPO_4.3H_2O$), tricalcium phosphate [$Ca_3(PO_4)_2$)], calcium phosphate dibasic ($CaHPO_4.2H_2O$) and struvite ($MgNH_4PO_4$). Each P standard was evaluated in an individual assay, following a completely randomized design, with six treatments and four replicates each, totaling 24 experimental units.

The treatments consisted of inoculating the five bacterial strains mentioned and a non-inoculated treatment for each P source (plus a control without P). These sources were individually incorporated as a powder (< 0.25 μm) into NBRIP medium, the pH was adjusted to 7.0 using hydrochloric acid 1:10 (v/v), and 50 mL of NBRIP medium was added into 125 mL Erlenmeyer's flasks before autoclaving for 20 min at 121 ºC. After cooling to room temperature, each flask received 1.0 mL of the inoculum. Finally, the treatments were incubated for seven days at room temperature on an orbital shaker and kept at constant stirring (110 rpm). After incubation, samples were placed in centrifuge tubes, centrifuged at 3900 rpm (~3214 g) for 10 min, and the supernatant was filtered through quantitative filter paper. Phosphate concentration (mg L^{-1}) in the supernatant was measured using inductively coupled plasma optical emission spectroscopy (ICP-OES). The pH was measured, and part of the extract was also used to identify and quantify organic acids.

2.4 Identification and quantification of organic acids of low molecular weights (OAs) after PSB incubation

According to the P-Ca and P-Mg solubilization results (Figure 1), the strains UFLA 04-155, UFPI B5-8A and UFLA 03-116 were chosen to identify and quantify OAs released (mg L^{-1}) in the medium using high-performance liquid chromatography (HPLC) with controller CBM-20A (Shimadzu corp., Kyoto, Japan). The retention times of analytical OAs standards were as follows: oxalic (9.18 min), citric/maleic (11.58 min), gluconic/tartaric (12.37 min), malic (13.65 min), malonic (14.05 min), lactic (17.09 min), formic (18.58 min) and fumaric (21.37 min). The spectra of the standard mix at a concentration of 10 mg L^{-1} are in Figure S1. The supernatant collected as mentioned and standards were filtered with a 0.45-μm membrane filter (Polyvinylidene fluoride) and injected (20 μL) into a Supelcogel 9 μm C-610H 30 cm × 7.8 mm chromatographic column (Supelcogel, Sigma Aldrich, Missouri, EUA). The mobile phase used was 0.1% H_3PO_4 (v/v) in a flow rate of 0.5 mL $minute^{-1}$ for 45 minutes and at 210 nm wavelength using a diode array detector (DAD). Based on the positive results from P release and OAs, the strains UFLA 04-155 and UFPI B5-8A were selected for the following P dissolution essay (poultry manure and biochar).

2.5 Processing and pyrolysis of poultry manure

Poultry manure biomass was collected in Lavras, Minas Gerais State, Brazil in a laying poultry farm with an average of 60% moisture. The biomass was oven-dried at 70 ºC until constant mass, ground, and sieved (< 850 µm) before pyrolysis. Some of the poultry manure was pre-treated with magnesium hydroxide [$Mg(OH)_2$] to achieve Mg/Ca ratios of 0.06, 0.15 and 0.26. Briefly, $Mg(OH)_2$ was mixed with dried poultry manure to achieve Mg/Ca ratios of 0.06, 0.15 and 0.26, soaked in deionized water (1:10, solid-liquid ratio), and stirred with a magnetic ball for 30 min. The mixture was oven-dried at 60 ºC (until constant mass). More details on Mg enrichment can be found elsewhere (Zhang et al., 2012). All biochars were produced in a laboratory-scale muffle furnace, and the process was performed with a heating rate of 5 ºC min^{-1} to the target temperatures of 350º C, 500º C, or 650 ºC, with a holding time of 30 min, and left to slowly cool down to room temperature. At the end of each cycle, the biochar yield was recorded. Characterization for total contents of P, Ca and Mg followed the nitric digestion procedure (Enders and Lehmann, 2012), and total elements were measured by ICP and the results are shown in Table 1.

Table 1. Elemental analysis of magnesium hydroxide modified poultry manure and biochar as a function of magnesium and calcium ratios.

Mg/Ca ratio	T (°C)	P	Ca	Mg	Biomass Yield
		g/kg			%
0.06	70	17.3 ± 0.3	117.5 ± 1.1	5.8 ± 0.1	-
	350	33.6 ± 0.1	215.7 ± 0.5	13.4 ± 0.1	49.9 ± 1.3
	500	32.4 ± 0.2	230.1 ± 2.6	13.4 ± 0.2	47.7 ± 0.4
	650	34.0 ± 1.0	230.1 ± 10.2	14.1 ± 0.5	46.3 ± 0.4
0.15	70	19.0 ± 0.3	121.0 ± 22.7	18.8 ± 1.4	-
	350	32.1 ± 0.5	218.1 ± 4.4	32.0 ± 0.3	53.6 ± 0.5
	500	35.9 ± 1.3	236.2 ± 10.2	35.2 ± 1.5	48.8 ± 0.3
	650	38.3 ± 0.1	245.8 ± 1.6	37.3 ± 0.3	48.3 ± 0.5
0.26	70	18.0 ± 0.7	97.5 ± 3.6	26.4 ± 1.1	-
	350	32.6 ± 0.4	184.9 ± 2.8	45.3 ± 0.9	52.7 ± 0.5
	500	36.9 ± 1.3	195.4 ± 5.5	50.8 ± 1.3	47.2 ± 0.3
	650	39.4 ± 0.5	202.9 ± 5.7	53.3 ± 0.6	42.4 ± 1.6

Note: mean value ± standard deviation (n=3).

2.6 Phosphorus dissolution from poultry manure and biochar

The strains UFLA 04-155 and UFPI B5-8A were selected to study P solubilization from poultry manure and biochar based on their potential for P release from Ca-P and Mg-P sources mentioned. P dissolution of poultry manure and biochar of different Mg/Ca ratios followed the same procedure of growth condition and inoculation of PSB as in the Ca-P and Mg-P solubilization experiment, except that a lower P concentration was used individually (100 mg L^{-1} of P) as biochar and poultry manure samples have much lower P concentration than P standards.

The P solubilization experiment of biochar and poultry manure followed a completely randomized design. Each temperature in which poultry manure and biochar were processed (70, 350, 500, or 650 ºC) and added to NBRIP medium at specific Mg/Ca ratios (0.06, 0.15 or 0.26), following in by inoculation of either with UFLA 04-155 or UFPI B5-8A. A non-inoculated control was added for each temperature, totaling nine treatments and four replicates each (36 experimental units). Description of treatments for each temperature as follows: Mg/Ca 0.06 (T1); Mg/Ca 0.06 + UFLA 04-155 (T2); Mg/Ca 0.06 + B5-8A (T3); Mg/Ca 0.15 (T4); Mg/Ca 0.15 + UFLA 04-155 (T5); Mg/Ca 0.15 + UFPI B5-8A (T6); Mg/Ca 0.26 NI (T7); Mg/Ca 0.26 + UFLA 04-155 (T8); Mg/Ca 0.26 + UFPI B5-8A (T9). As control treatments, individual essay containing K_2HPO_4 (100 mg L^{-1}) was included as positive control, and no P as negative control, both with and without inoculation (Figure S2). Similarly, after incubation, the samples were centrifuged at 3900 rpm for 10 min, and the supernatant was filtered through quantitative filter paper. The pH was measured. Phosphate concentration in the supernatant was measured using ICP. In addition, the remaining pellet in the centrifuge tubes at treatments 1 to 6 and (500 ºC) was dried (50 °C), milled (< 0.149 µm), and used for FTIR characterization.

2.7 Fourier transform infrared spectroscopy (FTIR)

Infrared spectroscopy analyzes of poultry manure and biochar post P dissolution essay were performed using a 600-IR FT-IR spectrometer (Varian, California, USA) with Fourier transform (FTIR), and a GladiATR accessory (Pike Technologies, Wisconsin, USA) coupled for measurements by attenuated total reflectance (ATR) at 45° with selenide crystal of zinc. The spectral range analyzed was from 4000−400 cm^{-1}, and resolution of 4cm^{-1} and 64 scans. Spectra were processed for baseline correction using Origin Pro v9.90 (Originlab Corp, Massachusetts, USA).

2.8 Bioassay experiment

A bioassay experiment was carried out at the Federal University of Lavras (Minas Gerais State, Brazil) to investigate how P availability is affected by Mg enrichment in poultry manure biochar and PSB inoculation. Biochars produced at 350 and 500 °C and Mg/Ca ratios of 0.06 and 0.15 were selected to study maize plant growth and P uptake. The experiment consisted of inoculated (UFPI B5-8A) and non-inoculated maize plants (*Zea mays* L., hybrid BM 915 PRO) grown in pots filled with 3.0 kg of an Oxisol (sandy loam), collected from the 0–20 cm layer in Itumirim (Minas Gerais State, Brazil, 21º 17' 16'' S e 44º 48' 07" W). Before the implementation of the experiment, the soil was air-dried and sieved (< 4.0 mm) and chemically characterized for available P, K, Fe, Zn, Mn and Cu (Mehlich-1), pH in water (1:2.5 w/v), exchangeable Ca, Al and Mg (KCl 1.0 mol L^{-1}) and organic matter content ($Na_2Cr_2O_7$ and H_2SO_4). Potential acidity (H+Al) was estimated with SMP buffer solution method, remaining P was measured after reacting 60 mg L^{-1} of P in 0.01 mol L^{-1} $CaCl_2$ solution. Boron (B) was measured colorimetrically after extraction with hot water, and sulfate (S-SO_4) was measured by ICP-OES after extraction with 500 mg L^{-1} calcium phosphate solution. Other soil fertility parameters (SB – sum of base; t – effective CEC; T – potential CEC; V – Ca+Mg+K saturation; and m – aluminum saturation) were calculated. Soil granulometry (sand, silt, and clay) were estimated using the densimeter method. The chemical and granulometry soil analysis were performed following methods from Silva et al. (2012) (Table 2).

Table 2. Soil characteristics before the implantation of the experiment.

pH	P	K	Ca^{2+}	Mg^{2+}	Al^{3+}	H + Al	SB	t	T	V	m
4.9	--- mg dm^{-3} ---		----------$cmol_c$ dm^{-3} ----------							-------%--------	
	0.0	28.5	0.5	0.2	0.3	3.0	0.8	1.1	3.8	21.9	26.3

OM	P-rem	Zn	Fe	Mn	Cu	B	S-SO_4	Sand	Silt	Clay
- g kg^{-1} -	- mg L^{-1} -	---------- mg dm^{-3} ----------						---------- g kg^{-1} ----------		
1.3	37.1	0.5	29.0	2.6	0.4	0.0	2.6	720	60	220

Note: pH (H_2O); available-P (Mehlich-1); SB – sum of exchangeable bases; t – effective cation exchange capacity; T – potential cation exchange capacity (pH 7.0); V – index of Ca+Mg+K saturation; m – aluminum saturation Index; MO – organic matter; P-rem – remaining P.

Liming was performed to increase the base saturation to 60% using calcium carbonate ($CaCO_3$) and magnesium carbonate ($MgCO_3$) (at 3:1 ratio). The soil was homogenized and incubated for 30 days with moisture maintained at 70% of the field capacity with water replacement by weight every week. The experiment consisted of 10 treatments conducted in a completely

randomized design (DIC) with four replicates and 40 experimental units. The treatments were set up based on biochar as a P source at a concentration of 100 mg kg^{-1} calculated according to total content P (modified dry-ashing digestion) and were added as a powder (<850 µm) before planting (Table S1). Treatment identification is as follows: T1 (TSP - Triple superphosphate), T2 (350 °C Biochar Mg/Ca 0.06), T3 (350 °C Biochar Mg/Ca 0.06 + UFPI B5-8A), T4 (350°C Biochar Mg/Ca 0.15), T5 (350 °C Biochar Mg/Ca 0.15 + UFPI B5-8A), T6 (500 °C Biochar Mg/Ca 0.06), T7 (500 °C Biochar Mg/Ca 0.06 + UFPI B5-8A), T8 (500 °C Biochar Mg/Ca 0.15), T9 (500 °C Biochar Mg/Ca 0.15 + UFPI B5-8A) and T10 (control - no P added).

Before planting, maize seeds were sterilized (98% ethanol and 2% sodium hypochlorite), washed, and incubated for 72 h at 28 °C for the emergence of rootlets. Four pre-germinated seeds were sown per pot. In treatments containing inoculation, 2 mL of bacterial culture was inoculated per seed (10^9 CFU per seed), and non-inoculated treatments received the liquid media (YM) without bacterial cells. Before basic fertilization, only two plants were left in each pot, and four days after planting, basic nutrient fertilization was added as a solution for all treatments (Novais, 1991). The nutrients were applied in mg per pot from the following sources: N [KNO_3 and $(NH_4)_2SO_4$ – 150], S [$(NH_4)_2SO_4$ – 40], K (KNO_3 – 50), B (H_3BO_3 – 0.8), Cu ($CuSO_4.5H_2O$ – 1.5), Fe ($FeCl_3$ – 3), Mg ($MnCl_2.4H_2O$ – 3.5), Mo ($Na_2MoO_4.2H_2O$ – 0.1), Zn ($ZnSO_4.7H_2O$ – 5). The N and K. After 15 and 30 days of sowing, shoots were harvested, oven-dried at 60 °C for 72 h and milled (< 1 mm) for chemical analysis. It was determined shoot-dry matter (g per plant) and P chemical composition in tissues (g kg^{-1} $_{dry\text{-}basis}$), P accumulation (mg per plant). Briefly, 200 mg (± 0.05 mg) of shoot tissues were digested in a block digestion system, progressively increasing temperature to achieve 200 °C (~4 h), using 6 mL of nitric acid and perchloric acid mixture at a ratio of 1:2 (2 mL HClO + 4 mL HNO_3) (Malavolta, 1980). Posteriorly, digested samples were diluted to 50 mL using deionized water, and P concentration was measured by ICP-OES.

3. Data analysis

Prior to other analyses, the collected data from P dissolution and greenhouse experiments were checked for normality and variance homogeneity by the Shapiro–Wilk's and Levene's tests, respectively. When the criteria for ANOVA analysis were not satisfied (as in P dissolution from Ca-P, Mg-P, poultry manure, and biochars), the significance of a generalized least squares (GSL) model was tested, observing the accuracy of the model based on the Akaike criterion (AIC)

(Akaike, 1974). When significant differences were observed, the means of the treatments were compared by the Tukey test ($p \leq 0.05$). When data met the criteria for ANOVA analysis (as in the greenhouse experiment), analysis of variance was performed, and the means of the treatments were clustered by the Scott-Knott test ($p \leq 0.05$). All data analysis was performed in *R software* with interface *RStudio*, v. 1.3.1056.

4. Results

4.1 Phosphorus release from Ca and Mg phosphates

Phosphorus released from Ca-P and Mg-P sources significantly increased with PSB inoculation, and solubilization potential varied between P sources and strains (Figure 1). Except for struvite ($MgNH_4PO_4$), the strains UFLA 04-155 and UFPI B5-8A released the highest amount of P for all phosphate sources. These strains completely solubilized the $CaHPO_4.2H_2O$ and $MgHPO_4.3H_2O$. However, the solubilization of $Ca_3(PO_4)_2$ and $Mg_3(PO_4)_2$ was at a much lower intensity, and the strain UFLA 04-155 was more efficient in solubilizing $Ca_3(PO_4)_2$, while the strain UFPI B5-8A was more efficient at $Mg_3(PO_4)_2$. For instance, UFLA 04-155 released 75% of the P supplemented as $Ca_3(PO_4)_2$, while UFPI B5-8A released around 60% of this P source. In contrast, at P supplemented as $Mg_3(PO_4)_2$, UFPI B5-8A released 80%, while UFLA 04-155 released 47%. For most P sources, the strain UFLA 03-116 had the lowest solubilization potential compared to the other strains studied. However, it was more efficient in solubilizing $MgNH_4PO_4$ than UFLA 04-155 and UFPI B5-8A, releasing 44% of the supplemented P, while the other two released less than 20%.

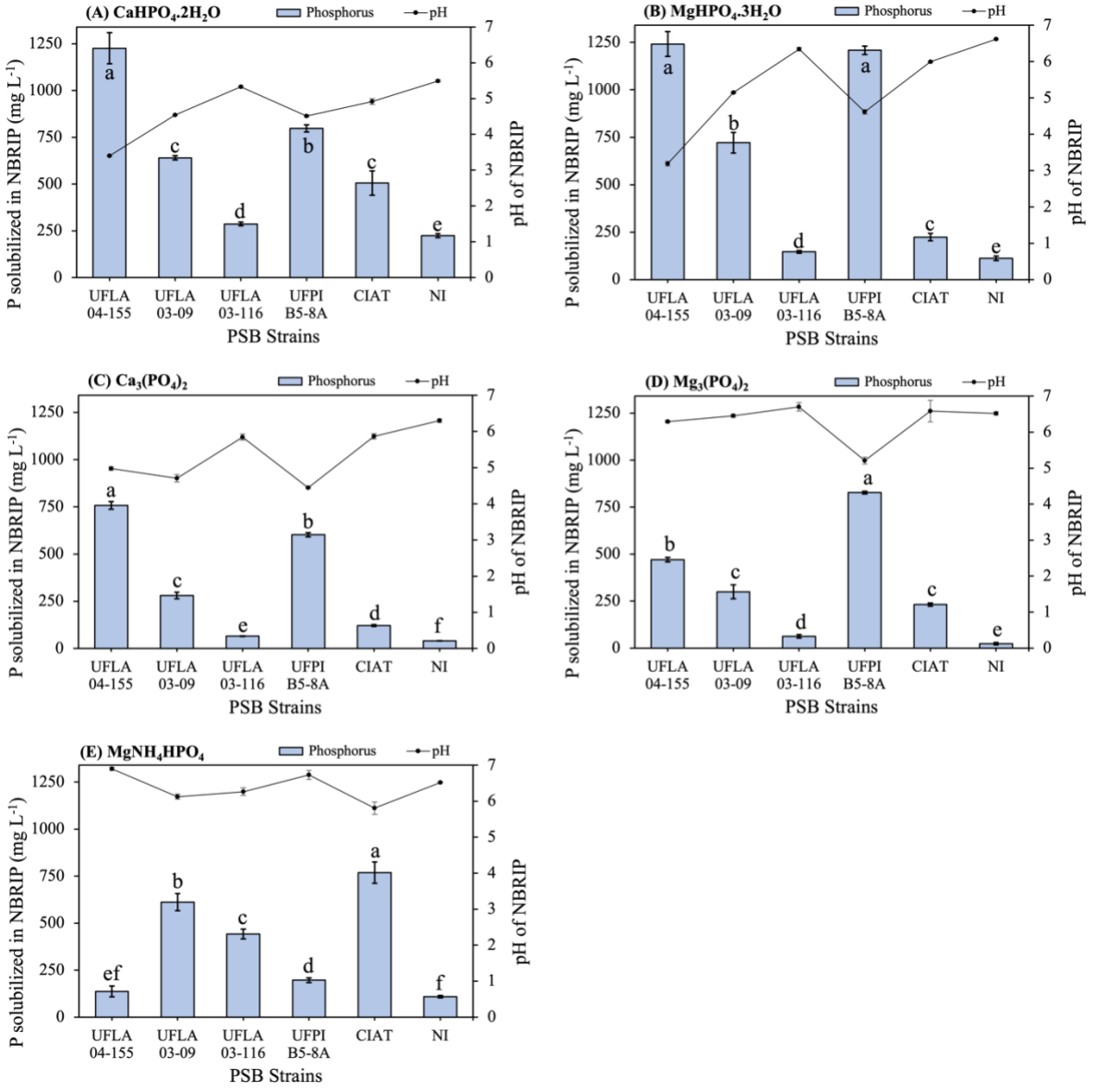

Figure 1. Soluble phosphorus (mg L^{-1}) and pH determined in liquid NBRIP medium containing phosphate sources after seven days after bacterial inoculation. Mean values ± standard deviation; n = 4. The letters above the bars compare the means of the treatments by the Tukey test ($p < 0.05$). Note: NI, non-inoculated.

The pH of NBRIP media after PSB solubilization decreased at high P solubilization treatments (Figure 1). However, pH varied more as a function of PSB inoculation. For instance, UFLA 04-155 decreased pH to around 3.3 for $CaHPO_4.2H_2O$ and $MgHPO_4.2H_2O$, and at a much lower intensity, decreased to 5.0 and 6.3 at $Ca_3(PO_4)_2$ and $Mg_3(PO_4)_2$ solubilization, respectively, while for $MgNH_4PO_4$, pH did not decrease. As for UFPI B5-8A, the pH was around 4.7 for all the

P sources except for $MgNH_4PO_4$, where the pH did not decrease when compared to control. However, pH decrease was not associated with higher P release for UFLA 03-116, where the highest solubilization level was recorded at pH 6.3 ($MgNH_4PO_4$). In contrast, for $Ca_3(PO_4)_2$ solubilization, this strain released less P at lower pH (5.8).

The organic acid release was associated with a high soluble P found in the medium after incubation. However, in agreement with soluble-P results, OAs production increased with PSB inoculation, and the amount and types varied more between strains than P sources (Table 3). For the strain UFLA 04-155, the acids released were mainly citric/maleic acids, in a concentration of ~200 mg L^{-1} for $Ca_3(PO_4)_2$, $CaHPO_4$, and $MgHPO_4$, and it was below detection limit for $MgNH_4PO_4$ and $Mg_3(PO_4)_2$, in which the P release was low for this strain. For UFPI B5-8A, the primary acid was gluconic/maleic at a concentration of ~1400 mg L^{-1} for all the sources studied, except for $MgNH_4PO_4$, where this acid was not identified, and a low P release was also recorded. For the strain UFLA 03-116, all the studied organic acids were undetected or detected in small amounts in P sources where this strain showed a low solubilization potential. However, for solubilization of $MgNH_4PO_4$, UFLA 03-116 released malic and fumaric acid at 251 and 35 mg L^{-1}, respectively. These acids were released about 25 and 5-fold higher than other strains at the same P source or other P sources studied, respectively.

Table 3. Identification and quantification of organic acids (mg L^{-1}) in liquid NBRIP medium containing phosphate sources after seven days of bacterial cultivation.

Strain	P source	Oxalic	Citric/ Maleic	Tartaric/ Gluconic	Malic	Malonic	Lactic	Formic	Fumaric	Total
		mg L^{-1}								
UFLA 04-155	$Ca_3(PO_4)_2$	0.9 ± 0.0	206.3 ± 11.7	2.8 ± 0.1	33.0 ± 1.0	-	-	0.1 ± 0.0	0.6 ± 0.0	245.7
	$CaHPO_4$	0.7 ± 0.0	208.7 ± 7.2	4.2 ± 0.1	8.9 ± 0.8	37.3 ± 3.8	0.2 ± 0.0	0.1 ± 0.0	0.5 ± 0.0	263.7
	$MgNH_4PO_4$	1.7 ± 0.8	-	-	-	-	0.8 ± 0.0	0.2 ± 0.0	0.6 ± 0.1	3.3
	$MgHPO_4$	0.6 ± 0.0	201.1 ± 5.5	43.7 ± 3.0	7.6 ± 1.4	29.0 ± 5.8	10.3 ± 0.6	0.7 ± 0.5	0.8 ± 0.1	428.6
	$Mg_3(PO_4)_2$	10.5 ± 0.3	-	99.6 ± 8.5	9.8 ± 1.6	48.4 ± 5.9	2.5 ± 0.1	1.0 ± 0.1	6.9 ± 0.7	218.0
UFPI B5-8A	$Ca_3(PO_4)_2$	1.2 ± 0.0	-	1595.0 ± 81.8	10.4 ± 2.0	45.5 ± 0.6	0.3 ± 0.0	0.5 ± 0.1	0.2 ± 0.0	1,653.0
	$CaHPO_4$	0.8 ± 0.1	-	684.4 ± 86.0	5.6 ± 1.0	29.0 ± 4.6	0.2 ± 0.0	0.3 ± 0.1	-	720.2
	$MgNH_4PO_4$	7.2 ± 2.6	-	-	-	9.6 ± 2.2		0.1 ± 0.0	-	16.9
	$MgHPO_4$	1.0 ± 0.2	-	1488.1 ± 42.6	7.0 ± 0.8	45.3 ± 17.3	0.2 ± 0.0	0.4 ± 0.1	0.2 ± 0.0	1,542.2
	$Mg_3(PO_4)_2$	0.7 ± 0.0	-	1830.0 ± 263.5	-	-	0.3 ± 0.0	0.7 ± 0.1	0.4 ± 0.0	1,832.1
UFLA 03-116	$Ca_3(PO_4)_2$	0.6 ± 0.0	-	4.0 ± 0.3	18.2 ± 2.0	-	0.4 ± 0.0	0.7 ± 0.0	0.4 ± 0.0	50.9
	$CaHPO_4$	0.6 ± 0.0	-	4.6 ± 0.2	5.0 ± 3.2	-	0.2 ± 0.0	0.4 ± 0.1	0.7 ± 0.2	21.1
	$MgNH_4PO_4$	5.1 ± 1.7	-	-	250.8± 35.6	-	-	-	34.9 ± 4.3	290.7
	$MgHPO_4$	0.6 ± 0.0	-	4.5 ± 0.2	11.5 ± 1.2	-	0.5 ± 0.2	0.7 ± 0.1	0.6 ± 0.0	36.2
	$Mg_3(PO_4)_2$		-	4.1 ± 0.1	41.9 ± 9.4	-	0.2 ± 0.0	0.4 ± 0.1	0.3 ± 0.0	46.8
NI	$Ca_3(PO_4)_2$	0.6 ± 0.0	-	5.6 ± 0.2	35.8 ± 3.2	-	-	0.3 ± 0.0	-	126.6
	$CaHPO_4$	0.56 ± 0.0	-	5.5 ± 0.1	12.8 ± 1.6	-	-	-	-	90.5
	$MgNH_4PO_4$	0.7 ± 0.0	-	5.8 ± 0.1	6.1 ± 1.4	-	-	0.1 ± 0.0	-	33.7
	$MgHPO_4$	0.6 ± 0.0	-	5.6 ± 0.1	14.2 ± 1.4	-	-	0.1 ± 0.0	-	87.9
	$Mg_3(PO_4)_2$	0.5 ± 0.0	-	5.5 ± 0.1	30.5 ± 4.0	-	0.1 ± 0.0	0.1 ± 0.0	-	60.1

Note: NI, non-inoculated. Mean values ± standard deviation; n = 4.

4.2 Properties of poultry manure and biochar

After pyrolysis, total P concentrations in biochar increased on average 2-fold irrespective of Mg addition or pyrolysis temperature (Table 2). However, total P increased more at higher temperatures in treatments that have received Mg. For instance, at 650 °C, the total P at Mg/Ca of 0.15 and 0.26 was 11.2 and 13.7% higher, respectively, than P at Mg/Ca ratio of 0.06. Total Ca increased with pyrolysis but decreased at the highest Mg/Ca ratio of 0.26. For instance, the total

concentration of Ca at Mg/Ca ratio of 0.26 corresponds, on average, to ~87% of total Ca recorded at Mg/Ca ratio of 0.06. Finally, total Mg increased as a function of Mg addition, but no relevant differences were observed among pyrolysis temperatures.

4.3 Phosphorus release from poultry manure and biochars

Regarding P release from biochars, the strain UFPI B5-8A released a higher amount at all pyrolysis temperatures studied (Figure 2). Besides, regardless of Mg/Ca ratios, P release from this strain was 2-fold higher compared to UFLA 04-155 and 4-fold higher compared to non-inoculated control. Concerning Mg/Ca ratios, at 350 °C, UFPI B5-8A and UFLA 04-155 released more P at the Mg/Ca ratio of 0.15, where these strains released 9.5% and 6.0% higher P compared to Mg/Ca of 0.06, representing an increase of 7.1 and 3.3 mg L^{-1} in P release. Furthermore, at 500 and 650 °C, Mg addition did not increase P solubilization.

For poultry manure (dried at 70 °C), the amount of soluble P was low for all treatments, regardless of Mg/Ca ratios and PSB inoculation. The maximum amount of P released was recorded for UFLA 04-155 at Mg/Ca of 3 (29 mg L^{-1}), which is 2.4 and 2.9-fold higher comparing the same Mg/Ca ratio for non-inoculated and inoculated with UFPI B5-8A, respectively.

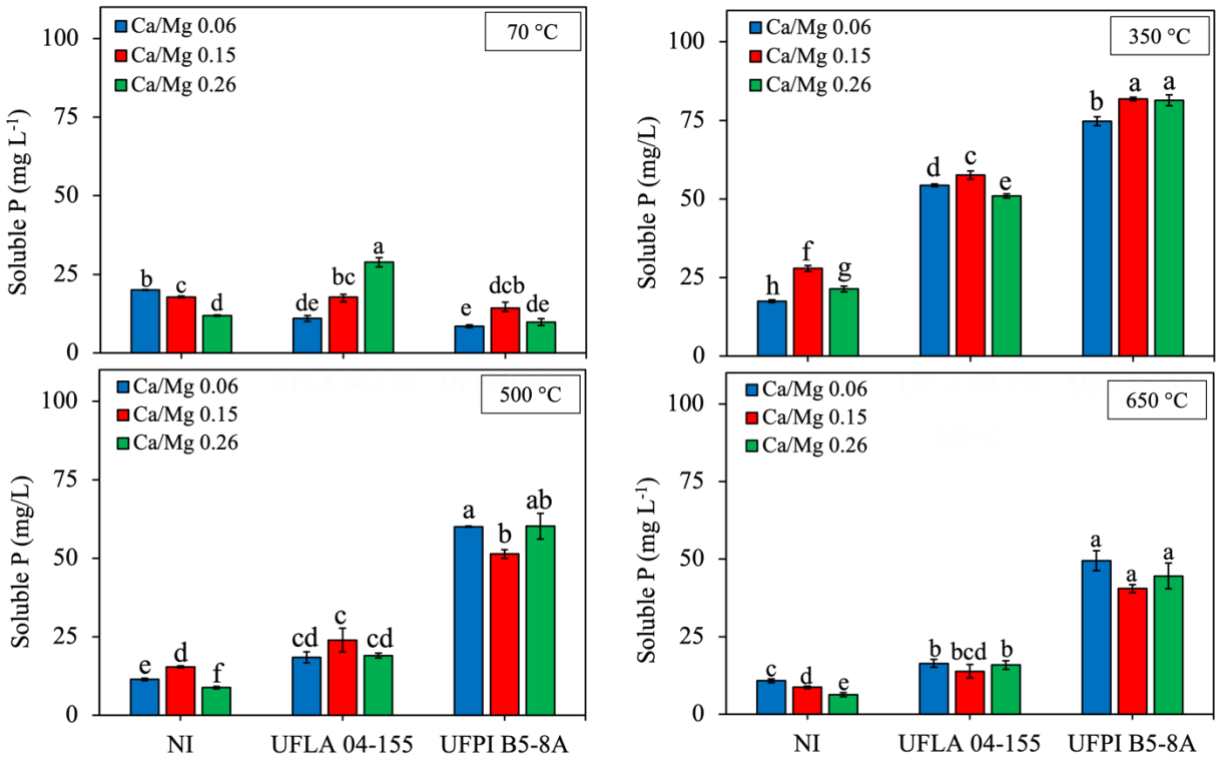

Figure 2. Soluble phosphorus (mg L^{-1}) in liquid NBRIP medium after 7 days incubation of poultry manure at several Mg/Ca ratios, pyrolysis temperature, and bacterial inoculation. Mean values ± standard deviation; n = 4. The letters above the bars compare the means of the treatments by the Tukey test ($p < 0.05$). Note: NI, non-inoculated.

The pH of biochar decreased when higher P solubilization was observed, but with less influence of Mg/Ca ratio or pyrolysis temperature. However, a lower pH value was not always in accordance with higher P release, but rather with the inoculated strain (Table 2), similarly as observed for Ca-P and Mg-P solubilization and control without P and with K_2HPO_4 (Table S2). The pH at inoculation with UFPI B5-8A was kept at an average of 4.3, and, as observed, the amount of P solubilization increased or decreased depending on the biochar. The same trend was observed with the inoculation of UFLA 04-155. For instance, for biochar produced at 500 and 650 °C, this strain kept media pH at an average of 5.2, while non-inoculated treatments have a pH of around 7.6 and with both presenting similar ranges of soluble P.

Table 4. pH of liquid NBRIP medium after 7 days incubation of poultry manure at several Mg/Ca ratios, pyrolysis temperature, and bacterial inoculation. P release referring to this pH in figure 2.

Mg/Ca	NBRIP pH		
	70 °C		
	NI	UFLA 04-155	UFPI B5-8A
0.06	7.0 ± 0.1	7.6 ± 0.2	8.1 ± 0.2
0.15	7.1 ± 0.1	8.3 ± 0.6	8.7 ± 0.1
0.26	7.4 ± 0.1	7.4 ± 0.1	8.0 ± 0.2
		350 °C	
0.06	7.3 ± 0.3	5.6 ± 0.1	4.4 ± 0.0
0.15	7.4 ± 0.1	5.4 ± 0.2	4.8 ± 0.2
0.26	7.6 ± 0.2	5.2 ± 0.1	4.6 ± 0.2
		500 °C	
0.06	7.3 ± 0.1	5.0 ± 0.1	4.4 ± 0.0
0.15	7.6 ± 0.0	5.0 ± 0.0	4.4 ± 0.0
0.26	7.7 ± 0.2	5.0 ± 0.4	4.3 ± 0.1
		650 °C	
0.06	7.6 ± 0.1	5.0 ± 0.1	3.7 ± 0.1
0.15	7.6 ± 0.0	5.7 ± 0.1	4.4 ± 0.2
0.26	7.9 ± 0.1	4.8 ± 0.1	3.5 ± 0.1

Note: NI, non-inoculated. Mean values ± standard deviation; n = 4.

4.4 FTIR spectra of biochar after phosphate-solubilizing bacterial inoculation

Most of the peaks still present in biochars after P dissolution are contained in the fingerprint region between 1600 and 400 cm^{-1}. The highest peak intensity in the FTIR spectra of biochar was observed at 1020 cm^{-1}, corresponding to P-O bond or C-O bending, and it can be attributed to stretching in Ca-P or Mg-P minerals (Bekiaris et al., 2016). This peak decreased after solubilization with UFPI B5-8A. The peaks lower than 1000 cm^{-1} also correspond to P-O bonds (Bekiaris et al., 2016; Li et al., 2016), and they decrease at peaks at 935, 592 and 549 cm^{-1} for the strain UFPI B5-8A, while for UFLA 04-155 only peak at 935 cm^{-1} decreased. At 1400 and 1558 cm^{-1}, peak intensities in biochar correspond to carboxylates C-O stretching and aromatic C=C stretching, respectively (Bekiaris et al., 2016; Farah Nadia et al., 2015). After P dissolution, the peak intensity at 1400 cm^{-1} decreases and peak at 1558 cm^{-1} increases with inoculation of UFLA 04-155 and UFPI B5-8A.

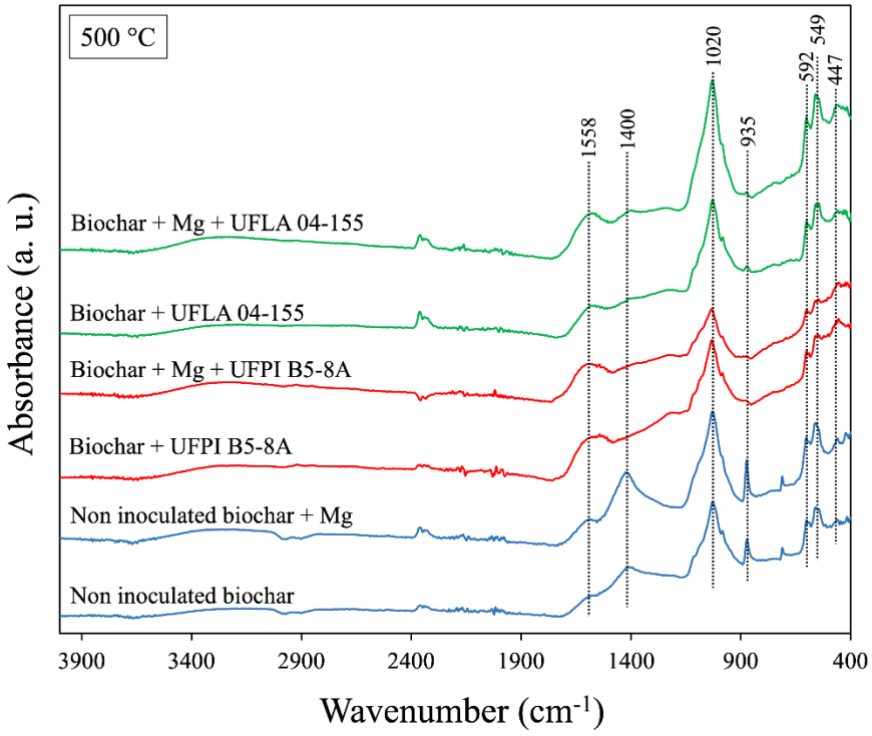

Figure 4. Fourier transform infrared spectroscopy (FTIR) spectra and spectral bands of unmodified biochar, Mg biochar, and phosphate-solubilizing bacterial inoculation.

4.4 Greenhouse experiment

4.4.1 Biomass production and P concentration in maize plants

At the harvest of 15 days after planting, the positive control (TSP) produced higher plant biomass compared to all other treatments (~2.8 g pot^{-1}) (Figure 5A). For biochar produced at 350 °C, treatments of Mg/Ca of 0.06 and 0.15 did not significantly differ among themselves for shoot dry matter production (~2.1 g pot^{-1}), which represents 75% of the TSP production. In contrast, all treatments containing biochar produced at 500 °C produced the lowest shoot biomass (~0.7 g pot^{-1}), representing only 33% of production observed in biochar at 350 °C, with no difference compared to the negative control (without P addition). Concerning the Mg/Ca ratio, the P concentration in maize shoots slightly increased at Mg/Ca of 0.16 and inoculation with UFPI B5-8A (Figure 5B). For instance, at biochar of 350 °C, the Mg/Ca of 0.15 showed 37% higher P concentration in maize shoots than observed with Mg/Ca of 0.06. The P concentration in Mg/Ca of 0.15 was 1.9 g kg^{-1}, while for Mg/Ca of 0.06, it was 1.2 mg kg^{-1}, the last not differing from the control without P. Inoculation of UFPI B5-8A increased P concentration in Mg/Ca of 0.06 to the same levels of Mg/Ca

of 0.15. Furthermore, achieving both ~77% of the P concentration when fertilized with TSP. At last, all treatments fertilized with biochar at 500 °C had the lowest P concentration in maize shoots, similar to the control without P.

The biochar at 350 °C and Mg/Ca ratio of 0.15 inoculated with UFPI B5-8A presented P accumulation in maize plants to similar levels of TSP (Figure 5C), while the non-inoculated biochars at Mg/Ca ratios of 0.06 and 0.15 did not significantly differ among themselves at this variable. Finally, in agreement with plant biomass production, P provided via biochars at 500 °C presented P accumulation similarly to the control without P.

At 30 days after planting, the positive control (TSP) produced higher amounts compared to all other treatments (~11.1 g per pot) (Figure 6A). At 350 °C, treatments with Mg/Ca ratios of 0.06 and 0.15 did not significantly differ for shoot biomass production (~7.1 g per pot). The shoot dry matter production observed for biochars at 350 °C represents 64% of TSP production, a slight reduction compared to plants harvested at 15 days. However, in contrast to 15 days after planting, biochars at 500 °C (Mg/Ca ratio of 0.06) produced 46% higher shoot biomass than Mg-biochar (Mg/Ca ratio of 0.15). As for P concentration in maize shoots, TSP was similar to biochars at 350 °C (~1.6 g kg^{-1}). At Mg-biochar at 500 °C, P concentration in plant shoots significantly differ from the control without P addition, but it was lower than 350 °C (Figure 6B). As for P accumulation, maize plant fertilized with TSP was higher than in any biochar. Finally, the level of P accumulation 30 days after planting agreed with plant biomass production, where TSP had the highest accumulation compared to all other treatments (Figure 6C).

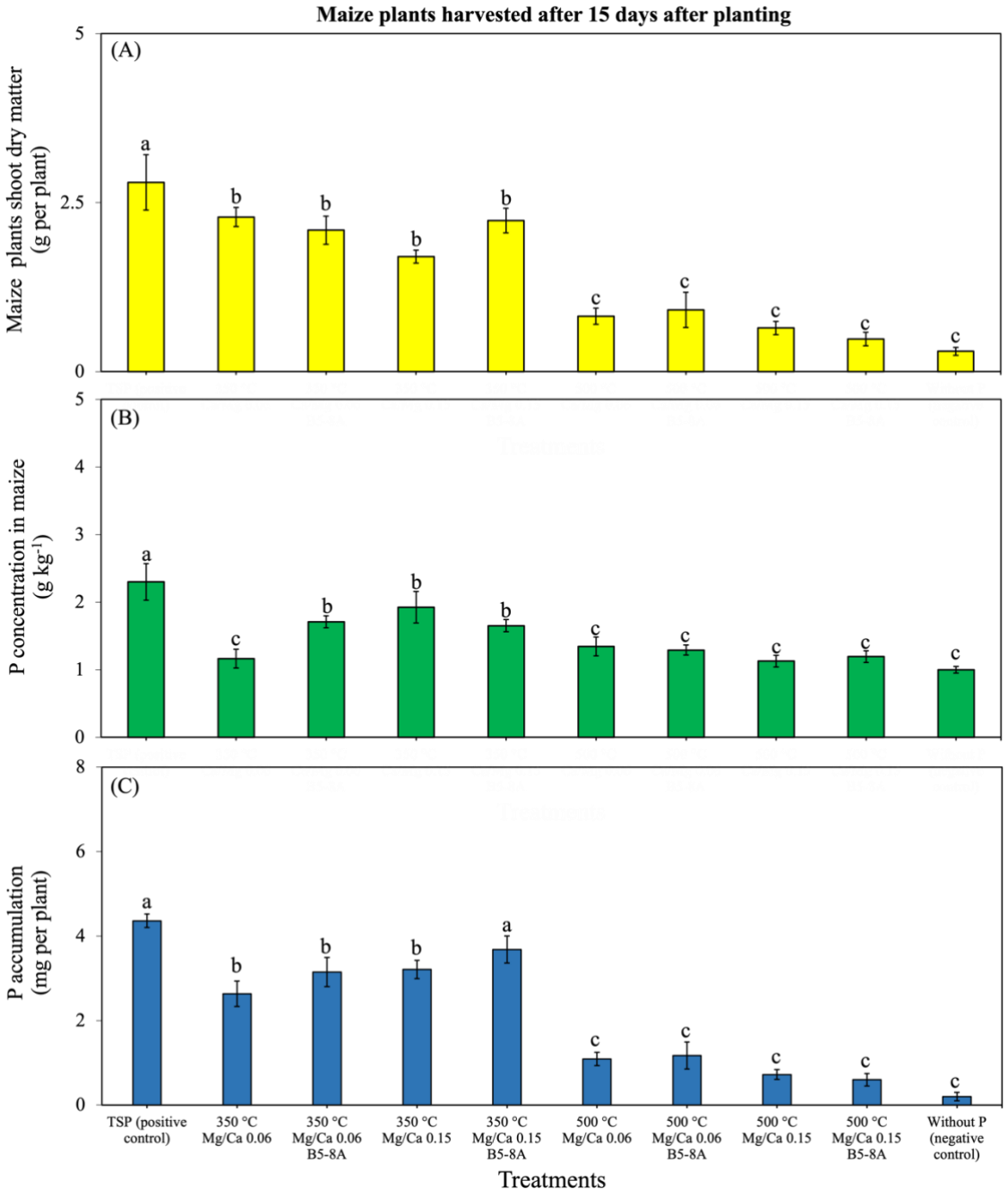

Figure 5. Maize plants shoot dry matter (g per plant) (A), phosphorus concentration in plants (g kg^{-1}) (B) and P accumulation in shoot tissues (mg per plant) (C) 15 days after planting as a function of biochar (Mg/Ca 0.06) and Mg-biochar (Mg/Ca 0.15) inoculated and non-inoculated with phosphate-solubilizing bacteria (UFPI B5-8A). TSP: Triple-superphosphate. Treatments followed by the same letter were grouped by the Scott-Knott test ($p < 0.05$). Mean values ± standard error; n = 4. P dose applied in soil: 100 mg dm^{-3}.

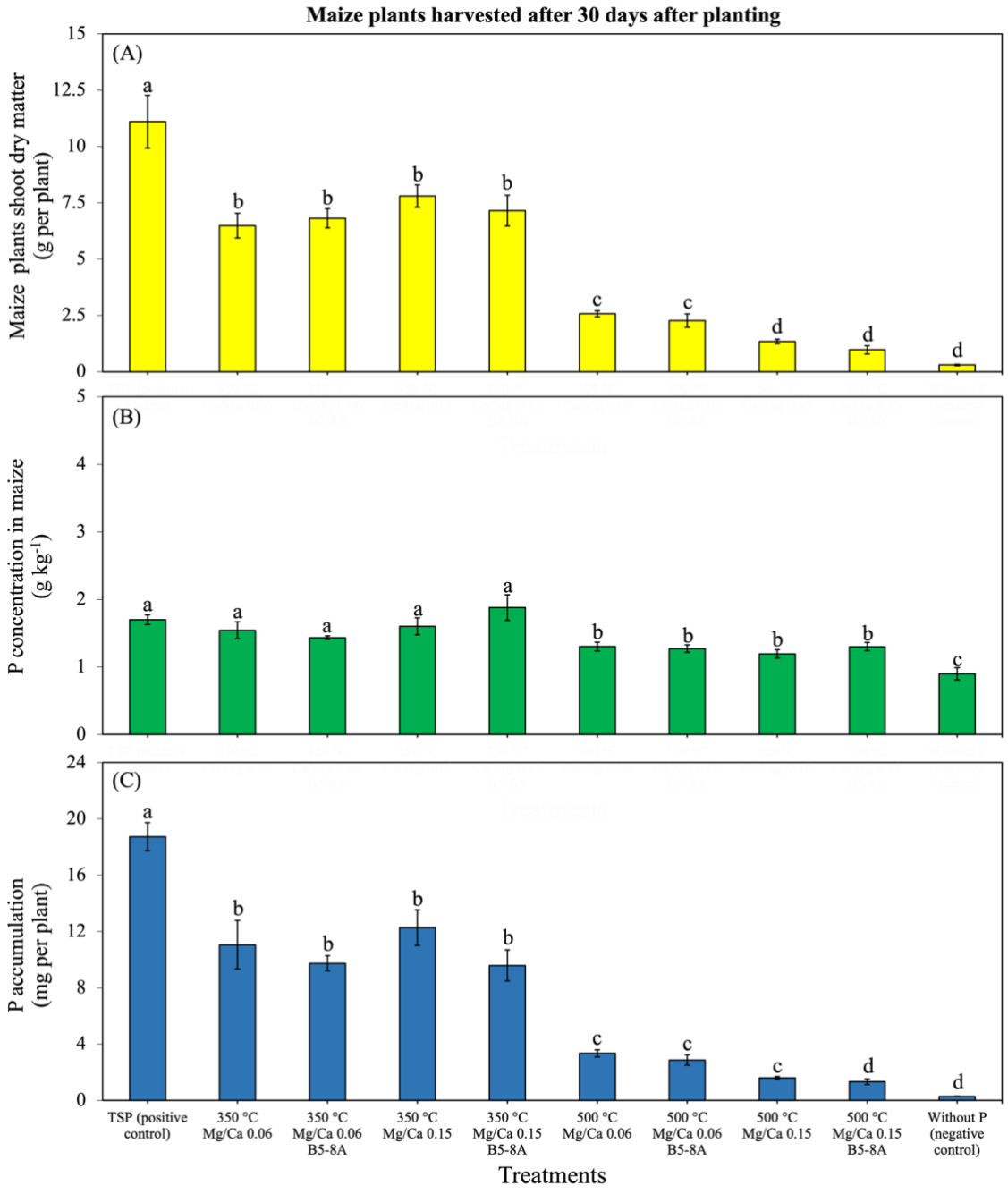

Figure 6. Maize plants shoot dry matter (g per plant) (A), phosphorus concentration in plants (g kg^{-1}) (B) and P accumulation in shoot tissues (mg per plant) (C) 30 days after planting as a function of biochar (Mg/Ca 0.06) and Mg-biochar (Mg/Ca 0.15) inoculated and non-inoculated with phosphate-solubilizing bacteria (UFPI B5-8A). TSP: Triple-superphosphate. Treatments followed by the same letter were grouped by the Scott-Knott test ($p < 0.05$). Mean values ± standard error; n = 4. P dose applied in soil: 100 mg dm^{-3}.

5. Discussion

5.1 Mg phosphates influence PSB solubilization potential and organic acids production

Phosphate-solubilizing bacteria showed contrasting solubilization potential between Mg and Ca phosphates (Figure 1). For instance, PSB inoculation was more efficient for $CaHPO_4.2H_2O$ and $MgHPO_4.3H_2O$ solubilization, phosphates that can be easily solubilized under acidic conditions since they have lower Ca/P and Mg/P ratio, and the lower is this ratio, the more acidic and soluble is the phosphate phase (Koutsoukos et al., 1979). In contrast, between $Ca_3(PO_4)_2$ and $Mg_3(PO_4)$, the strain UFLA 04-155 released more P from $Ca_3(PO_4)_2$ and the strain UFPI B5-8A from $Mg_3(PO_4)_2$, indicating that P source might induce changes on strains metabolism influencing P solubilization. In this case, organic acid production and acidification varied depending on the strain and on the P sources studied (Table 3). The strain UFLA 03-116 released malic and fumaric acids only in the presence of struvite, and the strain UFLA 04-155 have not produced citric acid for $Mg_3(PO_4)_2$ and struvite solubilization, and, as a result, P release was low. These results indicate that the P source might influence strain metabolism in favor of specific organic acid production, thus, influencing P solubilization.

The PSB strains studied also released similar concentrations of organic acids for both Ca-P and Mg-P sources, even at contrasting P solubilization (Table 3). The strain UFLA 04-155 released citric/maleic (~208 mg L^{-1}) acids in both mediums supplemented with $Ca_3(PO_4)_2$ and $Mg_3(PO_4)_2$, while the strain UFPI B5-8A released tartaric/gluconic acid (~1713 mg L^{-1}). Among solubilization mechanisms, organic acid production has already been reported as the main mechanism of inorganic P solubilization (Alori et al., 2017; Marra et al., 2019). However, metabolically pathways for its production are mainly driven by bacterial genes and environmental conditions that affect microbial growth, such as pH, C, N and P (Brown et al., 2022; Marra et al., 2015; Okoye et al., 2022). For instance, direct oxidation of glucose into high amounts of gluconic acid seems to be the primary mechanism of solubilization for the strain UFPI B5-8A since glucose is readily available in NIBRIP medium (10 g L^{-1}) (Vyas and Gulati, 2009; Whiting et al., 1976). However, it is still unknown which conditions divalent cations (e.g., Ca^{2+} and Mg^{2+}) influence the expression of genes related to organic acid production by these bacterial strains.

The differences in the amounts of organic acids released and P concentration could be explained by their potential for acidification. For instance, citric acid has lower pK_a and more carboxylic groups than gluconic acid; thus, the amounts observed in this study can be sufficient to

acidify and release P (Marra et al., 2019; Papagianni, 2007). In addition to organic acids release and acidification, medium acidification by H^+ from proton extrusion may also be a mechanism by which P release is enhanced in solubilization media (Illmer and Schinner, 1995). However, in this study, the pH of liquid media containing Ca-P and Mg-P sources was also altered as a function of the inoculated strain regardless of the P source. Thus, when adding a completely soluble P source (K_2HPO_4) in NBRIP media or at no P conditions (Figure S1), both the strains UFLA 04-155 and UFPI B5-8A decreased medium pH to similar levels as when there was insoluble P addition and solubilization (Table S2). Thus, acidification might not be solely altered driven by solubilization or in favor of higher P release but also a result of the strain metabolism, as observed for NH_4^+ assimilation and microbial respiration (de Freitas et al., 1997).

5.2 Phosphate-solubilizing bacteria enhances P release from Mg-enriched biochar

In biochars, higher P release was observed at lower pyrolysis temperature (350 °C), and as pyrolysis temperature increased, P release decreased for both strains studied (UFLA 04-155 and UFPI B5-8A) (Figure 2). That behavior is explained due to the increase in crystalline P forms in higher pyrolysis temperature biochar (Okoye et al., 2022; Xu et al., 2016), and as observed in Ca-P and Mg-P solubilization, these strains released lower amounts of P at high Ca/P and Mg/P ratio phosphates. However, besides pyrolysis temperatures, Mg addition into raw biomass before pyrolysis also influenced P release. In biochar of intermediate Mg addition (Mg/Ca 0.15), the strain UFPI B5-8A slightly released more P at 350 °C, consistent with what has been observed in Ca-P and Mg-P solubilization, where this strain released more P from $Mg_3(PO_4)_3$ than from $Ca_3(PO_4)_2$. Also, biochar may contain other P sources, such as iron and aluminum phosphates and hydroxyapatites (Bekiaris et al., 2016), which were not studied and can reduce the P release. In contrast, pyrolyzed and non-pyrolyzed biomass also influence the proportion of organic and inorganic P and P solubilization. In raw poultry manure solubilization, where a significant P proportion is in the form of organic-P (Roriz de Souza et al., 2012), the strains released lower amounts of soluble P, and had a lower potential to produce phosphatases under *in vitro* conditions (Leite et al., 2020).

Similarly to what has been observed in P release from Ca-P and Mg-P solubilization, the pH of the media containing poultry manure and biochar varied as a function of the inoculated strain (Table 4). Besides, when inoculated only minor differences were observed between pyrolysis

temperatures and the level of Mg enrichment regarding pH changes, except for pyrolyzed and non-pyrolyzed biomass. For instance, pH of unpyrolyzed poultry manure was recorded above 7 for UFLA 04-144 and UFPI B5-8A, consistent with low P release and Mg enrichment. However, pH was similar for each strain at all temperatures and levels of Mg enrichment, indicating that P release is more influenced by crystallinity and speciation of the P source, which is modified due to pyrolysis and Mg enrichment, and less with pH.

Generally, P release in biochar was higher for UFPI B5-8A than for UFLA 04-155, and the decrease in FTIR spectra peak intensities in P chemical bonds are consistent with this result (Figure 4). For instance, at 500 °C, inoculation of UFLA 04-155 did not reduce peak intensities of Ca-P and Mg-P at 1020, 592 and 594 cm^{-1} (Bekiaris et al., 2016; Li et al., 2016) decreasing only peak intensity at 935 cm^{-1}, which is attributed to lower crystallinity Ca-P. In contrast, all peak intensities concerning P bonds were reduced with UFPI B5-8A inoculation, which is consistent with the higher P release recorded for this strain. Regarding C chemical bonds, peak intensities at 1400 cm^{-1}, which corresponds to carboxylates C-O stretching (Bekiaris et al., 2016; Farah Nadia et al., 2015), decreased for the two strains, indicating that they might have assimilated this C source from biochar. Furthermore, an increase in peak intensity at 1558 cm^{-1} for inoculated treatments corresponds to C=C stretching (Bekiaris et al., 2016; Farah Nadia et al., 2015), which could be an increase in carbon from microbial biomass, indicating microbial growth even at lower P release as in UFLA 04-155. Conversely, it is still unknown if C from biochar pyrolyzed at different temperatures could influence types of organic acid production by these strains.

5.3 P accumulation in maize increased at lower pyrolysis temperature and PSB inoculation

Magnesium-added biochar and PSB inoculation increased P uptake and accumulation in maize shoot tissues, with similar effects at plants harvested at 15 and 30 days, and at the lower pyrolysis temperature (350 °C) (Figure 5). Mg-enrichment in biochar (e.g., Mg/Ca ratio of 0.15) seems to be part of a mechanism in which the strain UFPI B5-8A enhanced its capacity to solubilize P and consequently promoted higher P uptake. This may result from higher proportions of Mg-P sources at the lower pyrolysis temperature. The increase in P uptake at 15 days was minor, which also agrees with P release for this strain under *in vitro* (7 days) experiments containing Mg-biochar. However, for plants grown for 30 days, a trend can be observed in favor of higher plant growth in

Mg-biochar (Figure 6). For instance, plant shoots under Mg-biochar fertilization achieved 7.8 g per pot, while for biochar it was 6.5 g per pot, representing an increase of 20% for Mg-biochar.

For plants treated with biochars at 500 °C, the results were also in agreement with solubilization *in vitro*, where P release was lower. Besides, plants treated with biochar produced at this higher temperature showed similar levels regardless Mg addition or PSB solubilization. The lower plant growth and P uptake in soil containing biochars at 500 °C both at maize plants grown for 15 and 30 days, is contrary to our hypothesis, with no influence of Mg addition. Furthermore, even with Mg addition, P availability might take longer to be enhanced in soils fertilized with biochars of higher pyrolysis temperature, and higher doses than the ones applied in this study could be necessary to demonstrate the effect of the Mg addition on plant growth and P uptake. The effect of higher P uptake could be more pronounced in higher P fixing soils, as in soil with higher clay content, where soluble P fertilization efficiency is limited (Roy et al., 2016). Thus, more studies are needed to understand the mechanisms by which Mg addition prior to pyrolysis regulates P availability and plant P uptake in tropical soils fertilized with biochar.

Conclusion

The solubilization potential of PSB was strain-specific in each Ca-P and Mg-P source. In summary, P concentration was increased through organic acid production, mainly the citric/maleic and gluconic/tartaric acids. However, organic acid production also varied as a function of the P source, indicating that the P source induces changes in PSB in metabolite production.

From the strains studied, *Pseudomonas* sp. showed a higher potential of P release from Mg-enriched biochar and increased P uptake in maize plants cultivated for a short period (15 and 30 days). However, the positive effect of Mg-enrichment was restricted to biochar produced at 350 °C, which contrasts with our hypothesis. Thus, more studies are needed to understand the mechanisms by which Mg addition prior to pyrolysis and high pyrolysis temperatures (> 350 °C) regulates P availability and plant P uptake in tropical soils fertilized with biochar.

Acknowledgments

The first author received a scholarship from the Improvement of Higher Education Personnel (CAPES - Proex 88887.358193/2019-00). This study was also financed by CAPES and FAPEMIG and CNPq. The authors would like to thank the Central of Analysis and Chemical Prospecting of

the Federal University of Lavras, and Finep, Fapemig, CNPq and Capes for supplying the equipment and technical support for experiments involving infrared analyzes and HPLC analysis. We thank Livia Botelho, Mariene Duarte, Lidiany Lima, Franciane Campos, Daniella Queiroz, Thiago Costa and Giovanna Fontes for help with analyses.

References

Adeleke, R., Nwangburuka, C., Oboirien, B., 2017. Origins, roles and fate of organic acids in soils: A review. South African Journal of Botany 108, 393–406. https://doi.org/10.1016/j.sajb.2016.09.002

Akaike, H., 1974. A New Look at the Statistical Model Identification. IEEE Trans Automat Contr 19, 716–723. https://doi.org/10.1109/TAC.1974.1100705

Alori, E.T., Glick, B.R., Babalola, O.O., 2017. Microbial phosphorus solubilization and its potential for use in sustainable agriculture. Front Microbiol. https://doi.org/10.3389/fmicb.2017.00971

Bekiaris, G., Peltre, C., Jensen, L.S., Bruun, S., 2016. Using FTIR-photoacoustic spectroscopy for phosphorus speciation analysis of biochars. Spectrochim Acta A Mol Biomol Spectrosc 168, 29–36. https://doi.org/10.1016/j.saa.2016.05.049

Billah, M., Khan, M., Bano, A., Hassan, T.U., Munir, A., Gurmani, A.R., 2019. Phosphorus and phosphate solubilizing bacteria: Keys for sustainable agriculture. Geomicrobiol J. https://doi.org/10.1080/01490451.2019.1654043

Bindraban, P.S., Dimkpa, C.O., Pandey, R., 2020. Exploring phosphorus fertilizers and fertilization strategies for improved human and environmental health. Biol Fertil Soils. https://doi.org/10.1007/s00374-019-01430-2

Brown, R.W., Chadwick, D.R., Bending, G.D., Collins, C.D., Whelton, H.L., Daulton, E., Covington, J.A., Bull, I.D., Jones, D.L., 2022. Nutrient (C, N and P) enrichment induces significant changes in the soil metabolite profile and microbial carbon partitioning. Soil Biol Biochem 172. https://doi.org/10.1016/j.soilbio.2022.108779

Bünemann, E.K., Bossio, D.A., Smithson, P.C., Frossard, E., Oberson, A., 2004. Microbial community composition and substrate use in a highly weathered soil as affected by crop rotation and P fertilization. Soil Biol Biochem 36, 889–901. https://doi.org/10.1016/j.soilbio.2004.02.002

Buss, W., 2021. Pyrolysis Solves the Issue of Organic Contaminants in Sewage Sludge while Retaining Carbon - Making the Case for Sewage Sludge Treatment via Pyrolysis. ACS Sustain Chem Eng. https://doi.org/10.1021/acssuschemeng.1c03651

Cui, X., Yang, X., Sheng, K., He, Z., Chen, G., 2019. Transformation of Phosphorus in Wetland Biomass during Pyrolysis and Hydrothermal Treatment. ACS Sustain Chem Eng 7, 16520–16528. https://doi.org/10.1021/acssuschemeng.9b03784

da Costa, E.M., de Carvalho, F., Nóbrega, R.S.A., Silva, J.S., Moreira, F.M. de S., 2016. Bacterial strains from floodplain soils perform different plant-growth promoting processes and enhance cowpea growth. Sci Agric 73, 301–310. https://doi.org/10.1590/0103-9016-2015-0294

da Silva, K., de Souza Cassetari, A., Silva Lima, A., de Brandt, E., Pinnock, E., Vandamme, P., de Souza Moreira, F.M., 2012. Diazotrophic Burkholderia species isolated from the Amazon region exhibit phenotypical, functional and genetic diversity. Syst Appl Microbiol 35, 253–262. https://doi.org/10.1016/j.syapm.2012.04.001

Leite, A., de Souza Cardoso, A.A., de Almeida Leite, R., de Oliveira-Longatti, S.M., Filho, J.F.L., de Souza Moreira, F.M., Melo, L.C.A., 2020. Selected bacterial strains enhance phosphorus availability from biochar-based rock phosphate fertilizer. Ann Microbiol 70. https://doi.org/10.1186/s13213-020-01550-3

de Freitas, J.R., Banerjee, · M R, Germida, · J J, 1997. Phosphate-solubilizing rhizobacteria enhance the growth and yield but not phosphorus uptake of canola (Brassica napus L.), Biol Fertil Soils.

de Zutter, N., Ameye, M., Bekaert, B., Verwaeren, J., de Gelder, L., Audenaert, K., 2022. Uncovering New Insights and Misconceptions on the Effectiveness of Phosphate Solubilizing Rhizobacteria in Plants: A Meta-Analysis. Front Plant Sci. https://doi.org/10.3389/fpls.2022.858804

Elias, F., Woyessa, D., Muleta, D., 2016. Phosphate Solubilization Potential of Rhizosphere Fungi Isolated from Plants in Jimma Zone, Southwest Ethiopia. Int J Microbiol 2016. https://doi.org/10.1155/2016/5472601

Enders, A., Lehmann, J., 2012. Comparison of Wet-Digestion and Dry-Ashing Methods for Total Elemental Analysis of Biochar. Commun Soil Sci Plant Anal 43, 1042–1052. https://doi.org/10.1080/00103624.2012.656167

Farah Nadia, O., Xiang, L.Y., Lie, L.Y., Chairil Anuar, D., Mohd Afandi, M.P., Azhari Baharuddin, S., 2015. Investigation of physico-chemical properties and microbial community during poultry manure co-composting process. J Environ Sci (China) 28, 81–94. https://doi.org/10.1016/j.jes.2014.07.023

Farzadi, A., Bakhshi, F., Solati-Hashjin, M., Asadi-Eydivand, M., Osman, N.A.A., 2014. Magnesium incorporated hydroxyapatite: Synthesis and structural properties characterization. Ceram Int 40, 6021–6029. https://doi.org/10.1016/j.ceramint.2013.11.051

Halajnia, A., Haghnia, G.H., Fotovat, A., Khorasani, R., 2009. Phosphorus fractions in calcareous soils amended with P fertilizer and cattle manure. Geoderma 150, 209–213. https://doi.org/10.1016/j.geoderma.2009.02.010

Hilger, D.M., Hamilton, J.G., Peak, D., 2020. The influences of magnesium upon calcium phosphate mineral formation and structure as monitored by x-ray and vibrational spectroscopy. Soil Syst 4, 1–13. https://doi.org/10.3390/soilsystems4010008

Ibrahim, M., Iqbal, M., Tang, Y.T., Khan, S., Guan, D.X., Li, G., 2022. Phosphorus Mobilization in Plant–Soil Environments and Inspired Strategies for Managing Phosphorus: A Review. Agronomy. https://doi.org/10.3390/agronomy12102539

Illmer, P., Schinner, F., 1995. Solubilization of inorganic calcium phosphates-solubilization mechanisms. Soil Biol. Biochem 27, 257-263

Kannan, S., Lemos, I.A.F., Rocha, J.H.G., Ferreira, J.M.F., 2005. Synthesis and characterization of magnesium substituted biphasic mixtures of controlled hydroxyapatite/β-tricalcium phosphate ratios. J Solid State Chem 178, 3190–3196. https://doi.org/10.1016/j.jssc.2005.08.003

Koutsoukos, P., Amjad, Z., Tomson, M.B., Nancollas, G.H., n.d. / Crystallization of Calcium Phosphates Crystallization of Calcium Phosphates. A Constant Composition Study.

Lambers, H., 2022. Annual Review of Plant Biology Phosphorus Acquisition and Utilization in Plants. https://doi.org/10.1146/annurev-arplant-102720

Li, R., Wang, J.J., Zhou, B., Awasthi, M.K., Ali, A., Zhang, Z., Lahori, A.H., Mahar, A., 2016. Recovery of phosphate from aqueous solution by magnesium oxide decorated magnetic biochar and its potential as phosphate-based fertilizer substitute. Bioresour Technol 215, 209–214. https://doi.org/10.1016/j.biortech.2016.02.125

Li, W., Feng, X., Song, W., Guo, M., 2018. Transformation of Phosphorus in Speciation and Bioavailability During Converting Poultry Litter to Biochar. Front Sustain Food Syst 2. https://doi.org/10.3389/fsufs.2018.00020

Li, Z., Bai, T., Dai, L., Wang, F., Tao, J., Meng, S., Hu, Y., Wang, S., Hu, S., 2016. A study of organic acid production in contrasts between two phosphate solubilizing fungi: Penicillium oxalicum and Aspergillus Niger. Sci Rep 6. https://doi.org/10.1038/srep25313

Malavolta, E., 1980. Elementos de nutrição mineral de plantas. Piracicaba: Agronômica Ceres, 251p.

Maria De Oliveira Longatti, S., Marra, L.M., Maria De Souza Moreira, F., 2013. African Journal of Microbiology Research Evaluation of plant growth-promoting traits of Burkholderia and Rhizobium strains isolated from Amazon soils for their co-inoculation in common bean 7, 948–959. https://doi.org/10.5897/AJMR12.1055

Marra, L.M., de Oliveira-Longatti, S.M., Soares, C.R.F.S., de Lima, J.M., Olivares, F.L., Moreira, F.M.S., 2015. Initial pH of medium affects organic acids production but do not affect phosphate solubilization. Brazilian Journal of Microbiology 46, 367–375. https://doi.org/10.1590/S1517-838246246220131102

Marra, L.M., de Oliveira-Longatti, S.M., Soares, C.R.F.S., Olivares, F.L., Moreira, F.M. de S., 2019. The Amount of Phosphate Solubilization Depends on the Strain, C-Source, Organic Acids and Type of Phosphate. Geomicrobiol J 36, 232–242. https://doi.org/10.1080/01490451.2018.1542469

Marra, L.M., Sousa Soares, C.R.F., de Oliveira, S.M., Ferreira, P.A.A., Soares, B.L., de Carvalho, R.F., de Lima, J.M., de Moreira, F.M.S., 2012. Biological nitrogen fixation and phosphate

solubilization by bacteria isolated from tropical soils. Plant Soil 357, 289–307. https://doi.org/10.1007/s11104-012-1157-z

Martins da Costa, E., de Lima, W., Oliveira-Longatti, S.M., de Souza, F.M., 2015. Phosphate-solubilising bacteria enhance Oryza sativa growth and nutrient accumulation in an oxisol fertilized with rock phosphate. Ecol Eng 83, 380–385. https://doi.org/10.1016/j.ecoleng.2015.06.045

Matoso, S.C.G., Wadt, P.G.S., de Souza Júnior, V.S., Otero Pérez, X.L., 2022. Soil mineralogy-controlled phosphorus availability in soils mixed with phosphate fertiliser and biochar. Environmental Technology (United Kingdom). https://doi.org/10.1080/09593330.2022.2074318

Nautiyal, C.S., 1999. An efficient microbiological growth medium for screening phosphate solubilizing microorganisms. FEMS Microbiol Lett 170, 265–270

Ng, J.F., Ahmed, O.H., Jalloh, M.B., Omar, L., Kwan, Y.M., Musah, A.A., Poong, K.H., 2022. Soil Nutrient Retention and pH Buffering Capacity Are Enhanced by Calciprill and Sodium Silicate. Agronomy 12. https://doi.org/10.3390/agronomy12010219

Novais, R.F., Neves, J.C.L., Barros, N.F., 1991. Ensaio em ambiente controlado. In_ Oliveira, A.J., Garrido, W.E. Métodos de pesquisa em fertilidade do solo. Brasília, Embrapa-SAE, 189-254.

Okoye, C.O., Dong, K., Wang, Y., Gao, L., Li, X., Wu, Y., Jiang, J., 2022. Comparative genomics reveals the organic acid biosynthesis metabolic pathways among five lactic acid bacterial species isolated from fermented vegetables. N Biotechnol 70, 73–83. https://doi.org/10.1016/j.nbt.2022.05.001

Papagianni, M., 2007. Advances in citric acid fermentation by Aspergillus niger: Biochemical aspects, membrane transport and modeling. Biotechnol Adv. https://doi.org/10.1016/j.biotechadv.2007.01.002

Roriz de Souza, C., Kumar Ghosh, A., Ribeiro da Silva, I., Santiago de Alvarenga, E., Ferreira Novais, R., Luiz de Jesus, G., Professor, A., 2012. Phosphorus transformation in poultry litter and litter-treated oxisol of brazil assessed by 31 p-nmr and wet chemical fractionation. R. Bras. Ci. Solo 36, 1516-1527

Roy, E.D., Richards, P.D., Martinelli, L.A., Coletta, L. della, Lins, S.R.M., Vazquez, F.F., Willig, E., Spera, S.A., VanWey, L.K., Porder, S., 2016. The phosphorus cost of agricultural intensification in the tropics. Nat Plants 2. https://doi.org/10.1038/NPLANTS.2016.43

Silva, F.C., 2009. Manual de análises químicas de solos, plantas e fertilizantes. 2nd ed. Empresa Brasileira de Pesquisa Agropecuária, Embrapa Solos, Brasília, DF.

Song, W., Guo, M., 2012. Quality variations of poultry litter biochar generated at different pyrolysis temperatures. J Anal Appl Pyrolysis 94, 138–145. https://doi.org/10.1016/j.jaap.2011.11.018

Ullrich-Eberius, C.I., Novacky, A., van Bel, A.J.E., 1984. Phosphate uptake in *Lemna gibba* G1: energetics and kinetics. Planta, 161, 46-52.

Vyas, P., Gulati, A., 2009. Organic acid production in vitro and plant growth promotion in maize under controlled environment by phosphate-solubilizing fluorescent Pseudomonas. BMC Microbiol 9. https://doi.org/10.1186/1471-2180-9-174

Wang, Y., Lin, Y., Chiu, P.C., Imhoff, P.T., Guo, M., 2015. Phosphorus release behaviors of poultry litter biochar as a soil amendment. Science of the Total Environment 512–513, 454–463. https://doi.org/10.1016/j.scitotenv.2015.01.093

Whiting, P.H., Midgley, M., Dawes, E.A., 1976. The Regulation of Transport of Glucose, Gluconate and 2-Oxogluconate and of Glucose Catabolism in Pseudomonas aeruginosa.

Wieczorek, D., Żyszka-Haberecht, B., Kafka, A., Lipok, J., 2022. Determination of phosphorus compounds in plant tissues: from colorimetry to advanced instrumental analytical chemistry. Plant Methods. https://doi.org/10.1186/s13007-022-00854-6

Xu, G., Zhang, Y., Shao, H., Sun, J., 2016. Pyrolysis temperature affects phosphorus transformation in biochar: Chemical fractionation and 31P NMR analysis. Science of the Total Environment 569–570, 65–72. https://doi.org/10.1016/j.scitotenv.2016.06.081

Yu, X., Liu, X., Zhu, T.H., Liu, G.H., Mao, C., 2011. Isolation and characterization of phosphate-solubilizing bacteria from walnut and their effect on growth and phosphorus mobilization. Biol Fertil Soils 47, 437–446. https://doi.org/10.1007/s00374-011-0548-2

Zhang, M., Gao, B., Yao, Y., Xue, Y., Inyang, M., 2012. Synthesis of porous MgO-biochar nanocomposites for removal of phosphate and nitrate from aqueous solutions. Chemical Engineering Journal 210, 26–32. https://doi.org/10.1016/j.cej.2012.08.052

Supplementary information

Table S1. Amount of biochar applied to soil as the P source at greenhouse experiment. *Calculated based on total P from biochar.

Treatment	P	*Total applied
	g kg^{-1}	g per pot
PM biochar 350 °C	31.44 ± 0.16	9.54
Mg-PM biochar 350 °C	32.29 ± 0.30	9.29
PM biochar 500 °C	31.16 ± 1.60	9.63
Mg-PM biochar 500 °C	35.91 ± 0.36	8.25

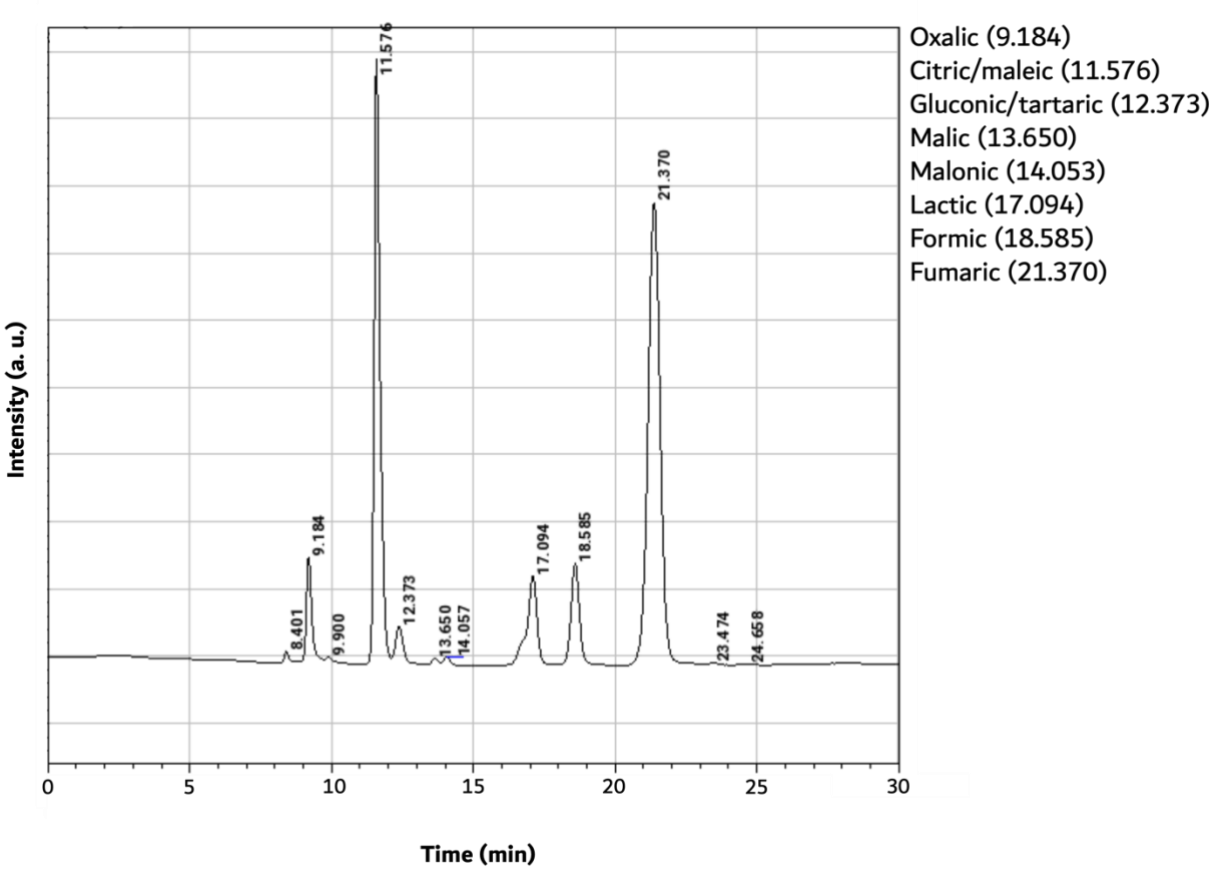

Figure S1. Retention time of low molecular mass organic acids (10 mg L^{-1}).

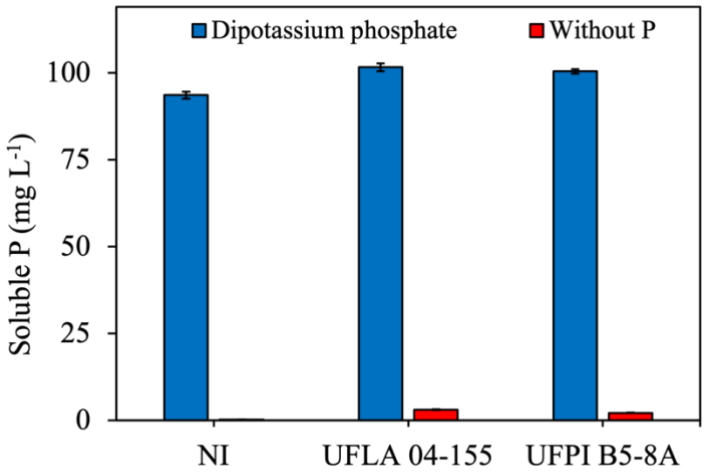

Figure S2. Soluble phosphorus (mg L^{-1}) in liquid NBRIP medium after 7 days incubation containing dipotassium phosphate and bacterial inoculation. Mean values ± standard deviation; n = 4. Note: NI, non-inoculated.

Table S2. pH of liquid NBRIP medium after 7 days incubation containing dipotassium phosphate (K_2HPO_4) and bacterial inoculation. P release referring to this pH at figure S2.

Strain	NBRIP pH	
	Positive control (K_2HPO_4)	Negative control (No P addition)
NI	6.6 ± 0.1	5.7 ± 0.3
UFLA 05-155	5.6 ± 0.1	4.0 ± 0.0
UFPI B5-8A	3.6 ± 0.0	4.2 ± 0.5

Note: NI: non-inoculated.

Final remarks

Producing biochar from poultry manure portrays an alternative to enhance the efficiency of P fertilization in tropical soils. Recycling and reintroducing P from organic residues into agriculture can diminish the shortage of P resources and diminish environmental contamination of water bodies with P and N present in poultry manure.

After pyrolysis, promising features were observed in biochar produced from the poultry manure enriched with Mg(OH)2. For instance, P speciation was modified, and new Mg-P compounds were observed predominantly in lower pyrolysis temperatures. These Mg-P sources might have been responsible for the augmented P availability observed in Mg-enriched biochar. In agreement with P speciation, the biochars produced at 350 °C and applied to soil as the P source for maize cultivation reached plant production levels near those observed by the conventional soluble phosphate source. In addition, due to the higher pH resulting from $Mg(OH)_2$ addition, a low water-soluble P fraction was also observed in poultry manure and biochar, which may help decrease P adsorption in tropical soils. Moreover, a lower water-soluble P fraction in poultry manure might aid in achieving efficient management for poultry manure application *in natura*.

Producing biochar from nutrient-rich biomass such as poultry manure increases the fertilizer value, reduces volumes, and facilitates land application. In addition, inoculating phosphate-solubilizing bacteria and applying Mg-enriched biochar to soil improved P concentration and accumulation in maize plant shoots in this work. The inoculation of bacterial strains is a sustainable approach to increase P use efficiency from sources of lower P availability, and as observed in this study, it is also an effective method for P solubilization from Mg-enriched biochar. However, it is still necessary to elucidate how Mg enrichment affects P losses and the residual effect of P at longer stages of plant cultivation.